
Doctoral Dissertations

Student Theses and Dissertations

Spring 2020

Polymeric nanoparticle as a new platform for high removal of endotoxins from biopharmaceutical solutions

Sidharth Razdan

Follow this and additional works at: https://scholarsmine.mst.edu/doctoral_dissertations



Part of the [Chemical Engineering Commons](#)

Department: **Chemical and Biochemical Engineering**

Recommended Citation

Razdan, Sidharth, "Polymeric nanoparticle as a new platform for high removal of endotoxins from biopharmaceutical solutions" (2020). *Doctoral Dissertations*. 2896.

https://scholarsmine.mst.edu/doctoral_dissertations/2896

This thesis is brought to you by Scholars' Mine, a service of the Missouri S&T Library and Learning Resources. This work is protected by U. S. Copyright Law. Unauthorized use including reproduction for redistribution requires the permission of the copyright holder. For more information, please contact scholarsmine@mst.edu.

POLYMERIC NANOPARTICLE AS A NEW PLATFORM FOR HIGH REMOVAL OF
ENDOTOXINS FROM BIOPHARMACEUTICAL SOLUTIONS

by

SIDHARTH RAZDAN

A DISSERTATION

Presented to the Graduate Faculty of the
MISSOURI UNIVERSITY OF SCIENCE AND TECHNOLOGY

In Partial Fulfillment of the Requirements for the Degree

DOCTOR OF PHILOSOPHY

in

CHEMICAL ENGINEERING

2020

Approved by:

Dr. Sutapa Barua, Advisor

Dr. Dipak Barua

Dr. Xinhua Liang

Dr. Manashi Nath

Dr. Jee-Ching Wang

© 2020

Sidharth Razdan

All Rights Reserved

PUBLICATION DISSERTATION OPTION

This dissertation consists of the following two articles, formatted in the style used by the Missouri University of Science and Technology:

Paper I, found on pages 43–103, has been published in *Scientific Reports Journal*.

Paper II, found on pages 104–151, is intended for submission to *Biotechnology Journal*.

ABSTRACT

Presently, approximately one-third of all biopharmaceutical drugs are derived from biological sources like gram-negative bacteria. Gram-negative bacteria like *E.coli* are much cheaper to cultivate and provide higher biotherapeutic yield compared to mammalian cells. On extracting the useful biotherapeutics from the gram-negative bacterial cells (*E.coli*), endotoxin present in the bacteria is released in the surrounding media thus contaminating the lifesaving biotherapeutics. Application of the endotoxin-contaminated therapeutics to humans or animals can cause serious health issues like septic shock, tissue injury and ultimately death. Hence, thorough purification of biotherapeutics before parenteral application is necessary. Although there are multiple methods for removing endotoxins, but achieving high protein recovery and purification efficiency are still a challenge.

We have demonstrated a cost-effective technology using a biocompatible polymer nanoparticle of approximately 800 nm diameter. The polymeric nanoparticle removed >99% endotoxins from water, phosphate buffer saline (PBS) and protein solutions including monoclonal antibodies (MAb). It also showed a high protein recovery of ~99%. Additionally, the polymeric nanoparticle was capable of being reused multiple times after being regenerated. Further, to enhance the throughput, flow properties and to scale up the whole system, the polymeric nanoparticles were incorporated in a portable and flat sheet biofilter. The biofilter is effective in removing >99% endotoxins from water and protein solutions with a protein recovery of > 90%. Finally, the whole filtration set-up being gravity driven minimized cost.

ACKNOWLEDGMENTS

First, I would like to express my sincere gratitude to my advisor Dr. Sutapa Barua, who created the valuable space for me to do this research and develop myself as a researcher in the best possible way. I greatly appreciate the freedom given to me to find my own path and the guidance and support offered by her when needed. Her mix of straightforward criticism combined with heart-warming support have given me great confidence as a researcher, and at the same time made me realize that I am only a beginner in this exciting profession. Thank you for all your feedback, encouragement, continuous pedagogic inputs, practical support, patience and motivation, which helped me during my PhD study and related research.

I am also thankful to my other PhD committee members, Dr. Dipak Barua, Dr. Xinhua Liang, Dr. Manashi Nath, and Dr. Jee-Ching Wang, for accepting to be on my committee, and investing their valuable time and providing valuable feedback.

I am also thankful to Mason Schneier, Allison M. Miller, and Maria E. Briceno for their contributions towards the literature review section of this dissertation.

I would also like to thank my fellow researchers in the lab, Raisul Abedin, Jawahar Khetan, Md Shahinuzzaman, Md Aminul Islam, Joseph Johnston, and Justin Adler for exchanging views and ideas that enabled me to widen my research from various perspectives during my various research activities.

Last but not the least, I would like to thank my family, my parents, grandparents, and my sister, for being a practical support to me and motivating me all through my research and life in general.

TABLE OF CONTENTS

	Page
PUBLICATION DISSERTATION OPTION	iii
ABSTRACT	iv
ACKNOWLEDGMENTS	v
LIST OF ILLUSTRATIONS	xi
LIST OF TABLES	xiii
LIST OF ABBREVIATIONS.....	xiv
 SECTION	
1. INTRODUCTION.....	1
1.1. BACKGROUND	1
1.2. BIOLOGICAL ENDOTOXIN DETECTION TECHNIQUES	2
1.2.1. Rabbit Pyrogen Test (RPT)	4
1.2.2. Limulus Amebocyte Lysate (LAL) Assay	4
1.2.3. Recombinant Factor C (rFC) Assay	10
1.2.4. Bovine Whole Blood Assay (bWBA)	11
1.2.5. Monocyte Activation Test (MAT)	11
1.3. BIOSENSOR TECHNIQUES	13
1.3.1. Electrochemical	13
1.3.2. Optical Techniques.....	16
1.3.3. Fluorescence and Luminescence Techniques.....	16
1.3.4. Surface Plasmon Resonance (SPR) and Mass-based Techniques.....	18

1.4. TECHNIQUES FOR DOWNSTREAM REMOVAL OF ENDOTOXINS	20
1.4.1. Ultrafiltration.....	20
1.4.2. Extraction	22
1.4.3. Ion Exchange Chromatography.....	23
1.4.4. Affinity Chromatography.....	25
1.4.5. Mixed-Mode Chromatography.....	36
1.4.6. Membrane Adsorption.....	36
1.5. DISCUSSION.....	37
1.6. CONCLUSION.....	41
1.7. DISSERTATION OVERVIEW	41

PAPER

I. POLYBALL: A NEW ADSORBENT FOR THE EFFICIENT REMOVAL OF ENDOTOXIN FROM BIOPHARMACEUTICALS	43
ABSTRACT	43
1. INTRODUCTION.....	45
2. MATERIALS AND METHODS	47
2.1. SYNTHESIS OF PCL NANOPARTICLES.....	47
2.2. CHARACTERIZATION OF PCL NANOPARTICLES.....	48
2.3. ADSORPTION STUDIES.....	49
2.4. PROTEIN RECOVERY	51
2.5. EFFECTS OF BUFFER AND pH ON LPS REMOVAL	51
2.6. EFFECT OF SALT CONCENTRATION ON PROTEIN RECOVERY.....	52
2.7. PCL NP REGENERATION STUDIES.....	52
2.8. SYNTHESIS OF CELLULOSE ACETATE (CA) MEMBRANE	52

2.9. MICROSCOPY AND MICROANALYSIS.....	53
2.10. PERMEATION STUDIES	54
2.11. QUANTIFICATION OF LPS REMOVAL USING PCL NPS IN CA MEMBRANES	54
2.12. CALCULATION OF LPS REMOVAL EFFICIENCY PER UNIT MASS AND SURFACE AREA OF PCL NPs.....	55
3. RESULTS.....	56
3.1. REMOVAL OF LPS FROM WATER AND PBS USING PCL NPs IN POWDER FORM.....	56
3.2. REMOVAL OF LPS FROM PROTEIN SOLUTIONS USING PCL NPs.....	61
3.3. LPS ADSORPTION BEHAVIOR ON PCL NPs.....	63
3.4. PROTEIN RECOVERY	64
3.5. EFFECT OF pH ON LPS REMOVAL IN DIFFERENT BUFFER CONDITIONS.....	66
3.6. EFFECT OF SALT CONCENTRATION ON PROTEIN RECOVERY.....	68
3.7. PCL NPs WERE REGENERATED TO REMOVE LPS.....	69
3.8. PCL NPs WERE EMBEDDED IN CA MEMBRANES.....	70
3.9. PERMEATION OF WATER USING CA MEMBRANES WITHOUT AND WITH PCL NPs.....	73
3.10. CA MEMBRANES WITHOUT AND WITH PCL NPs FOR REMOVING LPS FROM WATER	75
3.11. PRODUCT COMPARISON.....	77
4. DISCUSSION	79
5. CONCLUSION	83
ACKNOWLEDGMENTS.....	84
SUPPLEMENTARY INFORMATION.....	85

REFERENCES	95
II. UNDERSTANDING THE MECHANISM OF INTERACTION BETWEEN ENDOTOXIN AND POLYMER NANOPARTICLE	104
ABSTRACT	104
1. INTRODUCTION	105
2. MATERIALS AND METHODS.....	108
2.1. SYNTHESIS OF BARE PCL AND MODIFIED PCL NANOPARTICLES.....	108
2.2. CHARACTERIZATION OF BARE PCL AND MODIFIED PCL NANOPARTICLES.....	109
2.3. EFFECTS OF pH ON PROTEIN RECOVERIES	110
2.4. EVALUATION OF CONJUGATION EFFICIENCY OF MODIFIED PCL NANOPARTICLES	110
2.5. EVALUATION OF ENDOTOXIN REMOVAL EFFICIENCY OF PARTICLES (IN RO WATER AND PBS).....	111
2.6. SYNTHESIS OF CELLULOSE ACETATE (CA) BIOFILTER.....	112
2.7. MICROSCOPY AND MICROANALYSIS	113
2.8. WATER FLUX STUDIES	113
2.9. QUANTIFICATION OF ENDOTOXIN REMOVAL USING PCL NPS IN CA BIOFILTER	114
3. RESULTS	115
3.1. SYNTHESIS OF POLYCAPROLACTONE NANOPARTICLES	115
3.2. EFFECT OF pH ON PROTEIN RECOVERIES	117
3.3. ENDOTOXIN REMOVAL EFFICIENCY COMPARISON FROM WATER AND PBS USING PCL NPs AND POLYSTYRENE NPs.....	119
3.4. CONJUGATION EFFICIENCY OF CATIONIC LIGAND ON PCL NPs SURFACE.....	119

3.5. ENDOTOXIN REMOVAL EFFICIENCY COMPARISON FROM WATER AND PBS USING PCL NPs AND CATIONIC LIGAND MODIFIED PCL NPs	123
3.6. ENDOTOXIN REMOVAL FROM PROTEIN SAMPLES USING PCL NPs INCORPORATED CA BIOFILTER.....	123
4. DISCUSSION	130
5. CONCLUSIONS.....	135
ACKNOWLEDGMENTS.....	136
SUPPLEMENTARY INFORMATION.....	137
REFERENCES.....	147
SECTION	
2. CONCLUSIONS AND FUTURE WORK.....	152
2.1. CONCLUSIONS.....	152
2.2. FUTURE WORK.....	154
BIBLIOGRAPHY.....	155
VITA.....	171

LIST OF ILLUSTRATIONS

SECTION	Page
Figure 1.1. A simplified scheme of biopharmaceutical production, separation and purification steps.....	3
Figure 1.2. Schematic view of the chemical structure of endotoxin from E. coli and properties of endotoxin binding materials.	3
Figure 1.3. Endotoxin detection mechanism using LAL assay.	7
Figure 1.4. A new electrochemical endotoxin sensor.....	15
Figure 1.5. Fluorescent assay protocol for endotoxin detection.....	17
Figure 1.6. Chemical structures of various endotoxin binding ligands.	27
Figure 1.7. PolyBall nanoparticles based effective endotoxin removal.....	33
Figure 1.8. PolyBall nanoparticles incorporated cellulose acetate (CA) membrane for effective endotoxin removal.	34
PAPER I	
Figure 1. Characterization of PCL NPs.....	58
Figure 2. The LPS removal efficiency of PCL NPs from water and PBS.....	59
Figure 3. The LPS removal efficiency of PCL NPs from protein solutions.....	62
Figure 4. Freundlich adsorption isotherm fitting of LPS removal by PCL NPs from BSA and TTZ solutions in water and PBS.	64
Figure 5. Percentage of protein recovery as a function of (a) protein concentrations and (b) LPS concentrations.....	65
Figure 6. The effects of pH and salt concentrations on LPS removal by PCL NPs.....	67
Figure 7. PCL NP regeneration.....	70
Figure 8. Characterization of PCL NP embedded filter.....	71

Figure 9. Water flux performance of CA and PCL impregnated CA membrane	74
Figure 10. The LPS removal efficiency of PCL NP embedded filters	76
Figure 11. Endotoxin removal product comparison	78
PAPER II	
Figure 1. Characterization of PCL NPs..	116
Figure 2. The effects of pH on protein recovery using PCL NPs..	118
Figure 3. Comparison of endotoxin removal and binding efficiency of bare PCL NPs with Polystyrene NPs in water and PBS.	120
Figure 4. % Conjugation efficiency and zeta potential of PLL, PEI and chitosan ligand coated PCL NPs.	121
Figure 5. Comparison of endotoxin removal and binding efficiency of bare PCL NPs with cationic ligand modified PCL NPs in RO water and PBS.	124
Figure 6. Surface and cross-section morphology of biofilter.	125
Figure 7. Water flux through CA and PCL incorporated CA biofilter	128
Figure 8. The endotoxin removal efficiency and protein recovery of different proteins using CA and PCL incorporated CA biofilter.....	129

LIST OF TABLES

SECTION	Page
Table 1.1. A comparison chart eliciting three LAL test methods: the gel clot, turbidimetric and chromogenic method and rFC assay as available in commercial endotoxin detection kits.....	10
Table 1.2. Commonly used affinity-based ligands for endotoxin removal in chromatography.....	29
Table 1.3. Comparison of endotoxin removal products, their adsorption capacity, costs and regenerability.....	35
PAPER I	
Table 1. Comparison of PCL NPs and the NP containing membrane versus four commercially available endotoxin removal products.	78

LIST OF ABBREVIATIONS

Abbreviation	Description
EU	Endotoxin Unit
RPT	Rabbit Pyrogen Test
LAL	Limulus Amebocyte Lysate
bWBA	Bovine Whole Blood Assay
rFC	Recombinant Factor C
MAT	Monocyte Activation Test
BODIPY	4,4-difluoro-4-bora-3a,4a-diaza-s-indacene
SPR	Surface Plasmon Resonance
PCL NPs	Polycaprolactone Nanoparticles
LPS	Lipopolysaccharides
CA	Cellulose Acetate
PLL	Poly-l-lysine
PEI	Polyethyleneimine
SDS	Sodium Dodecyl Sulfate
PMB	Polymyxin-B
DEAE	Diethylaminoethane
PBS	Phosphate Buffer Saline
MMC	Mixed-Mode Chromatography
PVA	Polyvinylalcohol
BSA	Bovine Serum Albumin

TTZ	Trastuzumab
DMSO	Dimethyl sulfoxide
PS NPs	Polystyrene Nanoparticles
F.I	Fluorescence Intensity
pI	Isoelectric Point
SEM	Scanning Electron Microscope
DLS	Dynamic Light Scattering
ELS	Electrophoretic Light Scattering

1. INTRODUCTION

1.1. BACKGROUND

Pharmaceutical manufacturing deals with selection and optimization of the cell source, media composition and physico-chemical bioreactor operating conditions to maximize the culture yield and productivity (Figure 1.1) ¹⁻³. *Escherichia coli* is a cost effective and attractive choice for producing therapeutic monoclonal antibodies, recombinant proteins and other biopharmaceuticals due to their rapid growth, *minimal nutritional requirements, high product yield* and transformation capability ⁴⁻¹¹. With the millions of strains of bacteria, and gene-altering technology steadily improving, the possibilities are endless ¹². One of the most recognizable products derived from genetically engineered *E. coli* is the hormone insulin. Before being manufactured by bacteria, insulin was originally extracted from dogs and later pigs that was an extremely inefficient process, making the product rare and expensive ¹³. The advent of *E. coli* - produced insulin such as recombinant human insulin (Humulin) drastically increased its availability for diabetics ¹⁴. However, biopharmaceutical products manufactured using *E. coli* or other gram-negative bacteria are subject to endotoxin contamination ¹⁵⁻²¹.

Endotoxins are present in the outer cell wall of gram-negative bacteria that contribute to the organization and stability of the membrane ¹⁶⁻²². Endotoxin consists of three regions: a core polysaccharide, a long chain polysaccharide, and a non-polar lipid called Lipid A (Figure 1.2) ^{20,23}. The core polysaccharide has an outer hexose region and an inner heptose region and the long chain polysaccharide is a strain-specific surface antigen (O-antigen) that consists of repeating oligosaccharide subunits ^{17,20}. The core

polysaccharide and the O-antigen are both hydrophilic while Lipid A is hydrophobic. The toxicity of endotoxin is associated with Lipid A ²⁴⁻²⁶. Lipid A triggers the production of pro inflammatory cytokines ^{27,28} and activation of the coagulation cascade ^{20,29} which can lead to sepsis and septic shock ³⁰⁻³⁴. A pyrogenic reaction can be caused by as little as 1 ng of endotoxin per kilogram of body weight per hour ^{16-21,35}. The standard unit for endotoxin measurements is an endotoxin unit (EU), which is equal to the activity of 0.1 ng of *E. coli* endotoxin ^{36,37}. For intravenous applications, a maximum of 5 EU per kilogram of body weight can be administered to a patient per hour ^{36,38,39}, but acceptable concentrations in biopharmaceutical products vary depending on the required dose ^{40,41}. Endotoxin is highly stable and is resistant to destruction by heat or pH ^{25,39,42}. Additionally, endotoxins may form stable interactions with target therapeutic compounds that further complicates separations ^{23,43,44}. Downstream processing of recombinant protein products accounts for approximately 45-92% of the total manufacturing costs ^{10,45,46}. In addition to the downstream processing, the detection of endotoxins is absolutely critical for the safety of patients across the globe who rely on the purity of treatments prescribed ²⁸. The purpose of this review is to discuss these aspects of an array of endotoxin detection and removal technologies.

1.2. BIOLOGICAL ENDOTOXIN DETECTION TECHNIQUES

Biological detection techniques include rabbit pyrogen test (RPT), limulus amoebocyte lysate (LAL) assay and bovine whole blood assay (bWBA) that use natural methods of endotoxin detection, and are still in use today, although they are being phased

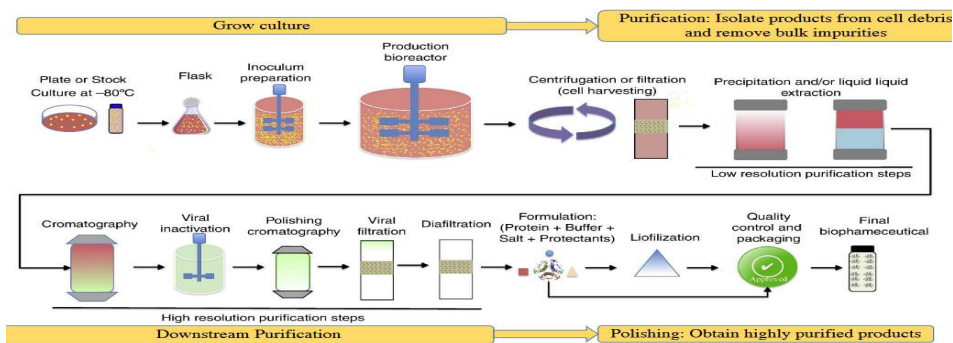


Figure 1.1. A simplified scheme of biopharmaceutical production, separation and purification steps. Biopharmaceutical manufacturing is divided into two areas: upstream fermentation or cell culture and downstream purification processes. Each area contains multiple unit operations. The primary downstream unit operation is chromatography that includes variations in modes such as affinity, cation-exchange, anion-exchange, ceramic hydroxyapatite, and hydrophobic-interaction chromatography. The process performance is mainly determined by the rate of molecule transport to the binding sites. In large chromatographic columns, small adsorbent particles provide high surface area for binding but generate a large pressure drop at high fluid velocity. On the other hand, large adsorbent particles minimize active binding site per volume as well as reduce mass transport. (Figure reproduced with permission from Jozala et. al., Ref. 3).

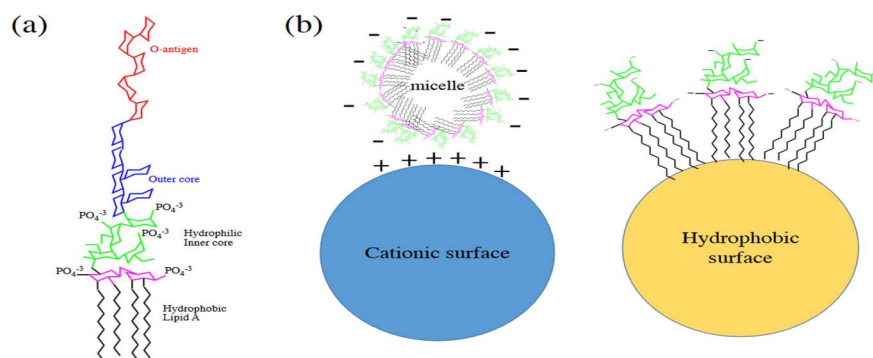


Figure 1.2. Schematic view of the chemical structures of endotoxin from E.coli and properties of endotoxin binding materials.(a) Schematic view of the chemical structure of endotoxin from E. coli. Endotoxins are lipopolysaccharides that consist of a heteropolysaccharide (O-antigen), the core oligosaccharide, and a non-polar lipid A tail. (b) Endotoxins form aggregates in micelle, cube, lamellar or vesicle forms exhibiting a net negative charge in pharmaceutical solutions. The negatively charged “micellar” endotoxins can be adsorbed on polycationic ligands, or the individual endotoxin monomers can be removed by hydrophobic lipid tail interactions with hydrophobic surface.

out by newer, more accurate testing methods such as biosensors that are described after the biological detection techniques.

1.2.1. Rabbit Pyrogen Test (RPT). The oldest and simplest of the endotoxin detection techniques, RPT involves injecting the biological sample in question into live rabbits and waiting for a fever to develop^{23,47}. This method works on the principle that rabbits and humans share similar fever patterns under influence of endotoxins. It was determined that a temperature increase of 0.5°C over a time span of 180 min after injection constituted a fever⁴⁸. It was also found that it has a detection limit of approximately 0.5 EU/ml (endotoxin unit/milliliter) or around 0.05 ng of endotoxin/ml of solution⁴⁹. As rudimentary as the technique seems, a detection rate as low as 0.1 ng was considered very accurate at the time of this methods development in 1912. This technique has been praised for its accuracy; being an in vivo technique, it is easy to accept the results of the test as researchers can physically see the test subject show symptoms of infection. Seeing the test subject suffering the effects of endotoxins provides a compelling argument to the presence of endotoxins in the sample. This method is often criticized⁵⁰. The scientific world is generally moving away from live test subjects where avoidable, in particular, animal testing. While this test was once considered the best in the industry, and is still being performed in parts of Japan, today it is criticized for its need for many samples, and its near-obsolete sensitivity and accuracy compared to other methods⁵¹.

1.2.2. Limulus Amebocyte Lysate (LAL) Assay. Unlike RPT, LAL assay developed in the 1960s does not involve live test subjects. It does, however, rely on an extract from the blood of the *Limulus polyphemus* species of horseshoe crab^{52,53}. The

extract is used in one of three ways. First and simplest, the gel-clot. This test involves mixing equal parts of extract and sample. If a gel has formed and the mixture remains intact in the bottom of the tube, the test shows positive ⁵⁴. This means the sample has at least enough endotoxins to trigger a positive reaction, the limit of this being around the range of 0.03 EU/mL to 0.06 EU/ml. The other two methods are turbidimetric and chromogenic methods. Both are referred to as photometric tests as they require an optical reader for analysis. The chromogenic assay is performed by replacing a natural substrate, coagulen, with a chromogenic, or colored one. The chromogenic substrate is cleaved by an endotoxin-activated enzyme coagulase, and the chromogenic molecule is released from the substrate into the suspension measured by spectrophotometry ⁵⁵. The turbidimetric method is similar to the chromogenic method, but instead measures the turbidity of the solution ⁵⁶. The rate of turbidity and absorbance (color change) are proportional to the endotoxin concentration. All three tests rely on the same protein, Factor C coagulation cascade found in horseshoe crabs' blood (Figure 3c). The endotoxin activates Factor C which goes onto activate Factor B following the formation of a clotting enzyme ^{57,58}. In gel clot and turbidity assays, the clotting enzyme transforms coagulen into coagulin, creating the gel in the gel clot test, as well as the clouding agent in the turbidity test. The chromogenic method follows the same pathway, but instead of using coagulen, it uses a complex of amino acids and p-nitroaniline (pNA), as the chromogenic factor. The enzyme trims the pNA off of the complex, turning the suspension a yellow color. This color is too faint to discern by the naked eye so a spectrometer must be used ²³. These tests are widely accepted as the official endotoxin test in the pharmaceutical community ⁵⁹. Every drug and medical device that is tested by the US Food and Drug

Administration (FDA) must undergo and pass a LAL test ^{60,61}. As previously mentioned, this method is much more accurate than RPT, particularly the photometric methods. This method still has its drawbacks. LAL assay gives both false negative and false positive results by the presence of test interferences. False negative results are observed when endotoxins are masked by product formulation matrices such as surfactants (*e.g.*, polysorbate 20, polysorbate 80 *etc.*), buffer constituents (*e.g.*, citrate, phosphate *etc.*) and cell culture medium, or by aggregation with products ⁶²⁻⁶⁴. As a result, endotoxin is not accessible to react with LAL reagents, a phenomenon well known as low endotoxin recovery (LER) ⁶⁵. In contrast, LAL assay also produces a falsely higher reading by the presence of (1→3)-β-D-glucans, a major cell membrane component that cause a false positive reaction triggering the protease enzyme Factor G pathway and form the same coagulin protein end product as found in LAL reactions ^{66,67}. The LAL test is challenging for measuring endotoxin activity in proteins, peptides and polymers because the active site of endotoxin binds with the products neutralizing the biological activity of endotoxins ⁶⁸⁻⁷¹. The protein cascades the LAL assay relies on is disrupted in samples with free metal ions, and similar to RPT, the method is subject to the same public outcry for its treatment of horseshoe crabs. While the phlebotomy itself is not fatal, an approximated 20% of the crabs fail to survive after being returned to sea ²³. Following the discovery of Factor C as endotoxin-activated portion of the protein cascade, attempts have been made to replace the conventional LAL test, with one using recombinant Factor C ⁷². As technology improves, alternative techniques are being developed to ease the pressure on the horseshoe crab population.

(a)

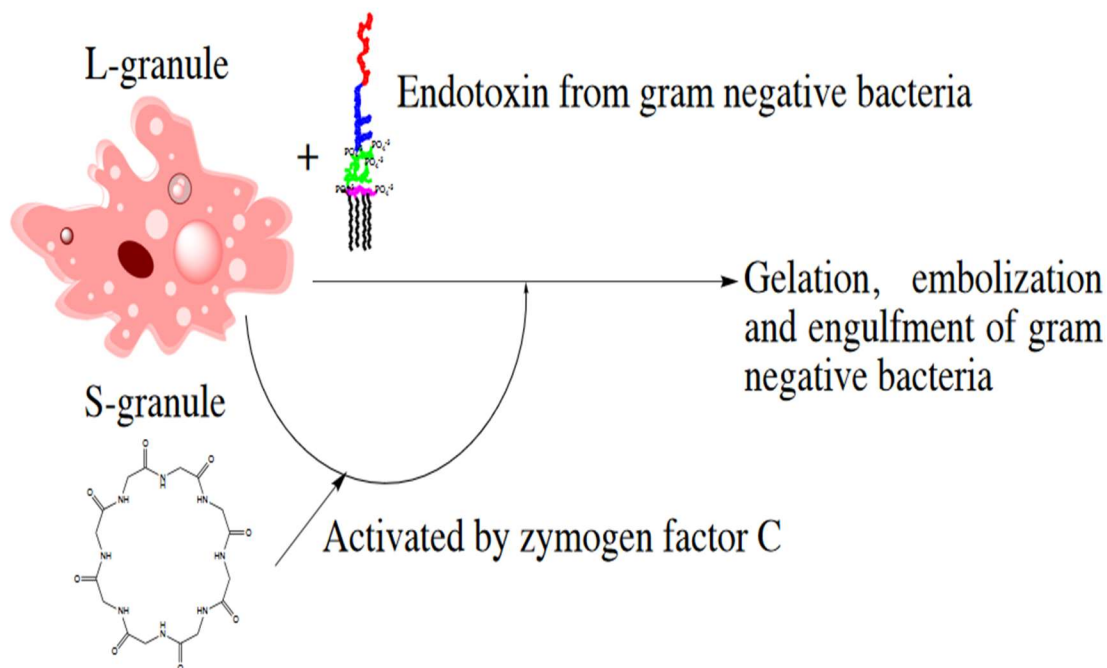


Figure 1.3. Endotoxin detection mechanism using LAL assay. (a) Endotoxin induced defense mechanisms in circulating hemolymphs of horseshoe crabs. The LAL assay is designed based on the immunogenic reactions developed in the blood of horseshoe crabs. Upon exposure to endotoxins, the electron dense large granules (L-granule) and less electron dense small granular (S-granule) amebocytes become activated by zymogen factor C. (b) Coagulation cascade in horseshoe crab blood. Endotoxin activates plasma membrane-bound factor C. Factor C is a single chain glycoprotein (M.W. = 123 kDa) comprising of a heavy chain (M.W. = 80 kDa) and light chain (M.W. = 43 kDa) that plays a major key role as an activator to immune system. Upon binding with endotoxins, an autocatalytic activity triggers with the cleavage of Phe-Ile bond resulting in an activated factor C that interacts with factor B converting it into a clotting enzyme. Clotting enzyme cleaves coagulogen at two terminal of peptide C at the Arg-Lys and Arg-Gly forming insoluble coagulin gel. (c) The proteolytic activity feature of the activated clotting enzyme in horseshoe crab's blood is used on synthetic chromogenic *i.e.* Gly-Arg-p-nitroaniline substrates instead of coagulogen to detect endotoxin as it separates *p*-Nitroaniline (*p*-NA). Upon addition of a chromogenic substrate, Ac-Ile-Glu-Ala-Arg-pNA, the activated protease, clotting enzyme catalyzes the release of *p*-nitroaniline (*p*NA), resulting in a yellow color that can be quantitated by measuring the absorbance at 405 nm (or absorbance at 340 nm) and extrapolating to a standard curve for correlating endotoxin concentrations.

(c)

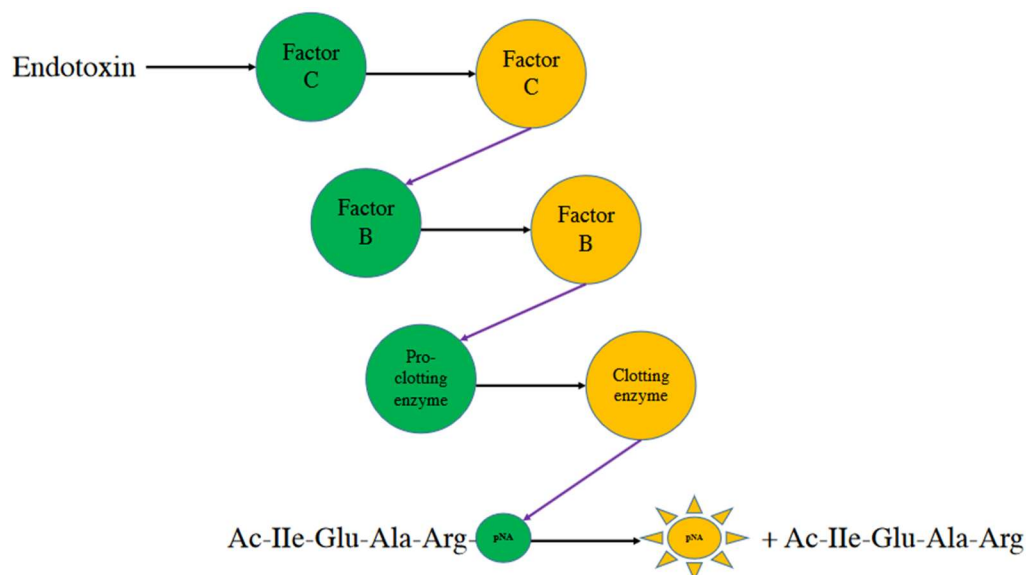


Figure 1.3. Endotoxin detection mechanism using LAL assay. (a) Endotoxin induced defense mechanisms in circulating hemolymphs of horseshoe crabs. The LAL assay is designed based on the immunogenic reactions developed in the blood of horseshoe crabs.

Upon exposure to endotoxins, the electron dense large granules (L-granule) and less electron dense small granular (S-granule) amoebocytes become activated by zymogen factor C. (b) Coagulation cascade in horseshoe crab blood. Endotoxin activates plasma membrane-bound factor C. Factor C is a single chain glycoprotein (M.W. = 123 kDa) comprising of a heavy chain (M.W. = 80 kDa) and light chain (M.W. = 43 kDa) that plays a major key role as an activator to immune system. Upon binding with endotoxins, an autocatalytic activity triggers with the cleavage of Phe-Ile bond resulting in an activated factor C that interacts with factor B converting it into a clotting enzyme.

Clotting enzyme cleaves coagulogen at two terminal of peptide C at the Arg-Lys and Arg-Gly forming insoluble coagulin gel. (c) The proteolytic activity feature of the activated clotting enzyme in horseshoe crab's blood is used on synthetic chromogenic *i.e.* Gly-Arg-p-nitroaniline substrates instead of coagulogen to detect endotoxin as it separates *p*-Nitroaniline (*p*-NA).

Upon addition of a chromogenic substrate, Ac-Ile-Glu-Ala-Arg-pNA, the activated protease, clotting enzyme catalyzes the release of *p*-nitroaniline (*p*NA), resulting in a yellow color that can be quantitated by measuring the absorbance at 405 nm (or absorbance at 340 nm) and extrapolating to a standard curve for correlating endotoxin concentrations (cont.).

1.2.3. Recombinant Factor C (rFC) Assay. rFC is an endotoxin sensitive synthetic protein that is cloned from factor C DNA to use as an alternative *in vitro* LAL test^{47,73-77}. In the rFC test, the binding of endotoxin activates the synthetic rFC molecule, which then cleaves a fluorescein substrate (amino-methylcoumarin), resulting in the generation of a fluorogenic compound. The fluorescence is measured twice, first at time zero and then after the endotoxin has been introduced using excitation/emission of 380/440 nm. The difference in fluorescence is proportional to endotoxin concentrations in the sample and is used to calculate a final endotoxin result. rFC is specific to endotoxin detection eliminating the dependence on nonspecific glycan binding like that in an LAL assay avoiding false positive results.⁷⁸ The enzymatic sensitivity range to endotoxin is 0.05-500 EU/ml.⁷³ A comparison of rFC with various LAL assays is summarized in Table 1.1. Despite its lower limit of detection under laboratory conditions, the rFC assay is prone to contamination in field environments that severely compromise its analytical utility.⁷⁹

Table 1.1. A comparison chart eliciting three LAL test methods: the gel clot, turbidimetric and chromogenic method and rFC assay as available in commercial endotoxin detection kits.

Kit	Model No.	Principle	Detection time (min)	Limit of Detection (EU/ml)
Lonza BioScience	QCL-1000	Endpoint chromogenic assay	16	0.1
	Pyrogent 5000	Kinetic turbidimetric assay	60	0.01
	Kinetci-QCL	Kinetic chromogenic assay	60	0.005
	PyroGene (rFC assay)	Endpoint fluorogenic assay	60	0.01
Thermo Scientific	Pierce LAL assay	Endpoint chromogenic assay	30	0.1
GenScript	LAL assay	Endpoint chromogenic assay	45	0.005
Associates of Cape Cod	Pyrosate kit	Gel clot assay	30	0.25

1.2.4. Bovine Whole Blood Assay (bWBA). The test works by taking the whole blood from the animal and introducing it to a solution containing the pharmaceutical being tested ⁸⁰. In response to endotoxin, the white blood cells in the blood produce the cytokine Prostaglandin E₂ (PGE₂) in an inflammatory response, similar to that of humans ⁸¹. The production of this cytokine is directly proportional to an increase in endotoxin concentration. According to several studies, the test is able to accurately detect endotoxins at concentrations of close to 0.25 EU/ml, whereas the concentration at which humans display symptoms of endotoxin exposure typically occurs around 0.30 EU/ml ⁸¹. This level of accuracy is very attractive for scientists looking to move away from LAL and RPT testing. The test also is easy to perform and takes few preparational steps ²³. The storage of bovine whole blood seems to be a little less problematic than human whole blood after 24 h of storage time at 4 °C, when the PGE₂ release is significant at >0.16 EU/mL ^{81,82}. The test is not without its limitations. The whole blood needed for the tests can only be obtained from very young calves which makes it difficult to amass in vast quantities ⁸³. Furthermore, due to cultural and religious practices, certain countries will not permit the collection or use of bovine blood. While its accuracy and ease of use is admirable, it still requires animal testing, and with the advancement of technology, this test may be replaced by other techniques.

1.2.5. Monocyte Activation Test (MAT). The Monocyte Activation Test, or MAT, has been in development since 1995 ⁸⁴. The commercially available MAT kit involves using cryopreserved monocytes in human blood to test for a reaction to endotoxins. The response to endotoxins is determined by measurement of the induced pro-inflammatory cytokine Interleukin – 1 β (IL-1 β) using enzyme-linked immunosorbent

assay (ELISA)^{85,86}. The ELISA is used by attaching a primary antibody to bind with the IL-1 β released by monocytes in the presence of endotoxins, while a secondary antibody is linked with avidin-conjugated horseradish peroxidase (Avidin-HRP) enzyme that metabolizes tetramethylbenzidine (TMB) substrate and develops a blue-green to yellow color product⁸⁷. The absorbance of yellow color density is then measured at 450 nm by spectrometers, similar to a chromogenic LAL test⁴⁹. The test also has the added benefit of testing all pyrogens and inflammatory materials that would prove harmful to human patients^{88,89}. It avoids animal testing and has a detection limit of as little as 10 EU/ml of endotoxin solution, and conveniently, this limit becomes even smaller, and the test becomes more accurate when using cryogenically-preserved human blood. This aids in storage and transportation of the human blood for testing if the blood can be cooled and preserved without sacrificing accuracy^{85,90,91}. The monocytes can be prepared in a variety of ways. Some experiments have used whole human blood, while others use monocytes harvested from leukocyte filters at blood donation centers⁹⁰. This method displays high precision by being able to detect non-endotoxic pyrogens and their effect on possible patients of the tested material. However, as there is often a limited supply of human blood to be used for simply testing, inconsistencies can arise when using large quantities of blood are used^{84,92}. The most important limitation for the MAT is the short half-life (< 2 h) of viable monocytes in human blood *in vitro*. An alternative endotoxin ELISA kit such as the competitive ELISA (cELISA) is available that uses a microtiter well plate pre-coated with an anti-endotoxin primary antibody.⁹³ Endotoxin containing sample or standards are added to the wells along with a fixed quantity of biotinylated detection antibody that competes for limited binding sites on the immobilized anti-

endotoxin antibody. Avidin-HRP conjugate and TMB are used like that in ELISA to generate and measure color changes from blue to yellow. The absorbance reading of coloration at 450 nm is quantitated for endotoxin concentrations present in samples.

1.3. BIOSENSOR TECHNIQUES

In attempts to modernize endotoxin detection methods, scientists have begun to develop techniques designed around more synthetic approaches. They involve more technology as opposed to pre-existing natural pathways. These techniques represent the up and coming detection methods that scientists hope will eventually replace the gold standard of RPT and LAL tests. These techniques can be split into three categories, electrochemical, optical, and mass-based.

1.3.1. Electrochemical. The majority of electrochemical biosensors are based on a principle called Electrochemical Impedance Spectroscopy, or EIS. Performing an EIS requires electrodes be placed within the solution desired to be tested and delivering a sinusoidal alternating current signal through the solution, usually ranging from 2-10 mV. By varying the frequency of these sinusoidal waves, an impedance spectrum can be created⁹⁴. The electrodes are coated in metal, to reduce electric resistance. Proteins that are highly selective to endotoxin components are then bound to these electrodes such that if the endotoxins come in contact with the electrode-protein complex, they bind to the proteins. These proteins are referred to as Endotoxin Neutralizing Proteins, or ENPs^{95,96}. When endotoxins bind to ENPs on the electrodes it increases the resistance of the electrode. This was the case in an experiment run by Yeo *et al.*⁹⁷ who constructed an electrode made of gold and a complex of human recombinant toll-like receptor 4

(rhTLR4) and myeloid differentiation-2 (MD-2) proteins (Figure 1.4). They exposed these electrodes to solutions of varying endotoxin concentrations and created impedance spectrums for each of these concentrations. The maximum current across all potential differences was lower at higher concentrations of endotoxin ⁸⁶. The study also reports that this particular biosensor has high specificity towards endotoxins, in order to prevent false positive results. It then goes on to state that the sensor had a detection limit of 0.0002 EU/ml. This is drastically lower than the standard LAL test limit of 0.03 EU/ml. A major limitation of this system is the single time use of electrodes once endotoxins are bound to TLR4-MD-2 complexes. Metal complexes immobilized upon a gold electrode have been used and were able to detect endotoxins at concentrations as low as 0.001 EU/ml ⁹⁸.

Porous silicon membranes (pSim) based electrochemical biosensors comprise of array of nano-channels which are modified using Polymyxin-B, with strong affinity to endotoxins. It shows the limit of detection of 18 EU/ml. These sensors showed ability to detect endotoxins from various bacterial strains like *E. coli* and *S. typhimurium* and all this is done in a label free manner ⁹⁹. Studies have also reported highly sensitive peptide modified gold electrode based electrochemical biosensors which are used for endotoxin detection with very low limit of detection of 0.04 EU/ml ¹⁰⁰. These methods are faster, more accurate, and in most cases, more cost effective than biological based techniques ¹⁰¹. Two other electrochemical techniques are amperometric and potentiometric methods. Amperometric transducers have been described as the most common of the electrochemical sensors used for endotoxin detection ¹⁰². They work on the relying on the same principle of EIS, wherein the concentration of the analyzed sample has a linear relationship with the current measured. This method is able to use premade, disposable

testing strips, for fast, cost-efficient testing¹⁰³. Potentiometric methods are worth noting because although their detection limits are relatively high, 1-5 EU/mL, they were the first biosensor to be able to detect endotoxins in real time^{94,104}. The methods in which the electrodes are created, as well as the ways in which they are measured and utilized, are more complicated and labor-intensive than the biological methods¹⁰⁵. They require more sophisticated personnel and equipment to be run effectively than RPT or LAL tests¹⁰⁶.

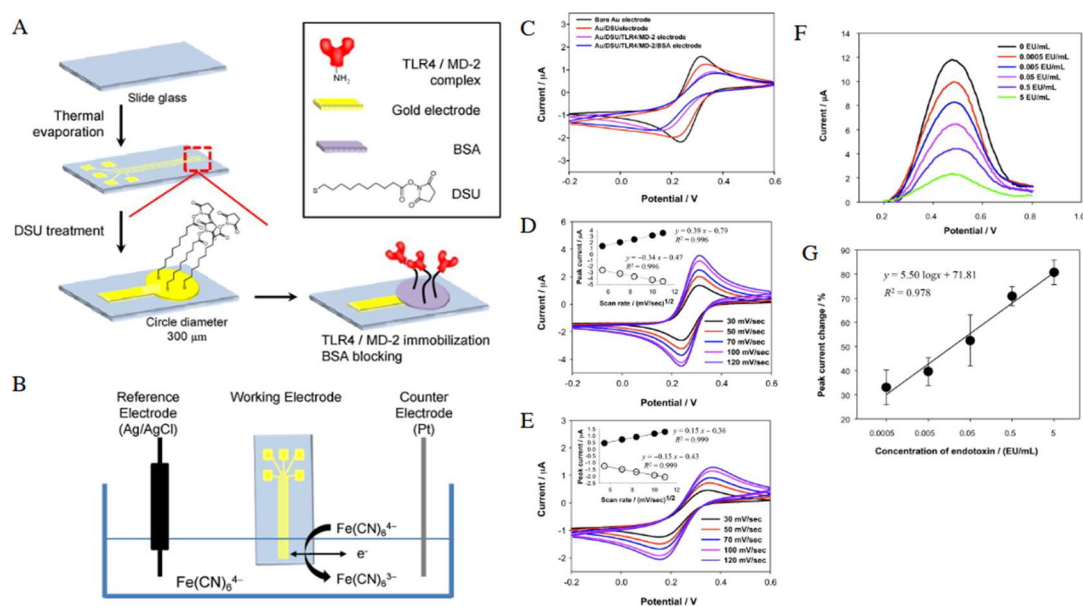


Figure 1.4. A new electrochemical endotoxin sensor. (A) and (B) The design and fabrication of a new electrochemical endotoxin sensor based on a human recombinant toll-like receptor 4 (rhTLR4) and myeloid differentiation-2 (MD-2) complex. The rhTLR4/MD-2 complex, which specifically binds to endotoxin, was immobilized on gold electrodes through a self-assembled monolayer (SAM) technique involving the use of dithiobis (succinimidyl undecanoate) (DSU). (C) – (F) The electrochemical signals generated from interactions between the rhTLR4/MD-2 complex and the endotoxin were characterized by cyclic voltammetry (CV) and differential pulse voltammetry (DPV). (G) A linear relationship between the peak current and endotoxin concentration was obtained in the range of 0.0005 to 5 EU/mL with a correlation coefficient (R^2) of 0.978. The estimated limit of detection (LOD) was fairly low, 0.0002 EU/ml. The rhTLR4/MD-2 based sensors exhibited no current responses to dipalmitoylphosphatidylcholine (DPPC) bearing two lipid chains, which is structurally similar to endotoxin, indicating the high specificity of the sensors to endotoxin. Reproduced with permission from Ref. 78.

1.3.2. Optical Techniques. One such example is that of liquid crystal (LC) based optical sensor for highly sensitive endotoxin detection. LC based optical biosensors are developed using endotoxin specific single-stranded DNA aptamers which are the endotoxin selective probes of the biosensors. The LC based aptamer optical biosensors have linear endotoxin detection range from 0.05 to 1000 EU/ml and a detection limit of 5.5 EU/ml. The biosensors have negligible cross-binding reactivity with the biomolecules thus maximizing their recovery¹⁰⁷. Broadly, these optical techniques can be divided into three distinct categories: luminescence, Surface Plasmon Resonance, and electrochemiluminescence that share the similar characteristic of relying on visual changes.

1.3.3. Fluorescence and Luminescence Techniques. The bioluminescence method is based on the same principle of the LAL assay except the end point material (pNA) of LAL tests is used as the starting material for the mutant firefly luciferase^{108,109}. Luciferin-modified pNA has been designed as the substrate for a mutated version of the North American luciferase (*Photinus pyralis*) that can quickly and precisely identify solutions containing endotoxins by a bioluminescence reaction¹⁰⁹. The reaction generates high luminescence intensity and shows a luminescence 10 times as intense as the standard, wild-type luciferase¹¹⁰. The lowest endotoxin concentration recorded was 0.0001 EU/mL, while the researchers report a detection limit of this mutant-type luciferase bioluminescence technique was 0.0005 EU/ml²³. Another important factor to mention is that this detection limit was reported in 15 minutes. This required time is rapid in comparison to the LAL gel-clot techniques estimated required time of 138 minutes to nearly 1.5 hours¹¹¹. Experiments have been performed using a peptide biosensor and

attached fluorescent probes, fluorescein-maleimide (F5M), and tetramethylrhodamine-5-maleimide (TMR5M)⁸⁵. Recently, a fluorophore BODIPY ((4,4-Difluoro-1,3,5,7,8-Pentamethyl-4-Bora-3a,4a-Diaza-s-Indacene) with excitation and emission wavelengths of 485/20 and 528/20 nm were used to quantify presence and removal of endotoxin from biological solutions (Figure 1.5)¹¹²⁻¹¹⁵. BODIPY dye which is a lipid biomarker, in presence of endotoxin quenches due to endotoxin binding to its surface signaling endotoxin contamination^{112,113,116}. The difference in the fluorescence of BODIPY which indicates the degree of quenching of the dye is plotted against the amount of corresponding endotoxin to generate standard curves. Endotoxin detection studies have been conducted using Alexa Fluor-labeled fluorescent endotoxin with excitation and emission wavelengths of 490 and 525 nm¹¹⁷. In this study, C-18 acyl chain modified Fe₃O₄/Au/Fe₃O₄ nanoflowers were used for simultaneous capture and detection of endotoxins from water samples¹¹⁷. The lowest endotoxin detection limit that was tested using this technique was 10 EU/ml¹¹⁷.

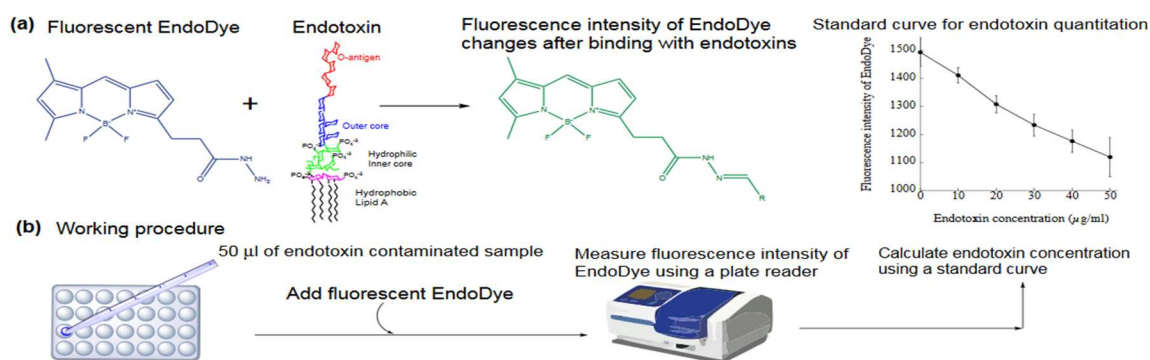


Figure 1.5. Fluorescent assay protocol for endotoxin detection. We have developed a fluorescence-based method that measures the changes in fluorescence intensity and the corresponding endotoxin concentration. The whole process is instantaneous and can detect endotoxin as low as 0.0001 ng/ml in solutions.

1.3.4. Surface Plasmon Resonance (SPR) and Mass-based Techniques. Zhang *et al.* have shown a smartphone biosensor platform using SPR. The disposable sensor chip utilizes the smartphone's built in flash as a light source and a compact diffraction grating and spectra dispersive unit ¹¹⁸, but this technology is still in development. Recent publication regarding antibiotic mediated plasmonic biosensors for endotoxin detection have shown a low limit of detection of 40 EU/ml ¹¹⁹. The plasmonic biosensor is based on a facile U-bent fiber optic probe (UFOP) technology that utilizes octadecyltrichlorosilanes (OTS) on the surface of optical fiber probes to hydrophobically entrap endotoxin from aqueous solutions. The binding of endotoxins has been monitored in real-time by measuring the change in refractive index (RI) in the evanescent layer ¹¹⁹. To add specificity and signal amplification, the bound endotoxins have been further tagged with antimicrobial polymyxin-B conjugated gold nanoparticles (PMB-AuNPs) in a sandwich format. The resulting evanescent wave absorbance-based fiber optic biosensor has excellent sensitivity with the total assay time of 1 h ¹¹⁹.

An example of mass-based techniques is electromagnetic piezoelectric acoustic sensors, or EMPAS that has been touted as being able to measure multiple types of pathogens, not exclusively endotoxins, as well as being able to detect endotoxins in real time within human blood plasma ¹²⁰. EMPAS uses ultra-high frequency acoustic wave sensing based on an ultrathin, oligoethylene glycol-based mixed surface platform coated on piezoelectric quartz discs. The glycol end on the surface of quartz has been functionalized with polymyxin B (PMB), a cyclic peptide antibiotic that shows high affinity for endotoxins and hence, has been used as the biosensor assay for endotoxin detection. Incubation of endotoxin-spiked whole blood with PMB-bead chemistry

resulted in the EMPAS resonant frequency shift (Δf) as a function of endotoxin concentration from 30-60 EU/ml ¹²⁰. Another mass-based method is magnetoelasticity that function by placing sensors directly on to dry testing surfaces, such as medical equipment or food. The sensor filaments, whose oscillation frequencies are monitored, fluctuate within a magnetic field. These sensors are coated in phages designed to bind with the target pathogen, like ENPs ¹²¹. When *Salmonella typhimurium* bind with the surface of sensors, the mass of sensor increases, resulting in a decrease in the sensor's resonant frequency. The resonant frequency of the sensors has been measured wirelessly and compared with their initial resonant frequency. Control sensors without phage do not show any shifts in the resonance frequency and have been used to compensate for environmental effects and nonspecific binding ¹²¹. The resonant frequency change of sample measurement sensors has been reported to be statistically different from that of control sensors down to 5×10^2 colony forming unit/ml, the detection limit for the work. The number of cells bound on the sensor surface have been imaged using scanning electron microscopy (SEM) that has been further verified the measured resonant frequency changes due to cell binding on the sensor surface. The total assay time of the presented methodology has been reported approximately 30 min. While the disadvantages of phage coated magnetoelastic sensor are non-regeneration of the surface, non-specificity and interferences from analytes, it may be advantageous as a disposable sensor due to low cost.

1.4. TECHNIQUES FOR DOWNSTREAM REMOVAL OF ENDOTOXINS

Downstream process for pharmaceutical manufacturing comprises of three steps: (1) initial recovery by extraction or isolation, (2) purification and (3) polishing 1-3. Endotoxin removal presents a unique challenge, which form stable interactions with themselves and possibly with target therapeutics.

1.4.1. Ultrafiltration. A single endotoxin molecule in its monomeric form has a molecular weight 10-30 kDa²² depending on the core polysaccharides and oligosaccharide chain, but endotoxins have the ability to aggregate and form micelles and vesicles with molecular weights above 1000 kDa²⁹ and diameters up to 0.1 μm ²⁰. The endotoxin micelles and vesicles can be separated from water, salts, and small target therapeutic molecules through size exclusion in ultrafiltration. Factors that affect the removal of endotoxins from aqueous solutions include the size distribution of the molecules in solution, the interactions between target molecules and endotoxin, therapeutic protein concentration and the presence of detergents. The effect of protein concentration on the endotoxin removal efficiency using ultrafiltration membranes has been explored^{22,122}. Ultrafiltration membranes with 100 kDa molecular weight cut off (MWCO) has been used to filter endotoxin contaminated protein solutions with concentrations varying between 2-30 mg/ml. The % endotoxin removal in the filtration permeate through the membrane ranges from 28.9% to 99.8%, depending on the level of protein concentration and endotoxin dilution²². The more dilute the protein samples are made, the higher is the rate of endotoxin removal due to the shift in equilibrium from endotoxin aggregates into monomers in dilute solutions and passing endotoxin monomers through the membrane.

Effects of detergent concentrations on the interactions between endotoxin molecules have been studied contributing towards efficient endotoxin removal. Multiple Tween 20 concentrations of 0.0%, 0.5%, 1.0%, and 2.0% have been added to the protein solutions to calculate the respective removal efficiency ²². An increase in the Tween 20 concentration has led to an increase in the passage of endotoxin into the permeate and thus removing endotoxin from proteins ²². These results demonstrate that the presence of a detergents decreases the size distribution of endotoxin aggregates. As the detergent concentration has been increased, the equilibrium has shifted from micelles and vesicles to monomers ^{22,122}. This method is undesirable for ultrafiltration where endotoxin monomers are to be trapped within the membrane and desired protein be allowed to pass as they are less likely to be stopped by the filtration membrane compared to endotoxin aggregates.

Ultrafiltration has been used to separate endotoxin molecules from small target therapeutic drug molecules. For example, ultrafiltration has been utilized to separate endotoxin aggregates from BMS-753493, a small aqueous drug molecule with a molecular weight of 1.57 kDa ¹²³. Two membrane sizes have been used to perform endotoxin decontamination of the drug molecules: 3 kDa and 10 kDa. The product permeates through the membrane while endotoxins are retained on the membrane. Both ultrafiltration membranes are effective in reducing the endotoxin concentration to below 0.03 EU/mg but compared to the MWCO of 3 kDa, the 10 MWCO has higher drug yield of around 95% unlike the 3 kDa membrane which shows around 55% loss of the desired product ¹²³. Thus, ultrafiltration membranes are an effective tool for removing endotoxins from aqueous drug molecules and other therapeutic products ¹²³.

The main limitation associated with the ultrafiltration technique is that in most cases it can be used to remove endotoxins from molecules that are magnitudes smaller than endotoxin aggregates. For this reason, this method is not applicable for most endotoxin separation scenarios. Ultrafiltration is best suited for removing endotoxin from water, salts, or small molecule therapeutics that do not have an affinity for endotoxin.

1.4.2. Extraction. Solvent extraction is used to separate endotoxins from target therapeutics based on their relative solubilities in two immiscible liquids. Endotoxins form partition in the organic phase, while hydrophilic target molecules remain in the aqueous phase. Endotoxins have been effectively removed from the bacteriophages T4, HAP1, and F8 using 1-octanol with endotoxin removal efficiencies varying between 64 - 99.9%.³⁶ Additional processing is required to remove any trace quantities of 1-octanol present in the aqueous phase as the presence of 1-octanol interferes with the LAL test for endotoxin detection³⁶. Even though solvent extraction technique gives high endotoxin removal from various therapeutics solutions, the product yield is significantly low and varies between 30-60% impacting the profits associated with the method where it may not be a practical choice for this application³⁶.

Two-phase extraction using detergent Triton X-114, a non-ionic surfactant¹²⁴, has been explored to remove endotoxins from target therapeutics. Endotoxin was successfully removed from the green fluorescent protein using Triton X-114 and temperature transitions. Triton X-114 is miscible with water at a temperature of 0°C, but a phase separation occurs at temperatures above 23°C¹²⁵. Endotoxins are partitioned in the detergent phase while the target therapeutics are partitioned in the aqueous phase. Endotoxin removal efficiencies using Triton X-114 ranged between 45-99%¹²⁵. In

addition to high endotoxin removal, Triton X-114 results in high product recovery of over 80%¹⁶. Triton X-114 isothermal extraction using sodium dodecyl sulfate (SDS) has also been very effective in removing endotoxins from pDNA with residual endotoxin concentration of around 16 EU/mg. Moreover, using this extraction technique, a pDNA recovery of over 80% was reported. While isothermal extraction was proven effective for plasmid-endotoxin removal, this method is not applicable for the removal of endotoxins from protein solutions because SDS completely denatures proteins causing significant changes to protein conformation¹²⁶. One major disadvantage of temperature transition extraction using Triton X-114 is that the repeated heating and cooling degrades therapeutic products¹²⁶. Extraction processes provide a rapid separation that is easily scalable and can achieve high removal efficiencies, especially with high initial concentrations^{36,125,127}. However, final endotoxin concentrations in the aqueous phase for both solvent extraction and Triton X-114 extraction remained above desired specifications, meaning additional processing is required.

1.4.3. Ion Exchange Chromatography. Anion exchange chromatography can be used to separate negatively charged endotoxin molecules from positively charged molecules, such as basic proteins. Proteins exhibit different charges at different pHs. A protein exhibits a neutral charge if the pH is equal to its isoelectric point (pI), a negative charge if the pH is > its pI, and a positive charge if the pH is < its pI¹²⁸. The pI of an endotoxin molecule is ~2^{16,20,129}, meaning endotoxins are negatively charged under conditions typically encountered during chromatography. At pH < 2, the target protein exhibits a net positive charge and is repelled by a positive stationary phase while the negatively charged endotoxins interact with the stationary phase and leaves the column at

a lower velocity^{130,131}. Anion exchange chromatography is not ideal for removing endotoxins from negatively charged target molecules, such as pDNA or acidic proteins^{132,133}.

If significant ionic interactions are present between target proteins and endotoxins or between the protein and the resin, a decrease in protein yield or an insufficient separation may be observed. If the protein and the endotoxin have a strong interaction, endotoxins leave the column bound to the target protein. If there is a strong attractive interaction between the target protein and the resin, the protein yield is low¹²⁹.

To lessen undesirable interactions, the pH of the protein solution is adjusted. The effects of resin volume and contact time in addition to pH and conductivity on the efficiencies of endotoxin removal have been explored for therapeutic products like, antigens NY-ESO-1, Melan-A, and SSX-2¹²⁹. The pIs of these antigens were 9.1, 8.7, and 6.2, respectively. NY-ESO-1 and Melan-A are both hydrophobic molecules while SSX-2 is hydrophilic¹²⁹. All tests were run using equilibrated Q XL resin. An increase in resin volume and endotoxin-resin contact time had a positive effect on endotoxin removal and the concentration of endotoxins in the permeate consistently decreased with increase in above variables. Low endotoxin concentration of ~ 0.4 EU/ μ g was obtained in the permeate and a protein recovery of > 80 % was obtained consistently at almost all resin volumes¹²⁹. While positively charged proteins are less likely to interact with the resin and remain in the column, they may also demonstrate an undesirable attraction to endotoxins. To minimize protein- endotoxin interactions, the pH chosen should be high enough to avoid giving the protein a strong positive charge. Effect of different pHs on the removal of endotoxin from protein Melan-A, a hydrophobic protein with a pI of 8.7 has been

studied. Melan-A exhibited a strong ionic interaction with endotoxins below its pI, causing endotoxins to leave the column with the target protein. To remedy this, the pH was increased to weaken such interactions¹²⁹. The pH tested were 7.9, 8.4, 8.9, and 9.2, which corresponded to endotoxin concentrations in the permeate of 1.4, 1.8, 0.6, and 0.5 EU/ μg ¹²⁹. As the pH was increased above the protein's pI, the endotoxin concentration decreased dramatically and with no significant impact on the protein yield¹²⁹.

The success of ion-exchange chromatography is highly dependent on the target molecule, but in general ion-exchange chromatography can achieve an endotoxin reduction of five orders of magnitude for concentrated solutions (>1,000 EU/ml) or three to four orders of magnitude from dilute endotoxin solutions (<100 EU/ml)²⁰. The resin involved with an ion exchanger can be regenerated by washing with detergents to separate endotoxins from the resin surface and additional washing steps¹³⁴.

1.4.4. Affinity Chromatography. Affinity chromatography is used to separate endotoxins from target molecules using highly specific interactions between endotoxins and a ligand bound to a stationary phase¹³⁵. Because of the specificity of the ligand, there is little to no product loss during separation³⁵. The target therapeutic molecule will elute with a greater velocity than endotoxin molecules due to specificity. The ligand chosen should have a strong interaction with endotoxins and a weak interaction with the target therapeutic molecule at separation conditions. Affinity chromatography is applicable to a wide range of target molecules, including proteins and pDNA^{136,137}.

It is important to note that the exact structure of endotoxins varies between bacteria strains based on the core polysaccharides and the long chain polysaccharide. For this reason, ligands are typically designed to interact²⁰ with the most conserved section

^{23,25,29,138} of the endotoxin molecule, Lipid A , through hydrophobic ¹²⁹ and electrostatic interactions ²⁰. Common ligands used in affinity chromatography include PMB, histidine, dimethylamine ligands, deoxycholic acid and polycationic ligands ^{17,139}. Hydrophobic polymers in the form of nanoparticles have been explored for removing endotoxins from water and protein solutions.^{112,113}

One of the most commonly used ligands is PMB, a cyclic lipopeptide with a high affinity for endotoxin (Figure 1.6). As a ligand, PMB induces the dissociation of endotoxin aggregates ¹⁴⁰ and binds to the Lipid A section of endotoxins ¹⁴¹ through hydrophobic interactions ¹⁴². PMB's affinity to endotoxin can be attributed to the terminal amidine groups that are spaced such that interactions between amidine groups and the two phosphate groups on Lipid A can occur simultaneously ¹⁴³. In addition to being used as a ligand, PMB is an antibiotic used to treat gram-negative bacterial infections. Despite PMB's high affinity for endotoxin, columns utilizing PMB may experience a higher than average product loss ²⁰. This is because there are positive charges on the amino acid groups on PMB that may attract negatively charged target molecules. Additionally, PMB is both neurotoxic and nephrotoxic, which may cause a problem if the ligand is released from the column ²⁵. Work has been going on to develop peptides with similar compositions to PMB but with a decreased toxicity. These peptide analogs displayed a strong affinity to endotoxin as well as a decreased lethality when introduced intravenously into mice ¹⁴⁴.

The nitrogenous bases adenine, cytosine, histidine and histamine all display an affinity for endotoxin. Of these, histamine and histidine are equally as effective as

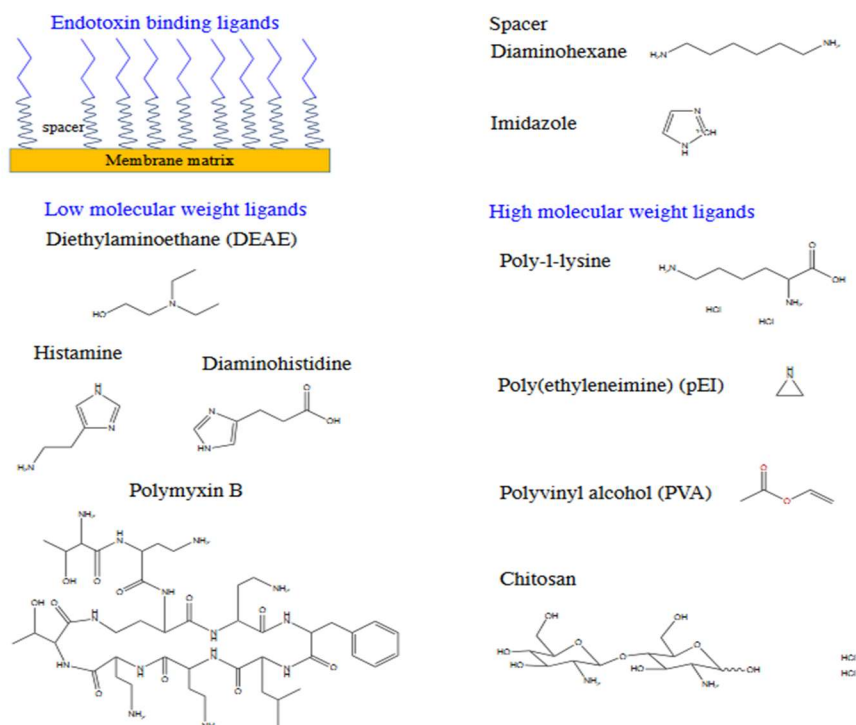


Figure 1.6. Chemical structures of various endotoxin binding ligands. Since endotoxins are negatively charged, anion exchange ligands are employed, e.g., diethylaminoethane (DEAE), polymyxin B, histamine, histidine, poly-L-lysine, polyethyleneimine (pEI) and chitosan.

polymyxin B and have been successful with separating endotoxin molecules from albumin, insulin, lysozyme, myoglobin, and others. Although histamine and histidine are considered equally effective, histamine is biologically active and may create immunogenic response in the body²⁰. On the other hand, histidine may work well for small sample volumes with a limited reduction of endotoxins, however, at the expense of large sample volumes, product losses cause low yield^{20,138}. Deoxycholic acid (DOC) is another ligand option that may offer a higher product recovery due to a low charge density that reduces ionic interactions with negatively charged proteins²⁰. While recombinant protein purification is primarily based on the use of tags, tag-free

alternatives have emerged as a convenient and popular approach because of less processing time. Such an example is the purification of PspA4Pro protein with one step by washing contaminant proteins using a cationic detergent, cetyltrimethylammonium bromide (CTAB) and centrifugation to remove endotoxins in aggregates, or, cryo-precipitation of contaminants in the precipitate and recovery of PspA4Pro protein in the supernatant ¹⁴⁵. Comparison of CTAB wash and cryo-precipitation with ion-exchange chromatography shows higher protein recovery (~92%) and intermediate recovery (47.8%) in CTAB and cryo-precipitation, respectively than 35-62% using chromatography ¹⁴⁵. The % endotoxin removal were 96.5%, 99.9% and 99.5-99.9% for CTAB, cryo-precipitation and chromatography, respectively ¹⁴⁵. This new strategy enables does not require the use of affinity tags, thus reducing the overall costs of protein purification.

Cost effective ligand and its binding capacity are key factors for endotoxin removal in a purification process. Poly- ϵ -lysine and polymyxin-B are two commonly used ligands in protein purification. Table 1.2 provides a reference list of these ligands with regards to endotoxin binding capacity, protein recovery, regenerability and cost that are commercially available for use in several different product names ^{112,113,115,146-151}. Additionally, the contact time required between the solution and ligand will affect the cost. A process with a high contact time will required a larger column and therefore a greater initial investment.

The pore size of the resin should also be considered. A small pore size will increase the retention of endotoxin in the column by size exclusion, while larger pore sizes will reduce the ionic interactions with anionic proteins ²⁰. Studies have been

Table 1.2. Commonly used affinity-based ligands for endotoxin removal in chromatography.

Ligand used	Product Name (Supplier)	Maximum Endotoxin Binding capacity (EU/ml)	% Protein recovery	Regenerability	Cost (\$)	Reference
Poly-ε-lysine immobilized on agarose beads	ToxOut endotoxin removal resins (BioVision)	1.5×10^9 (eliminates >99% of endotoxins)	> 97 %	5 times	\$ 195 (5 ml)	[145]
Poly-ε-lysine immobilized on porous cellulose beads	Pierce High capacity endotoxin removal resins (Thermo Fisher)	2.0×10^6 (eliminates >99% of endotoxins)	> 85 %	10 times	\$ 341 (10 ml slurry)	[146]
Polymyxin B immobilized resins	Toxin Eraser endotoxin removal resins (GenScript)	2.0×10^6 (eliminates >99% of endotoxins)	> 90 %	5 times	\$ 60 (1 ml)	[147]
Polymyxin B immobilized on agarose beads	PurKin endotoxin removal resins (Abbkine)	2.0×10^6 (eliminates >99% of endotoxins)	> 85 %	5 times	\$ 208 (10 ml)	[148]
(information not available)	Proteus endotoxin removal resin (BioRad)	1.0×10^6 (eliminates >95% of endotoxins)	> 90 %	2 times	\$ 500	[149]
(information not available)	Endo Trap Red (Lionex)	$> 2.0 \times 10^6$ (eliminates >99.9% of endotoxins)	> 95 %	3 times	\$ 170 (1ml column)	[150]
(information not available)	Endo Trap HD (Lionex)	$> 5.0 \times 10^6$ (eliminates >99.9% of endotoxins)	> 95 %	10 times	\$ 345 (1ml column)	[150]
No ligand (PCL nanoparticles alone)	PolyBall (not commercially available)	1.5×10^6 (eliminates >98% of endotoxins)	> 90 %	3 times	\$ 2.4 per 1 g	[112, 113, 115]

conducted to study the effect of pH and ionic strength solutions on endotoxin removal efficiencies from hemoglobin samples using an Acticlean Etox affinity column. Endotoxins have been reported to form stable complexes with hemoglobin, thus complicating separation^{43,152}. The effect of ionic strength on endotoxin removal efficiency and hemoglobin recovery have been studied using two different salt solutions (NaCl and CaCl₂). The endotoxin removal efficiency displayed a decreasing trend as the ionic strength was increased. However, the endotoxin removal efficiency for CaCl₂ solutions displayed a more drastic initial decrease than that for NaCl solutions. These results indicate that not only do ionic interactions play a role in affinity chromatography, but the types of cations matter as well⁴³.

Unlike the endotoxin removal efficiency, the ionic strength and cation type had a limited effect on the product recovery from hemoglobin-endotoxin solutions. For all endotoxin contaminated hemoglobin solutions tested, the recovery of hemoglobin showed an increasing trend as the ionic strength was increased. Beyond, the ionic strength of 0.10 M, the hemoglobin recoveries remained relatively constant or displayed a gradual decrease with values over 95%. Though there existed interactions between endotoxins and hemoglobin that hindered separation but all the endotoxin contaminated hemoglobin solutions prepared with either NaCl or CaCl₂ had hemoglobin recoveries above 99% for ionic strengths of 0.1 M, indicating that there is both an attraction between hemoglobin and the affinity resin and between hemoglobin and endotoxin which are weakened at an ionic strength of 0.1 M⁴³.

The effect of pH on endotoxin removal efficiency and hemoglobin recovery was tested using different buffer solutions. The endotoxin removal efficiency of resins was

governed by the pI. There was a continuous and gradual decrease in endotoxin removal efficiency as the pH was increased from 4.5 to 8, and then the removal efficiency plummeted when the pH was increased from 8 to 9 because the pI of the affinity resin was 8. As the pH was increased from 4.5 to 8, the resin became less positively charged and was therefore less effective at attracting negatively charged endotoxins through electrostatic interactions but other affinity mechanisms were still present. As the pH was increased beyond 8, the resin moved from having a neutral charge to a negative charge that repelled endotoxins and overpowered some of the attractive affinity interactions. On the other hand, the pH or pI had a minimal effect on hemoglobin recovery; the recovery of hemoglobin from endotoxin solutions was above 97% for all pHs tested^{43,143}.

Commercial resins employing hydrophobic and/or cationic ligands to remove endotoxin from proteins and biological solutions use porous nano and/or microparticles and have shown great promise in protein purification, but the type of ligand immobilized or incorporated within the matrix still governs its intravenous application. Many of these resins have shown reasonable endotoxin binding efficiency from therapeutic proteins and biological solutions but suffer from major shortcomings like low recombinant protein recovery and difficulty in intravenous application due to nephrotoxicity and neurotoxicity associated with the endotoxin binding ligands. Toxicity related shortcoming can surely be addressed by using biocompatible endotoxin selective polymers which are non-toxic. Another major concern associated with most of the porous resins used for endotoxin removal is that they come in packed bed form which suffer from major drawbacks like high pressure drop (due to combined effect of bed consolidation and column blinding) and poor mass transfer (as intraparticle diffusion is responsible for transport of solute to

the binding sites), thus making their application expensive and adding significant cost to downstream purification.

The toxicity, pressure drop and mass transfer related shortcomings were addressed by using biocompatible, rigid and non-porous particles where adsorption takes place on the surface. One such study focused on using biocompatible and environment friendly polymer, poly- ϵ -caprolactone (PCL) nanoparticles ~ 800 nm to remove endotoxins from water and protein solutions ^{112,113}. The PCL nanoparticles (PolyBalls) were non-porous in nature and thus the endotoxin binding took place on the surface of the particles (Figure 1.7 (a)). PolyBalls showed high endotoxin removal efficiency of $>99\%$ from phosphate buffer saline (PBS) solution. These particles were also effective in removing endotoxin from protein solution prepared in water with more than 90% removal efficiency ¹¹². The removal efficiency was $>99\%$ when protein solutions were prepared in phosphate buffer saline (PBS) ¹¹². The research also reported high endotoxin binding capacity of $\sim 1.5 \times 10^6$ endotoxin unit (EU) per mg of particles ¹¹². In addition to high endotoxin removal the particles offered high protein recovery in excess of 90% thus maximizing therapeutic product recovery. High endotoxin removal in presence of PBS was attributed to the creation of shielding effect in presence of lyotropic sodium chloride salt. Considering larger-scale industry applications, combinatorial techniques were applied to construct PolyBall containing flexible and multifunctional biofilters (Figures 1.7 and 1.8). Contaminated samples were allowed to flow from one side of the filter to the other. The kinetics of endotoxin removal efficiency were determined as a function of concentration that also removed $>99\%$ endotoxins from water.

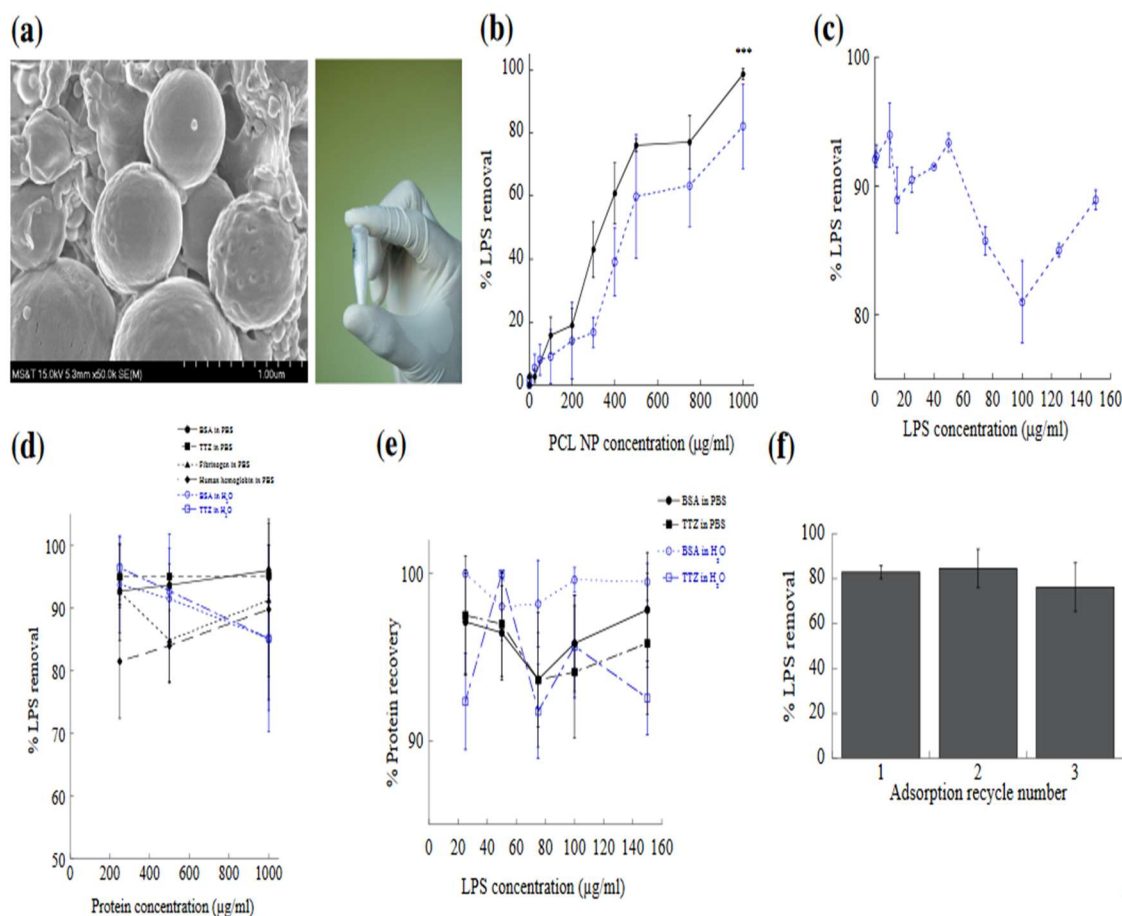


Figure 1.7. PolyBall nanoparticles based effective endotoxin removal. (a) PolyBall nanoparticles are synthesized using the solvent diffusion method. (b) PolyBalls can be lyophilized in white powder form and stored at room temperature ($\sim 22^\circ\text{C}$). (c) PolyBalls are effective in removing $>99\%$ endotoxins ($> 2 \times 10^6$ EU/ml) from water (dotted line) and PBS (pH 7.4) (solid line). Change in LPS concentrations does not compromise PolyBall's endotoxin removal efficiency. (d) PolyBalls efficiently remove endotoxins from a variety of protein solutions at different concentrations. (e) Removal of endotoxins does not affect protein recovery ($>95\%$ recovery) indicating minimal product loss and PolyBall's specificity towards endotoxins even in endotoxin mixed protein solutions. (f) PolyBalls can be regenerated to remove endotoxins further. Figures reproduced with permission from Ref. 97 (Razdan et. al.).

One major advantage of the biocompatible PolyBalls and multifunctional biofilters is that they can be reused for endotoxin binding quite effectively without a major loss in binding efficiency. PolyBalls can be regenerated by breaking endotoxin-

nanoparticle complexes which makes the endotoxin removal process more efficient and scalable.

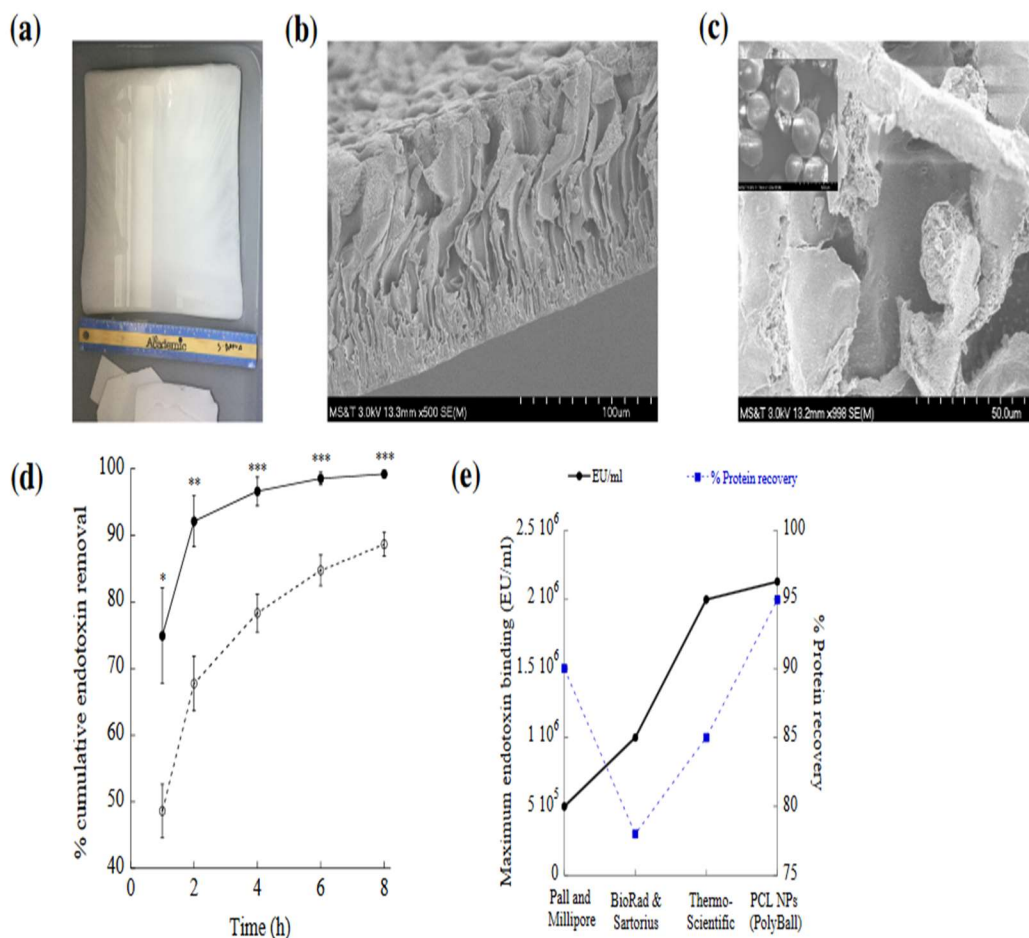


Figure 1.8. PolyBall nanoparticles incorporated cellulose acetate (CA) membrane for effective endotoxin removal. (a) PolyBall nanoparticles are embedded in a cellulose acetate (CA) biofilter. (b) Cross-sectional view of a CA filter without any nanoparticles (negative control) using SEM. (c) SEM image of a biofilter with PCL nanoparticles impregnated in it. (d) Our biofilter removes >99% endotoxins (solid line) while filter without PCL nanoparticles (negative control) is not as effective as the biofilter in removing endotoxins indicating the role of PCL nanoparticles in binding and removing endotoxins from solutions. (e) Comparison of the endotoxin removal efficiency (solid line) and protein recovery (dotted line) between our filter and other commercial endotoxin removal filters. Our filter outperforms others while removing >99% endotoxins and maintaining >95% protein recovery. Figure reproduced with permission from Ref. 97 (Razdan et. al.).

Figure 1.8 (e) and Table 3 showcase a comparison of different endotoxin removal products in terms of binding capacity, protein recovery and cost. Although, non-porous particles solve the mass transfer related limitation but the problem of high pressure drop during purification operation still persists. Due to the specificity of the ligand, affinity interactions offer a low product loss with a wide range of applications. Both mixed-mode chromatography and membrane adsorption use similar mechanisms and experience benefits.

Table 1.3. Comparison of endotoxin removal products, their adsorption capacity, costs and regenerability.

Product Name	Maximum Binding (EU/ml)	Endotoxin capacity	Cost (\$)	Reusability
Pall Acrodisc Unit with Mustang E membrane	5.0×10^5		\$ 9.2 per 1 cm^2 membrane area	Yes
Millipore charged Durapore membrane filters	$>5.0 \times 10^5$		\$ 2.7 per 1 cm^2 membrane area	Yes
BioRad Proteus Endotoxin Removal Kits (Membrane based)	$5.0 \times 10^5 - 10^6$		\$ 12.4 per 1 cm^2 membrane area	Yes
Sartobind membrane adsorbers (Sartorius)	1.0×10^6		NA	Yes
Thermo scientific Pierce High capacity endotoxin removal resins	2×10^6		\$ 20.2 per ml of resin slurry	Yes
PCL nanoparticles	1.45×10^6		\$2.4 per 1 g	Yes
PCL nanoparticles incorporated membrane	2.8×10^6		\$ 0.05 per 1 cm^2 membrane area	Not tested yet

1.4.5. Mixed-Mode Chromatography. Mixed-mode chromatography is a growing separation technique in the biopharmaceutical industry^{45,153,154}. While traditional chromatographic methods rely on a single dominant interaction between the ligand and the targeted molecule, mixed-mode chromatography (MMC) utilizes multiple interaction modes for an increased separation^{45,154,155}. When compared to traditional chromatographic methods, MMC offers an increased retention and selectivity of the targeted compound^{156,157}, especially for polar charged molecules^{153,154}. Many ligands used in affinity chromatography, such as histamine and histidine can be considered mixed-mode ligands due to their beneficial secondary interactions^{133,157-159}.

1.4.6. Membrane Adsorption. Membrane adsorption exploits the same mechanisms used in affinity and ion-exchange chromatography, but offers a reduced processing time and initial investment. Similar to affinity chromatography, a product yield near 100% can be achieved^{35,160}. In membrane adsorption, the same ligands used in affinity chromatography or resins used in ion-exchange chromatography are bound to a support medium. The use of a membrane greatly improves flow rates and nearly eliminates diffusion limitations. Membranes can be made of nylon, PVA, PEVA, PVDF, cellulose acetate and cellulose^{25,112,160}. The membrane capsules are single-use, meaning there is no need for eluting, cleaning, or regenerating. Benefits of single-use membranes include a decreased chance of product contamination as well as a decreased process time and buffer volume due to the decrease in required cleaning steps³⁸. Membrane adsorption requires a low initial investment when compared to traditional chromatographic methods, but membranes must be continually purchased, which will affect manufacturing costs³⁸.

In the past, membrane adsorbers have not been widely adopted because it had a lower binding capacity than that of traditional chromatography methods. Endotoxin removal efficiencies of histidine immobilized on a nylon membrane for different endotoxin concentrations have been carried out. The ligand density for the membrane adsorbers studied was 7.38 mg/g. As the initial endotoxin concentration was increased, the removal efficiency was greatly decreased. This demonstrates the limited binding capacity using membrane adsorbers. Even at the lowest endotoxin concentration of 387 EU/ml, the removal efficiency was only 65%²⁵. These results are consistent with those from previous studies that saw endotoxin removal efficiencies of approximately 70% with an initial endotoxin concentration of 6,000 EU/mL¹⁶¹. Recently, membrane adsorbers with high efficiency endotoxin removal and binding have been synthesized. One such example of membrane adsorbers is that of amphiphilic carbonaceous particles (ACPs) incorporated in the polyvinylidene fluoride (PVDF) matrix. The adsorbers have been successful at removing endotoxins from BSA protein solutions at >99.8% efficiency with >90 % protein recovery.¹⁶⁰ Another study with PCL nanoparticle incorporated in the cellulose acetate membranes have been able to effectively remove endotoxins from water. The endotoxin binding capacity offered by the membrane adsorber was $\sim 2.7 \times 10^6$ EU per mg particle compared to endotoxin binding capacity of $\sim 1.4 \times 10^6$ EU per mg particle offered by PCL nanoparticles in suspension¹¹².

1.5. DISCUSSION

The biopharmaceuticals industry has experienced a rapid and consistent growth over the past few years¹⁶²⁻¹⁶⁵. It is predicted that half of all drugs under development will

be biopharmaceuticals within the next 5-10 years³. Developing endotoxin removal methods that are both effective and cost efficient is an ongoing challenge⁴⁵ due to the high purity required and the potential interactions present between endotoxin and target molecules. Affinity and mixed-mode chromatography are the most promising methods for a widely applicable removal method due to the highly selective interactions between endotoxins and the chosen ligand. Additional research is still required to further develop additional methods for removal and ligands that demonstrate a high affinity to endotoxins with a low toxicity and cost. There is also ongoing research to develop endotoxin-free *E. coli* strains that would eliminate the need for endotoxin removal and decrease downstream processing costs^{10,166,167}. Another development is the use of alternative expression systems other than *E. coli* such as mammalian cell lines (*e.g.*, Chinese hamster ovary and human embryonic kidney 293) or engineered yeasts¹⁶⁸. However, endotoxin contamination may originate from other sources such as additives, buffers, cell culture medium, reagents, serum, supplements and water¹⁶⁹. Therefore, biomanufacturing processes focus on developing innovative and effective technologies for in-line endotoxin detection sensors and removal of endotoxins and other contaminants from process solutions.

Biological techniques led the way, starting with the RPT, a crude, yet effective method of testing medicines before injecting them into humans. This was a good start, but with a detection limit of 0.5 EU/ml, and taking over two hours to perform, as well as requiring live rabbits for test subjects, it was quickly outclassed by other methods. Following close behind RPT, was LAL assay testing. The LAL assay became the industry standard in medicine and equipment testing¹⁷⁰. A number of parental

pharmaceutical products such as Ampicillin, Cytarabine, Diclofenac, Dexamethasone, Heparin, Insulin, Gentamicin, Glucose, Saline solution, Vaccine, Vitamin, plasmid DNA, proteins *etc.* are routinely screened for endotoxin detection using LAL tests ^{171,172}. It still falls short of being fast enough to keep up with the modern world of testing needs, not to mention the need to move away from using horseshoe crab blood in order to protect their dwindling population. bWBA and MAT are similar to LAL in that they fall short on keeping up with the needs of the modern world. While they present attractive qualities, MAT being able to use recycled monocytes from blood banks and bWBA requiring very little preparation, they still require collection and storage of blood from living beings. This would create difficulties in collecting proper amounts of blood stores to handle testing requirements. These traditional endotoxin detection assays also suffer from masking of endotoxins by the constituents present in drug formulations when spiked with endotoxins (LER phenomena) ⁶²⁻⁶⁴. This poses potential risks of underestimated endotoxin contamination in pharmaceutical products. Electrochemical techniques offer nearly endless combinations of sensor and protein-complexes, able to be designed specifically for a testing solution that could prove difficult for other tests. Optical detection methods offer incredibly high precision testing, with results ready in a matter of seconds, provided the equipment can be afforded and operated correctly. Finally, with the rise of mass-based resonance detection, the future of detection methods relies on more accurate, real-time detection, with increasingly cheap and easy to use. A reliable analytical method for endotoxin detection and analysis will also serve as a useful tool in the monitoring of drinking water purification processes and water reclamation plants.

There is no single purification method that fits all separation scenarios¹⁷³. The method chosen will depend greatly on the properties of the target molecule¹³⁹.

Ultrafiltration is well suited for removing endotoxins from water, salts, or small molecule therapeutics, but it is not applicable to most separation scenarios. Extraction provides a high endotoxin removal efficiency for highly contaminated samples, but can possibly lead to an undesirable level of product loss. Ion Exchange chromatography provides adequate separation with acceptable product loss for molecules with a weak positive charge. Anion exchange chromatography is the most commonly used method for endotoxin removal. Endotoxin has been removed from plasmid DNA influenza vaccine solutions using ion-exchange chromatography with 97% purity and 47-88% yield^{174,175}. Due to the specificity of the ligands, affinity chromatography and mixed-mode chromatography offer an adequate separation with high product recovery for a wide range of therapeutic monoclonal antibodies. Membrane adsorption offers a reduced processing time and initial cost with a high product recovery, but has a low binding capacity that limits removal efficiencies. While there is no single method that is applicable to all scenarios, ion-exchange, affinity, and mixed-mode chromatography all offer consistently high removal efficiencies and product recoveries under appropriate operating conditions. Even so, additional research is needed to develop more widely applicable and cost-effective methods that reduce product loss while meeting all governing regulations for endotoxin concentrations in biopharmaceutical products.

1.6. CONCLUSION

There is an increased demand for techniques capable of producing quality products at a decreased cost. This is especially true for biopharmaceuticals produced using gram-negative bacteria, where endotoxin contamination is a concern. Animal-based endotoxin detection techniques will become obsolete in favor of electronic biosensors or fluorescence-based techniques. Developing endotoxin removal methods that are both effective and cost efficient is an ongoing challenge due to the high purity required and the potential interactions present between endotoxins and target molecules. Affinity and mixed-mode chromatography are the most promising methods for a widely applicable removal methods due to the highly selective interactions between endotoxins and the chosen ligand. Additional research is still required to further develop additional methods for removal and ligands that demonstrate a high affinity to endotoxins with a low toxicity and cost. These innovations will allow for an increase in product quality and yield with a decrease in manufacturing cost.

1.7. DISSERTATION OVERVIEW

In paper-1, biocompatible and recyclable polymeric polycaprolactone (PCL) nanoparticles (NPs) ($d_p = 780 \pm 285 \text{ nm}$) were synthesized at a relatively low cost and demonstrated to possess sufficient binding sites for endotoxin adsorption and removal. The PCL NPs removed ~82% and ~90% endotoxins from water and protein solution using only one milligram (mg) of NPs, which was equivalent to $\sim 1.23 \times 10^6$ and $\sim 1.45 \times 10^6$ endotoxin units (EU) per mg of particle. The endotoxin removal efficacy increased to a higher level (~98% and ~99%) when phosphate buffered saline (PBS; 150

mM NaCl) was used in place of water and in proteins. In addition to high endotoxin removal efficiency the protein recovery values were > 95 % for a wide concentration range of protein solutions (20 – 1000 µg/ml). The PCL NPs were also highly effective in different buffers and pHs. To scale up the process even further and increase the throughput, PCL NPs were incorporated into a matrix of cellulose acetate membrane which enhanced the endotoxin adsorption further up to ~100% just by running the endotoxin-containing water through the membrane under gravity.

In paper-2, The goal was to test the validity of the hypothesis that synergistic combination of van der Waals and hydrophobic interactions were responsible for endotoxin binding on polycaprolactone (PCL) nanoparticle's (NPs) surface. This hypothesis was tested by evaluating endotoxin removal efficiency of a material which shows surface hydrophobicity similar to that of PCL NPs. Polystyrene (PS) nanoparticles, ~ 800 nm, with surface properties similar to PCL NPs were used as a control to test the hypothesis. Additionally, this work demonstrated that acidic (pH 2.8) and basic (pH 11.5) conditions do not have a major impact on protein recovery using PCL NPs. Six different types of proteins with molecular weights varying from 14 kDa - 341 kDa and isoelectric points (pI) from 4.5-10.7 showed protein recovery > 92 % under extreme operating pH. Finally, in order to increase the throughput and address the mass transfer limitations, the PCL NPs incorporated cellulose acetate (CA) biofilter were synthesized and applied to different protein solutions with a maximum endotoxin removal efficiency ~ 99 % and protein recovery >92 %.

PAPER**I. POLYBALL: A NEW ADSORBENT FOR THE EFFICIENT REMOVAL OF
ENDOTOXIN FROM BIOPHARMACEUTICALS**

Sidharth Razdan, Jee-Ching Wang and Sutapa Barua

Department of Chemical and Biochemical Engineering, Missouri University of Science
and Technology, Rolla, MO 65409

Tel: 573-341-7551

Email: baruas@mst.edu

ABSTRACT

The presence of endotoxin, also known as lipopolysaccharides (LPS), as a side product appears to be a major drawback for the production of certain biomolecules that are essential for research, pharmaceutical, and industrial applications. In the biotechnology industry, gram-negative bacteria (e.g., *Escherichia coli*) are widely used to produce recombinant products such as proteins, plasmid DNAs and vaccines. These products are contaminated with LPS, which may cause side effects when administered to animals or humans. Purification of LPS often suffers from product loss. For this reason, special attention must be paid when purifying proteins aiming a product as free as possible of LPS with high product recovery. Although there are a number of methods for removing LPS, the question about how LPS removal can be carried out in an efficient and economical way is still one of the most intriguing issues and has no satisfactory solution yet. In this work, polymeric poly- ϵ -caprolactone (PCL) nanoparticles (NPs) ($d_p = 780 \pm$

285 nm) were synthesized at a relatively low cost and demonstrated to possess sufficient binding sites for LPS adsorption and removal with ~100% protein recovery. The PCL NPs removed greater than 90% LPS from protein solutions suspended in water using only one milligram (mg) of NPs, which was equivalent to $\sim 1.5 \times 10^6$ endotoxin units (EU) per mg of particle. The LPS removal efficacy increased to a higher level (~100%) when phosphate buffered saline (PBS containing 137 mM NaCl) was used as a protein suspending medium in place of water, reflecting positive effects of increasing ionic strength on LPS binding interactions and adsorption. The results further showed that the PCL NPs not only achieved 100% LPS removal but also ~100% protein recovery for a wide concentration range from 20 – 1000 $\mu\text{g}/\text{ml}$ of protein solutions. The NPs were highly effective in different buffers and pHs. To scale up the process further, PCL NPs were incorporated into a supporting cellulose membrane which promoted LPS adsorption further up to ~100% just by running the LPS-containing water through the membrane under gravity. Its adsorption capacity was $\sim 2.8 \times 10^6$ EU/mg of PCL NPs, approximately 2 -fold higher than that of NPs alone. This is the first demonstration of endotoxin separation with high protein recovery using polymer NPs and the NP-based portable filters, which provide strong adsorptive interactions for LPS removal from protein solutions. Additional features of these NPs and membranes are biocompatible (environment friendly) recyclable after repeated elution and adsorption with no significant changes in LPS removal efficiencies. The results indicate that PCL NPs are an effective LPS adsorbent in powder and membrane forms, which have great potential to be employed in large-scale applications.

1. INTRODUCTION

In biotechnology industries, gram-negative bacteria are widely used for the production of therapeutic biomolecules including proteins, peptides, and nucleic acids¹⁻⁶. These biomolecules are recovered by cellular rupturing that leads to the release of a large number of bacterial cell-wall components containing endotoxins, also known as lipopolysaccharides (LPS)⁷⁻⁹. When the LPS contaminated products are administered to animals or humans even in small quantities (0.05–0.1ng/ml), a systemic inflammatory reaction can occur, leading to multiple pathophysiological effects, such as septic shock, tissue injury, and lethality^{10,11}. Removing undesirable LPS from solutions is thus an important aim in the pharmaceutical industry and in clinical practice. Conventional treatments such as coagulation and membrane filtration are adequate for removing bacteria cells and debris but not effective for removing dissolved endotoxins to a significant extent. Therefore, it is highly desirable and also the focus of this project to develop a biodegradable and inexpensive means that can tackle both aspects of LPS removal.

A number of approaches have been developed and typically utilized to reduce LPS concentration in pharmaceutical solutions and therapeutic products or in purified water^{8,12-33}. These approaches employ activated carbon^{34,35}, gel filtration chromatography¹²⁻¹⁵, ion exchange or size exclusion chromatography¹⁶⁻²⁰, sucrose gradient centrifugation³⁶⁻³⁸, Triton X-114 phase separation³⁹⁻⁴¹, ultrafiltration^{21,22}, microfiltration^{21,22} and affinity adsorbents²³⁻²⁸, functionalized with L-histidine⁴², poly(ethylene imine) (pEI)²³, poly- ϵ -lysine, poly(γ -methyl L-glutamate), or polymyxin

B^{8,29-33} and chemical means such as ozonation and chlorination^{35,43}. More recently, nanoparticle (NP)-based methods have also been attempted and shown great promise⁴⁴⁻⁴⁶. Polymyxin B capped silver (Ag) NPs have been used to remove LPS from aqueous solutions, up to 97% efficiency, based on the ionic interaction between the cationic peptide on Polymyxin B and the anionic phosphate on Lipid A of LPS⁴⁴. Surface modified iron oxide (Fe₃O₄) gold (Au) core-shell nanoflowers (NFs) have been explored for simultaneous reduction and detection of LPS as alternatives to classical methods of endotoxin sensing⁴⁷. Also, NPs with a polystyrene core and a polyglycidyl methacrylate shell have been synthesized and further modified with amine-based, amino acid based, PEI, tetracaine, or Polymyxin B ligands for LPS removal from water and salt solution⁴⁶. The parent particles modified with amine-based (ethylene diamine, hexamethylene amine, and dodecyl diamine) and PEI ligands showed significant LPS removal efficiency around 90% from both water and salt solution, whereas those modified with tetracaine, amino acid lysine, and amines (histamine and tryptamine) showed a higher LPS removal efficiency from water, also around 90%, than from salt solution⁴⁶. While showing great promise, these approaches at present still have their shares of limitations and disadvantages in terms of cost, efficiency, degradability, side effects, and/or accompanying toxicity brought by the reagents. For examples, the methods utilizing porous functionalized NPs are reasonably effective in reducing the LPS concentration; however, their operations are relatively expensive due to the use of high-pressure equipment that adds significant cost to downstream purification and are contingent on the slow processes of intraparticle diffusion and solute retention on the binding sites⁴⁸⁻⁵⁰. Polymyxin B, a polypeptide antibiotic, can also cause neurotoxicity and nephrotoxicity.

A key step forward with the NP-based approach is to establish a high throughput, low-cost method that is not subject to high pressure-drop limitation, slow solute transport, or accompanying toxicity. To this end, poly- ϵ -caprolactone (PCL) NPs without any modification have been manufactured in the PI's laboratory, which are non-porous solid adsorbent nanoparticles with solute binding sites situated on the particle surface. The NPs were found to be capable of adsorbing and removing LPS from protein solutions at efficiency up to 100%. Their prospects for technological application were further substantiated by the processing feasibility of incorporating PCL NPs into membrane filters and high LPS reduction and removal from biological solutions using cellulose membranes embedded with PCL NPs. In either powder form or in a spread bed of a fat sheet membrane, PCL NPs offer high adsorption capacity per unit mass of the adsorbents. Since PCL and cellulose are both low-cost biocompatible polymers⁵¹⁻⁵³, the use of such PCL NP-embedded membranes represents a novel LPS separation system that requires low capital costs but provides desirable ease of manufacturing, excellent performance, disposability, and biodegradability.

2. MATERIALS AND METHODS

2.1. SYNTHESIS OF PCL NANOPARTICLES

PCL NPs were synthesized by the solvent evaporation method which utilized high-speed homogenization and sonication, followed by solvent evaporation, centrifugation to remove surfactants, and then lyophilization.⁵⁴⁻⁵⁸ A PCL solution at a concentration of 10 mg/ml in ethyl acetate was injected using a syringe pump to a 1%

w/v polyvinyl alcohol (PVA) solution prepared with reverse osmosis (RO) water. The mixture was homogenized by using a homogenizer rotating at 3000 rpm while being placed in a sonication bath. Ethyl acetate was removed by stirring the mixture at 300 rpm for two days. The obtained particles were washed five times using RO water and centrifuged for 30 minutes at 10,000 rcf. The resulting products were freeze-dried, weighed, and stored at 4°C until further use. To test the effects of cationic charges on bare PCL NP, 10 mg of freeze-dried PCL NPs were coated with cationic PLL solution by incubating with 1 ml of 0.1 % (w/v) PLL (Sigma) for 1 h. Post incubation the particle suspension was centrifuged for 30 min at 16,000 rcf and the supernatant was separated to obtain positively charged PLL coated PCL NPs.

2.2. CHARACTERIZATION OF PCL NANOPARTICLES

The morphology of PCL NPs was observed using Hitachi S-4700 scanning electron microscope (SEM) at an accelerating voltage of 15 kV. Samples were sputter coated with Denton Au/Pd coater before inserting it into the microscope. The average PCL particle size was measured by analyzing the SEM images using the ImageJ software (version 1.51w). The average particle size was reported as mean \pm standard deviation (SD) based on the diameters of 200 randomly selected particles. The hydrodynamic size and surface charge of NPs were characterized by dynamic light scattering (DLS) and zeta (ζ) potential measurements, respectively using Malvern NanoZS90 Zetasizer. The hydrodynamic diameter of PCL NPs was measured at 25°C using He-Ne Lasers at 90° scattering angle. The size distribution was obtained based on three independent experiments utilizing 100 successive runs. Zeta potential values were reported based on

three independent experiments with each experiment utilizing 15 successive runs and the results were reported as millivolts (mV) \pm SD.

2.3. ADSORPTION STUDIES

Escherichia coli O111 : B4 LPS (Sigma Aldrich) was used to study the adsorption capacities of PCL NPs in aqueous solutions in batch experiments. Initial experiments were carried out using a constant LPS concentration (150 μ g/ml) treated with different PCL concentrations (0.1, 25, 50, 100, 200, 300, 400, 500, 750 and 1000 μ g/ml) in: (i) RO water (pH \sim 6); (ii) phosphate buffered saline (PBS; 150 mM, pH \sim 7.4); (iii) bovine serum albumin (BSA) solutions in water and PBS; (iv) Trastuzumab (TTZ; Genentech) solutions in water and PBS; (v) Fibrinogen (Alfa Aesar) in PBS and (vi) Human Hemoglobin (MP Biomedicals) in PBS. The composition of PBS is as follows: 137 mM NaCl, 10 mM phosphate, and 2.7 mM KCl at 25°C. The LPS binding capacity to PCL NPs was analyzed using Bodipy (BOD) fluorescence displacement assay technique.^{58,59} BOD is a fluorescent molecule that quenches its fluorescence intensity (F.I.) when it binds to LPS. The F.I. of BOD was used to determine the LPS concentration in solution using a known standard calibration curve (Figure. S1 and Figure. S2). The F.I. measurements were carried out using a microplate reader (BioTek). Excitation and emission wavelengths for BOD were 485/20 and 528/20 nm, respectively. RO water was used as a negative control. The background fluorescence intensities were subtracted to avoid any interferences. The percentage (%) LPS removal by PCL NPs from water and PBS was calculated using equation (1):

$$\%LPS \text{ Removal} = \frac{FI_{BOD.LPS.PCL} - FI_{BOD.LPS}}{FI_{BOD} - FI_{BOD.LPS}} \times 100 \quad (1)$$

where FI_{BOD} , $FI_{BOD.LPS}$, and $FI_{BOD.LPS.PCL}$ represent the F.I. of BOD alone, LPS mixed with BOD, and LPS mixed with BOD and PCL NPs, respectively.

The % LPS removal by PCL NPs from protein solutions was calculated using equation (2):

$$\%LPS \text{ Removal} = \frac{FI_{BOD.Protein.LPS.PCL} - FI_{BOD.Protein.LPS}}{FI_{BOD} - FI_{BOD.Protein.LPS}} \times 100 \quad (2)$$

where FI_{BOD} , $FI_{BOD,Protein,LPS}$, and $FI_{BOD,Protein,LPS.PCL}$ represent the F.I. of BOD alone, LPS mixed with BOD and protein, and LPS mixed with BOD, protein and PCL NPs, respectively.

The adsorption capacity at equilibrium (q_e) was evaluated using the following equation:

$$q_e = \frac{(C_0 - C_e)}{W} \times V \quad (3)$$

where C_0 , C_e , W , and V represent the initial LPS concentration ($\mu\text{g/ml}$), the corresponding LPS concentration at equilibrium ($\mu\text{g/ml}$), the PCL NP's mass amount (mg), and the solution volume (ml), respectively. The isotherm data were fitted into the linear Freundlich model equation (4) to describe the adsorption equilibria:

$$\ln q_e = \ln K + \frac{1}{n} \ln C_e \quad (4)$$

where, q_e , K , n and C_e represent the adsorption based binding capacity (μg LPS per mg PCL NPs), Freundlich (binding affinity) constant (μg LPS per mg PCL NPs), Freundlich exponent and equilibrium LPS concentration (μg LPS/ml solution), respectively.

2.4. PROTEIN RECOVERY

Protein recovery in LPS spiked sample solutions was quantified using BCA assay kit (Pierce). The absorbance at 562 nm was measured in a microplate reader (BioTek). Different concentration of BSA, TTZ, fibrinogen and human hemoglobin were used for plotting the individual protein's standard curves (Figure. S3). All assays were performed by the manufacturer's instructions.

2.5. EFFECTS OF BUFFER AND pH ON LPS REMOVAL

The effect of different buffers on LPS binding efficiency was analyzed by interacting a fixed PCL NP concentration (1000 $\mu\text{g}/\text{ml}$) with a constant LPS concentration (150 $\mu\text{g}/\text{ml}$) prepared using different buffer solutions recipes (Table S1) each having fixed ionic strength of 100 mM (0.1 M). Six different buffer pH values from 2.8-9.6 were tested. Glacial acetic acid was used to obtain a pH value of 2.8. Phosphate buffers were prepared from monobasic and dibasic salts of 0.2 M sodium phosphate to

obtain pH values of 5.8, 6.8 and 8.⁶⁰⁻⁶² PBS of sodium bicarbonate were used to prepare pH 7.4 and 9.6 buffers, respectively.⁶⁰⁻⁶²

2.6. EFFECT OF SALT CONCENTRATION ON PROTEIN RECOVERY

To investigate the effect of salt concentration on % protein recovery, 1000 µg/ml of each BSA and TTZ were spiked with 150 µg/ml of LPS in the different range of PBS concentrations: 0, 0.1, 1, 10, 100 and 150 mM. Protein concentrations were measured before and after LPS spiking and used to further calculate the % protein recovery.

2.7. PCL NP REGENERATION STUDIES

PCL NP suspension was interacted with fixed LPS concentration (270 µg/ml) in RO water and then centrifuged to obtain the supernatant which was reacted with BOD to calculate the percent LPS removal efficiency using equation (1). The PCL NP pellet was resuspended in 0.2 N sodium hydroxide (NaOH) solution for 2 h and then centrifuged to remove the NaOH supernatant. The PCL NP pellet was washed five times using RO water before reusing it again for LPS binding. This regeneration cycle was repeated three times to measure any loss in LPS binding efficiency for PCL. The LPS removal efficiency of PCL NPs after each washing cycle was measured using the BOD fluorescence assay.

2.8. SYNTHESIS OF CELLULOSE ACETATE (CA) MEMBRANE

The CA membranes with or without PCL NPs were prepared by a non-solvent induced phase separation process.⁶³ A casting solution was prepared by dissolving 10

wt.% each of CA and 5 wt.% Pluronic F127 in dimethyl sulfoxide (DMSO) (control). For membranes with NPs, 1 wt.% of PCL NPs was dispersed in the casting solution under vigorous stirring (1100 rpm) at 50°C for 1 h to allow homogenous mixing and the solution was then left for 2 h to allow the complete release of bubbles. The final solution was cast on a casting plate and then immersed in RO water coagulation bath for 30 min. Finally, the water wet membrane was immersed in 30% glycerol (plasticizer) for 15 min, which in addition to improving the mechanical properties also help in dry storage of the membrane for at least 300 days with no major loss in membrane flux and removal properties.⁶⁴ The mass loading of PCL NPs in CA membranes was quantified by comparing the weights of 10 randomly freeze-dried membrane pieces of the same area (1.8 cm²) before and after adding the NPs. The measured weight difference of the membranes with and without NPs is the mass of PCL NPs added to the membrane and was used to calculate LPS removal per unit mass of PCL NPs.

2.9. MICROSCOPY AND MICROANALYSIS

The CA membranes with or without PCL particles were dried using the freeze-fracture method.⁶⁵ Samples were attached to an SEM stub and sputter coated with Denton Au/Pd coater. The membrane surface and cross sections were imaged using the Hitachi S-4700 SEM operated at 3 kV. The membrane surface and cross-sectional morphology, pore size, and thickness were analyzed using ImageJ software (version 1.51w). The average membrane pore size and thickness were based on 100 randomly selected pores and points from different images. The results were reported as average \pm standard deviation (SD). The presence of PCL NPs in the membrane was further verified using

fluorescein isothiocyanate (FITC; 1wt%) incorporated PCL NPs and fluorescence microscopy (Zeiss) equipped with $470 \pm 40/525 \pm 50$ nm excitation/emission filters.

2.10. PERMEATION STUDIES

The measurement of permeation flux was conducted using a custom-made membrane test apparatus (Figure. S4). The apparatus was made of two polyvinyl chloride flow pipes that hold the membrane in between like a sandwich. Each flow pipe is 1.5 cm wide. The top and bottom pipes are 20 cm and 10 cm long, respectively. The membrane area was 1.8 cm^2 . In each experiment, a volume of 20 ml water or solution was fed to the top pipe in a batch setup and flowed through the membrane by gravity. For LPS mixed water, a concentration of 270 $\mu\text{g/ml}$ LPS in 20 ml water was used. Water was collected from the end of the bottom pipe. The water volume was measured at 1 h interval for 8 h to calculate the change in water flux.

2.11. QUANTIFICATION OF LPS REMOVAL USING PCL NPs IN CA MEMBRANES

The determination of LPS removal by CA membranes with or without PCL particles was also carried out by BOD fluorescence displacement assay technique^{58,59} and the apparatus introduced above. A volume of 20 ml RO water containing 270 $\mu\text{g/ml}$ of LPS was fed to the top flow pipe to flow through a sandwiched membrane by gravity. A fixed volume (277 μL) of the LPS feed and the permeate was collected every hour until 8 h. The samples were mixed with BOD (262.11 $\mu\text{g/ml}$) and the F.I. of BOD was measured using a plate reader (BioTek). The percent (%) LPS removal was calculated using equation (5),

$$\text{Cumulative \% LPS removal} = \left(1 - \frac{FI_{BOD} - FI_{BOD.LPS \text{ in permeate}}}{FI_{BOD} - FI_{BOD.LPS \text{ in feed}}}\right) \quad (5)$$

where FI_{BOD} , $FI_{BOD.LPS \text{ in permeate}}$, and $FI_{BOD.LPS \text{ in feed}}$ are the F.I.s of BOD alone, BOD mixed with LPS in permeate, and BOD mixed with LPS in the feed solution, respectively. Each value used here was based on triplicate measurements from three independent experiments. The mean differences and standard deviations were also evaluated.

2.12. CALCULATION OF LPS REMOVAL EFFICIENCY PER UNIT MASS AND SURFACE AREA OF PCL NPs

The LPS removal efficiency per unit mass and surface area were calculated for PCL NPs used in powder form or in the CA membrane. This required the calculation of the number of PCL NPs per unit solution volume using equation (6).

$$\text{Number of PCL} \frac{NPs}{ml} = \frac{6c \times 10^{12}}{\rho \pi d_p^3} \quad (6)$$

where c is the concentration of particles in solution in g/ml, ρ is the density of PCL NPs in g/ml, and d_p is the particle diameter in μm . The mass loading of PCL NPs entrapped in a CA membrane was measured from the mass difference of the freeze-dried CA membranes with and without NPs. The LPS removal efficiency per unit cm^2 and per unit milligram of NPs was calculated based on the mass of LPS in the feed solution and the maximum % LPS removal.

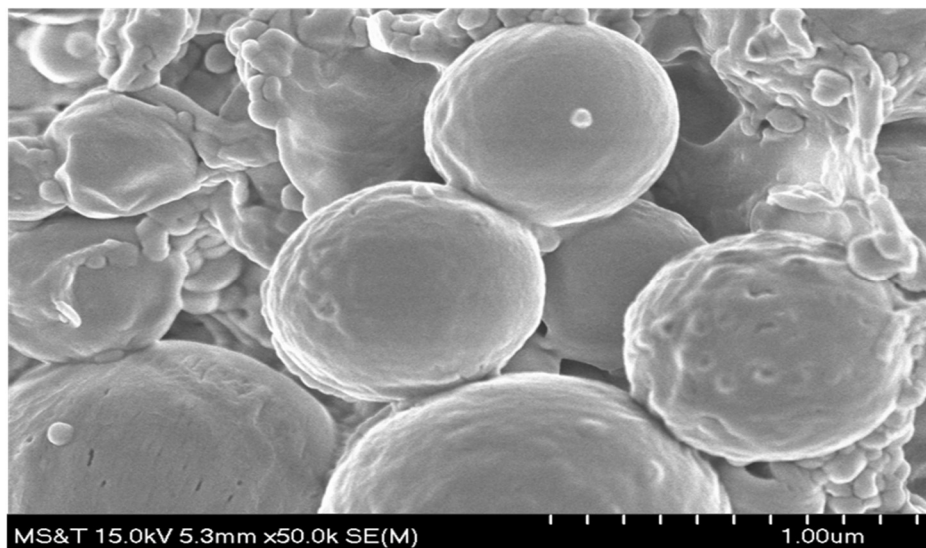
3. RESULTS

3.1. REMOVAL OF LPS FROM WATER AND PBS USING PCL NPs IN POWDER FORM

The size of PCL NPs was observed to be 780 ± 285 nm in diameter by analyzing SEM images (Figure. 1a) and DLS technique (Figure. 1b), which, relatively speaking, is fairly uniform with a low level of dispersity in size. The surface morphology shows that the NPs were of highly spherical shape and their surfaces appeared to be closely packed without apparent pores leading into the interior of the particles. The ζ potential of PCL NPs was found to be -20 ± 5 mV in water (Figure. 1c) indicating a stable dispersion that resists aggregation. LPS adsorption tests were carried out with PCL NPs in both water (open circles; dotted line; Figure. 2a) and PBS (filled, solid circles; solid line; Figure. 2a) where initially the concentration of PCL NPs was systematically varied from 0 to 1000 $\mu\text{g/ml}$ in both cases at a fixed LPS spiked concentration of 150 $\mu\text{g/ml}$ and then the concentration of PCL NPs was fixed and the concentration of LPS was varied from 0.1 to 150 $\mu\text{g/ml}$ in RO water. It was clear and important to note first that PCL NPs were effective in adsorbing and removing LPS from solutions regardless of the presence or absence of salts (PBS). In general, the removal efficiency of LPS by PCL NPs increased with increasing PCL NP concentration, which was to be expected due to increasing numbers of active sites available in the system for binding to LPS. The maximum level of LPS removal achieved was 98% when the PCL NP concentration of $c=1000$ $\mu\text{g/ml}$ was used under the positive influence of salts. Without salts, the LPS sequestration from water was only $\sim 1.8\%$ at a low NP concentration of 0.1 $\mu\text{g/ml}$ and increased to 9% and 82% when the NP concentration became 100 and 1000 $\mu\text{g/ml}$, respectively. The result

at $c = 1000 \mu\text{g/ml}$ was used to evaluate the LPS removal efficiency with varying LPS concentrations of 0–150 $\mu\text{g/ml}$ in water (Figure. 2b). The maximum LPS removal efficiency was $\sim 95\%$, which was approximately $\sim 2040 \text{ endotoxin units (EU)}/\text{cm}^2$ or $\sim 1.3 \times 10^6 \text{ EU}/\text{mg}$ of PCL NPs (Table S2). Across the whole concentration range, the LPS adsorption increased with the addition of salt (PBS; pH 7.4) to water (solid circles; Figure. 2a). This positive effect was clearly exhibited by the data beyond any uncertainty of measurement and indicated that increased ionic strength by the addition of salts resulted in higher LPS adsorption on the PCL NP surface. It is possible that at this high salt concentration (150 mM PBS) a strong interaction between water molecules and salts creates a shielding off effect leaving less water available for the induction of interactions between LPS and PCL. This behavior is consistent with the previously published literature.⁶⁶⁻⁷¹ Another possible explanation could be an electrostatic screening effect that reduces the repulsive interaction between two moieties carrying the same type of charges. Although both LPS and PCL can generally be considered hydrophobic molecules, the former exhibits a net negative charge due to its phosphate groups³³ and the latter also possesses partial negative charges in its carbonyl oxygen atoms. The repulsion between these negative charges can be understood to be weak relative to the van der Waals and hydrophobic binding⁴⁶ between the two massive molecules and hence unable to impede the overall binding interaction and adsorption between LPS and PCL. However, this repulsion can be further weakened, thereby giving rise to stronger binding interaction and heightened adsorption, by the presence of salt ions in proximity to the negative charges that shield their like-charge interactions.

(a)



(b)

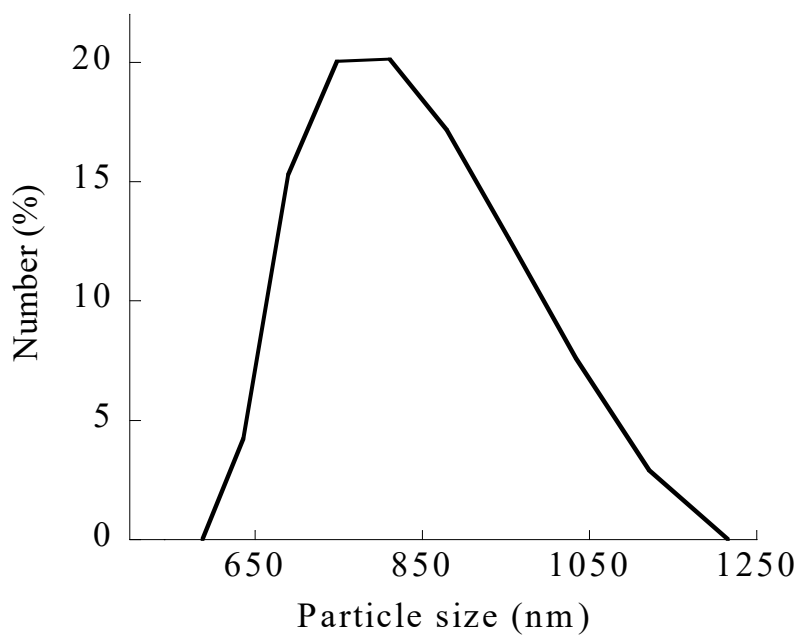


Figure 1. Characterization of PCL NPs. (a) An SEM image of PCL NPs at 50,000 X magnification. (b) Plot showing size distribution of PCL NPs. (c) Zeta potential of PCL NPs in water. Three colors indicate three independent runs.

(c)

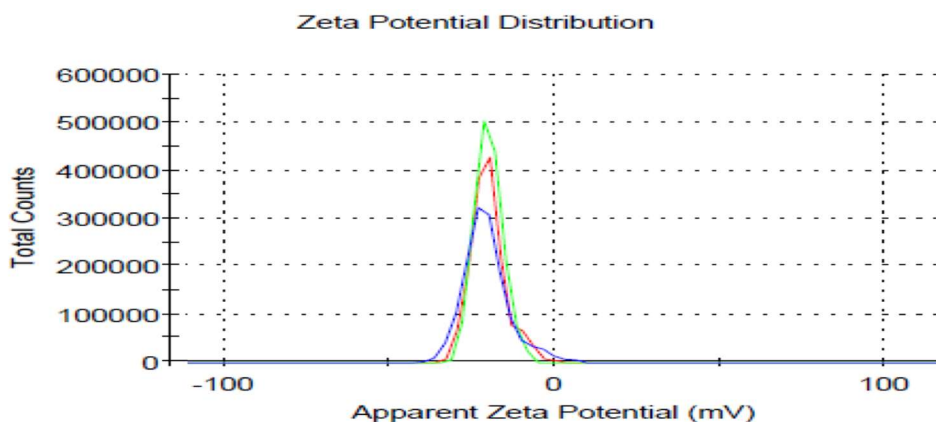


Figure 1. Characterization of PCL NPs. (a) An SEM image of PCL NPs at 50,000 X magnification. (b) Plot showing size distribution of PCL NPs. (c) Zeta potential of PCL NPs in water. Three colors indicate three independent runs (cont.).

(a)

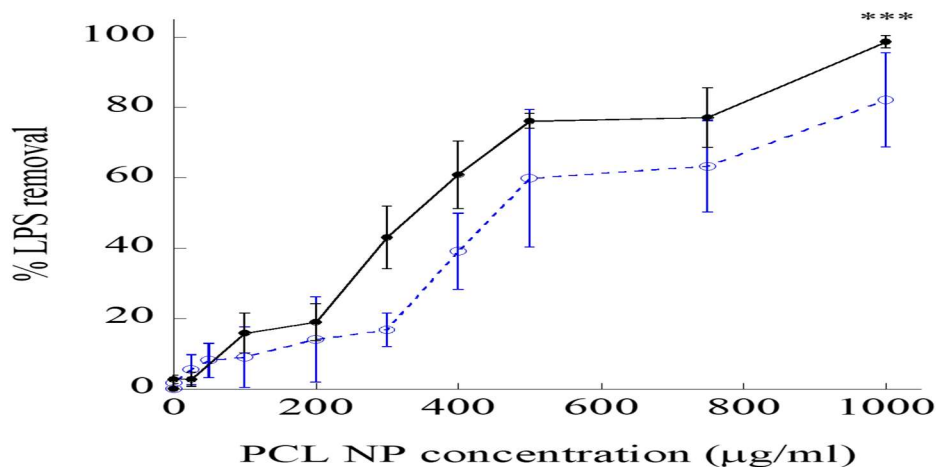


Figure 2. The LPS removal efficiency of PCL NPs from water and PBS. (a) The percent (%) LPS removal from water (open circles, ○; dotted line) and PBS (filled, solid circles, ●; solid line) following adsorption on PCL NPs. *** indicates the p-value < 0.005 showing a statistically significant difference between % LPS removal in water and PBS. A fixed LPS concentration of 150 µg/ml was used in this study. (b) Water containing low (0.1 µg/ml) to high (150 µg/ml) LPS concentrations were treated with 1000 µg/ml of PCL NPs that gives ~95% LPS removal.

(b)

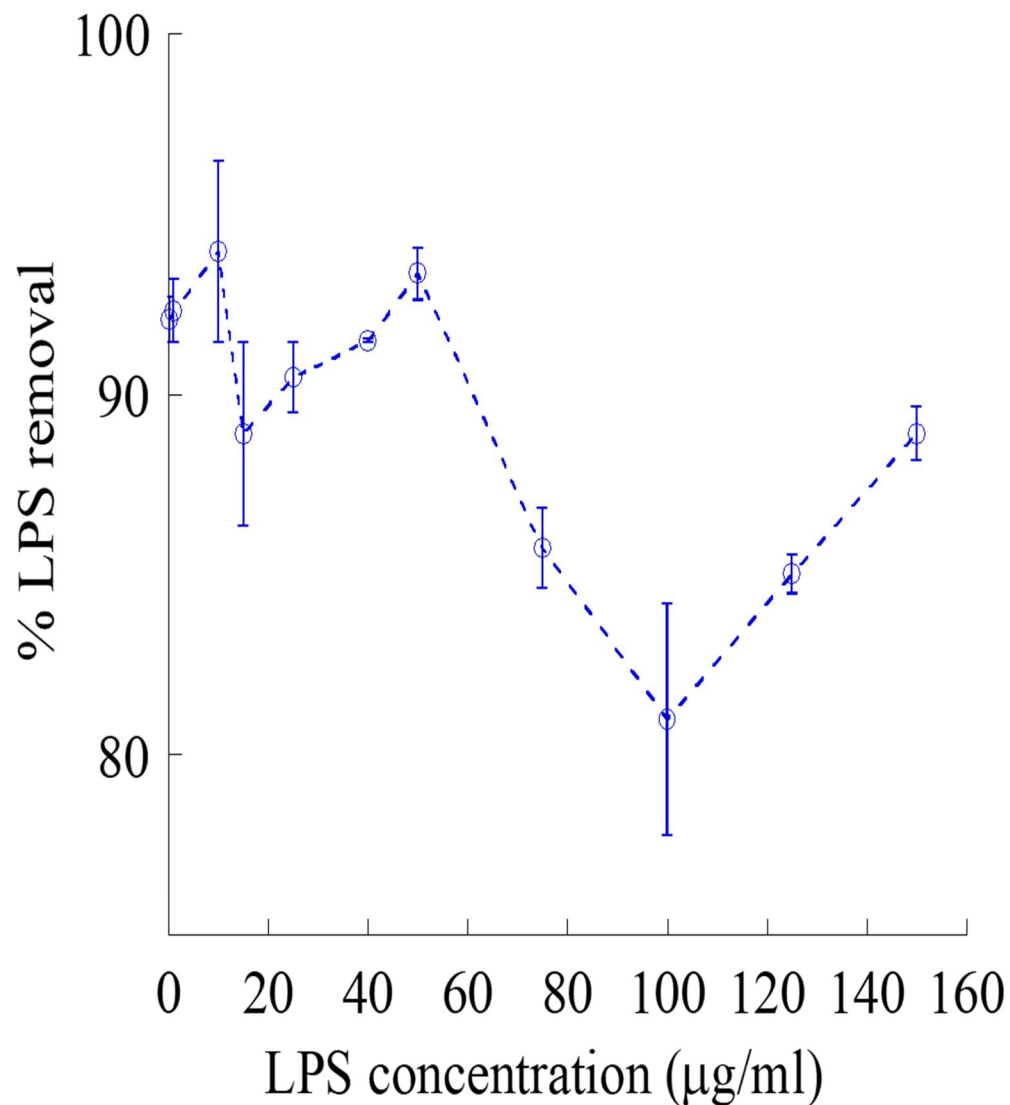


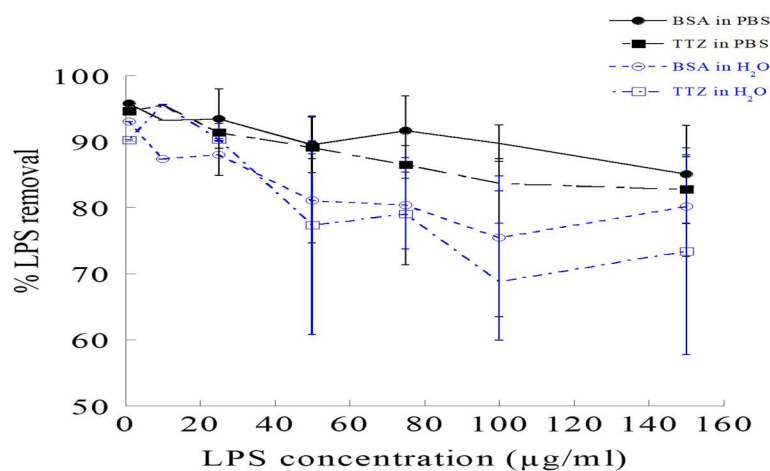
Figure 2. The LPS removal efficiency of PCL NPs from water and PBS. (a) The percent (%) LPS removal from water (open circles, \circ ; dotted line) and PBS (filled, solid circles, \bullet ; solid line) following adsorption on PCL NPs. *** indicates the p-value < 0.005 showing a statistically significant difference between % LPS removal in water and PBS. A fixed LPS concentration of 150 $\mu\text{g/ml}$ was used in this study. (b) Water containing low (0.1 $\mu\text{g/ml}$) to high (150 $\mu\text{g/ml}$) LPS concentrations were treated with 1000 $\mu\text{g/ml}$ of PCL NPs that gives ~95% LPS removal (cont.).

3.2. REMOVAL OF LPS FROM PROTEIN SOLUTIONS USING PCL NPs

To study the effectiveness of PCL NPs on removing LPS at the common contamination level from 0–150 $\mu\text{g}/\text{ml}$ in biopharmaceutical solutions, two protein solutions were investigated. For this purpose, BSA and TTZ protein solutions ($\sim 1 \text{ mg}/\text{ml}$) in PBS of pH 7.4 and RO water containing either low or high levels of LPS were exposed to 1000 $\mu\text{g}/\text{ml}$ PCL NPs (Figure. 3a). It is worth noting that the % LPS removal was higher (90–100%) in PBS (solid lines, Figure. 3a) than in water (dotted lines, Figure. 3a) indicating that PCL NPs were effective in removing LPS from pharmaceutical protein formulations.⁷² We further tested the effects of protein concentration on LPS removal by analyzing four different protein solutions spiked with a fixed concentration (150 $\mu\text{g}/\text{ml}$) of LPS (Figure. 3b). Increasing protein concentrations from 250 to 1000 $\mu\text{g}/\text{ml}$ did not alter the $\sim 90\%$ LPS removal efficacy in PBS (solid lines, Figure. 3b) by PCL NPs (1000 $\mu\text{g}/\text{ml}$). In the case of BSA and TTZ in water, the % LPS removal dropped from 95% to $\sim 80\%$ with the increment in protein concentrations. This reduction of LPS binding on PCL NPs at high protein concentrations in water could be either due to: (i) exchange of low affinity of the highly abundant protein binding with the NP surface by the lower abundance of LPS with a higher affinity for the NP surface; and/or (ii) formation of large aggregates between LPS-protein molecules desorbing LPS from the NP surface. In PBS, the % LPS removal from protein solutions was higher than that in water presumably due to more stable LPS-PCL NP complex formation surrounded by ions in bulk solution. On a preparative scale, an important indicator of desirable properties from such NP adsorbents is the adsorption capacity per unit mass. For this purpose, the equilibrium LPS adsorption capacity of PCL NPs was calculated up to $1.4 \times 10^6 \text{ EU}/\text{mg}$ with $\sim 100\%$

LPS removal capacity from BSA, TTZ, fibrinogen and human hemoglobin solutions in PBS of pH 7.4 (Table S3-S6).

(a)



(b)

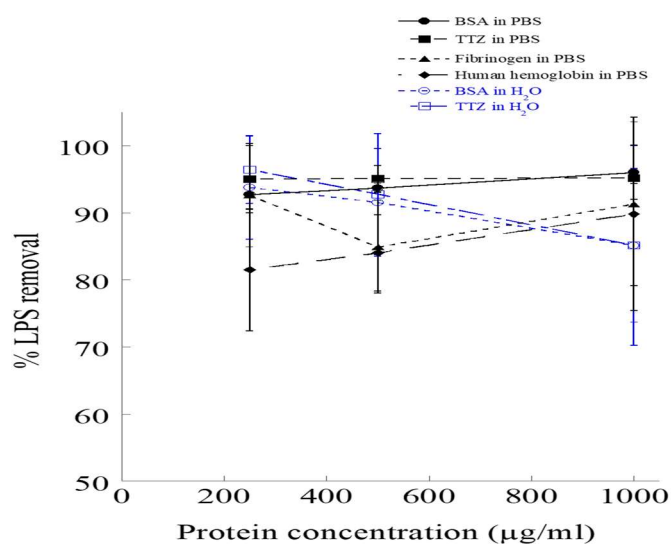


Figure 3. The LPS removal efficiency of PCL NPs from protein solutions. (a) Increasing LPS or (b) protein concentrations have no significant effect on the % of LPS removal from protein solutions prepared in water and PBS. Symbols ●, ○, ■, ▲, ◆ indicate LPS containing BSA solutions in PBS, BSA in water, trastuzumab (TTZ) solutions in PBS, TTZ in water, Fibrinogen in PBS and Human hemoglobin in PBS respectively.

3.3. LPS ADSORPTION BEHAVIOR ON PCL NPs

Based on the experimental data of LPS binding on PCL NPs, binding-dependent parameters were calculated using the Freundlich isotherm model that rationalizes the contribution of favorable adsorption on the NP surface. The experimental data fit the Freundlich model ($R^2 > 0.98$) where the slope $\frac{1}{n}$ accounts for the intensity of adsorption and intercept, K measures the binding affinity ($\mu\text{g LPS}/\text{mg PCL NPs}$) (Figure. 4). $n > 1$ represents favorable adsorption associated with multilayer LPS formation on the PCL surface.^{73,74} From Table S7, it can be seen that the binding intensity (n) values vary from 1.1 – 1.4 thus indicating that the NPs have favorable LPS binding adsorption performance for all tested conditions.⁷⁵ The binding affinity constant, K was found to vary between 9.5 – 11.7 $\mu\text{g LPS}/\text{mg PCL NPs}$ ($\sim 10^5$ - 10^6 EU/mg) depending on the solution (water and PBS) and protein types (BSA and TTZ). The K values were compared with previously reported sorbents⁷⁶⁻⁷⁹ which indicated that PCL NPs were 10 to 40 log orders of magnitude better in LPS binding capacity than most of the commonly used adsorbents such as Polymyxin B conjugated cellulose microspheres and Histidine immobilized silica gels, among others.⁷⁶⁻⁷⁹ To ease out the interactions between LPS and PCL NPs, the NPs were coated with a cationic polymer, PLL (Figure S5). The PLL coated PCL NPs showed a significant decrease in % LPS removal from 80% to 60% in water and from 100% to 20% in PBS. These findings reassert the selective hydrophobic interactions between LPS and PCL NPs.

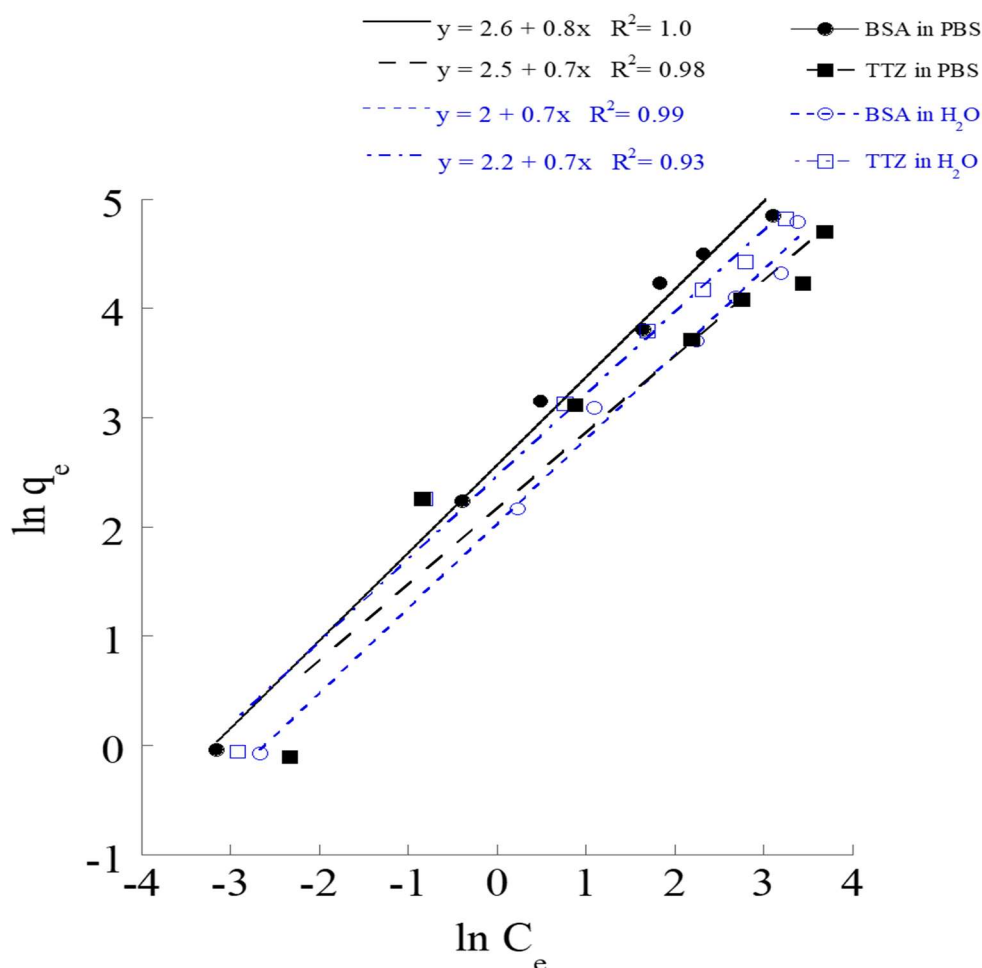


Figure 4. Freundlich adsorption isotherm fitting of LPS removal by PCL NPs from BSA and TTZ solutions in water and PBS.

3.4. PROTEIN RECOVERY

Most biopharmaceutical purification processes suffer from product loss. Protein recovery is as important as LPS removal to reflect an interaction of the protein with LPS binding sites. Figure. 5 shows the results of protein recovery at varying (a) LPS and (b) protein concentrations. As it is seen that protein recoveries were close to 100% for a wide range of LPS (0 – 160 $\mu\text{g}/\text{ml}$) and protein (0 – 1000 $\mu\text{g}/\text{ml}$) concentrations. These results

further confirm the selectivity of PCL NPs for LPS while showing 100% protein recovery.

(a)

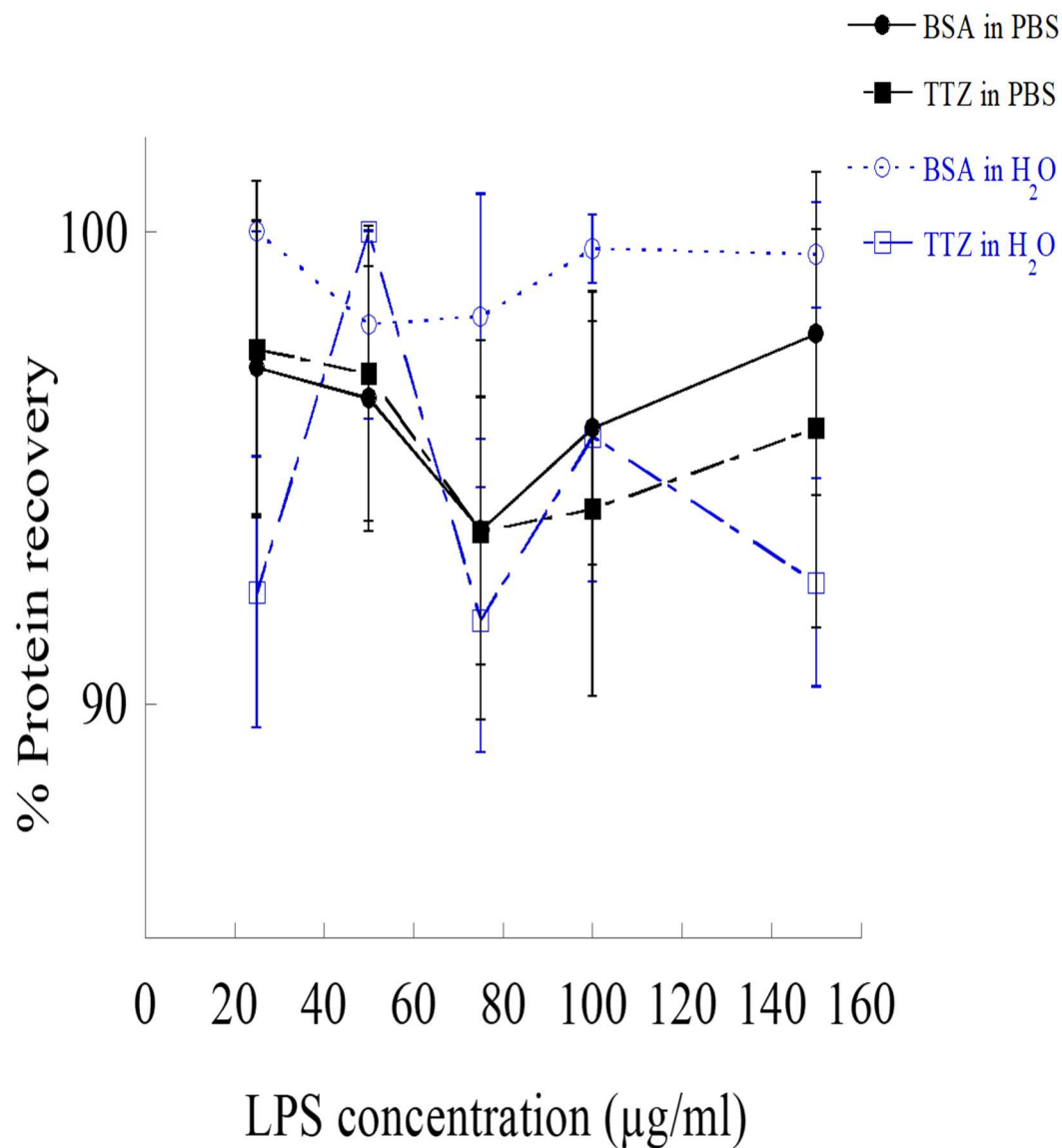


Figure 5. Percentage of protein recovery as a function of (a) protein concentrations and (b) LPS concentrations. The amount of PCL NPs used was 1000 µg/ml.

(b)

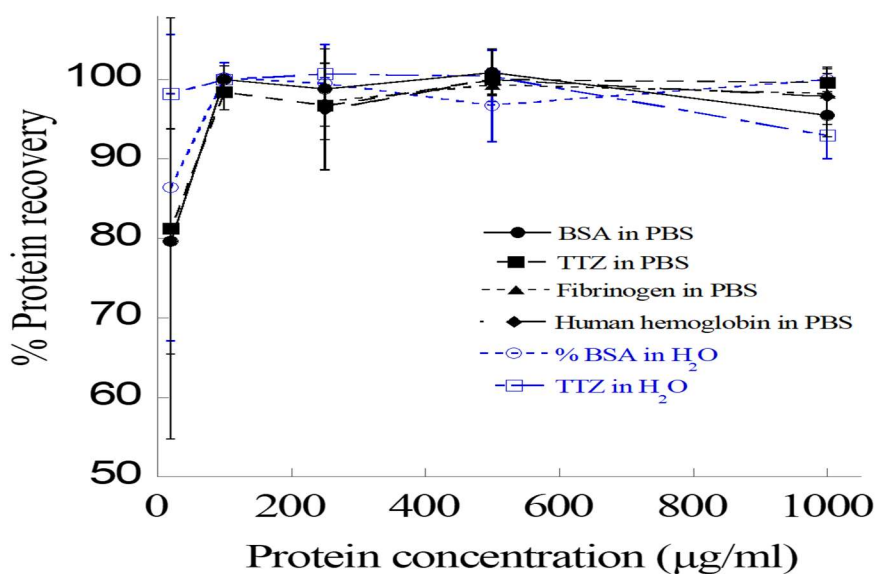


Figure 5. Percentage of protein recovery as a function of (a) protein concentrations and (b) LPS concentrations. The amount of PCL NPs used was 1000 µg/ml (cont.).

3.5. EFFECT OF pH ON LPS REMOVAL IN DIFFERENT BUFFER CONDITIONS

The percentage of LPS removal was predicted to be dependent on the changes in buffer pH (Figure. 6a). LPS binding on PCL NPs show reasonably strong dependence on pH for different buffers of variable pHs. The ionic strength for all buffers was maintained constant at 100 mM (0.1 M). At the pH of 2.8, i.e., near and below the isoelectric point (pI 2) of LPS,⁸⁰ the binding of LPS with PCL NPs increased close to ~90% possibly due to low LPS solubility near the pI and high hydrophobic interactions between non-polar LPS and PCL resulting in increased LPS removal from the solution. On the other hand above the pI of LPS, at pHs between 5.8 and 8, average LPS removal efficiencies were

found to be increased from 30% up to 90% in an alkaline buffer pH of 9.6. The enhancement in LPS removal at high pH is most likely due to hydrophobic interactions between non-polar LPS and PCL NPs that segregate the polar ions and water molecules and minimizes the area of contact between polar and nonpolar molecules in the solution.⁸¹ The phase separation of LPS was further enhanced up to ~99% by PBS of higher ionic strength (0.15 M, pH 7.4) driving the self-assembly of LPS-PCL NP hydrophobic effects. In summary, PCL NPs can operate in acidic to neutral conditions (pH 2.8 to pH 9.6). The highest LPS removal (~100%) was found in PBS of pH 7.4 followed by >85% recovery in acetic acid and sodium bicarbonate buffer of pH 2.8 and 9.6, respectively.

(a)

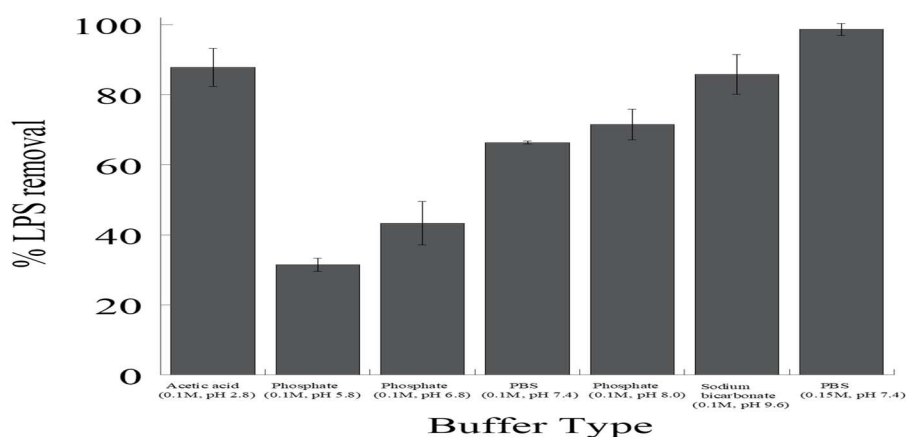


Figure 6. The effects of pH and salt concentrations on LPS removal by PCL NPs. (a) The effect of pH and buffers on the % LPS removal. Four different types of buffers (acetic acid, phosphate, PBS and sodium bicarbonate) covering pH range from 2.8-9.6 were used. (b) Dependence of protein recovery on salt concentrations in LPS and PCL NP systems. Solid line with filled, solid circles (●) represents BSA and the dotted line with filled, solid squares (■) indicates TTZ.

(b)

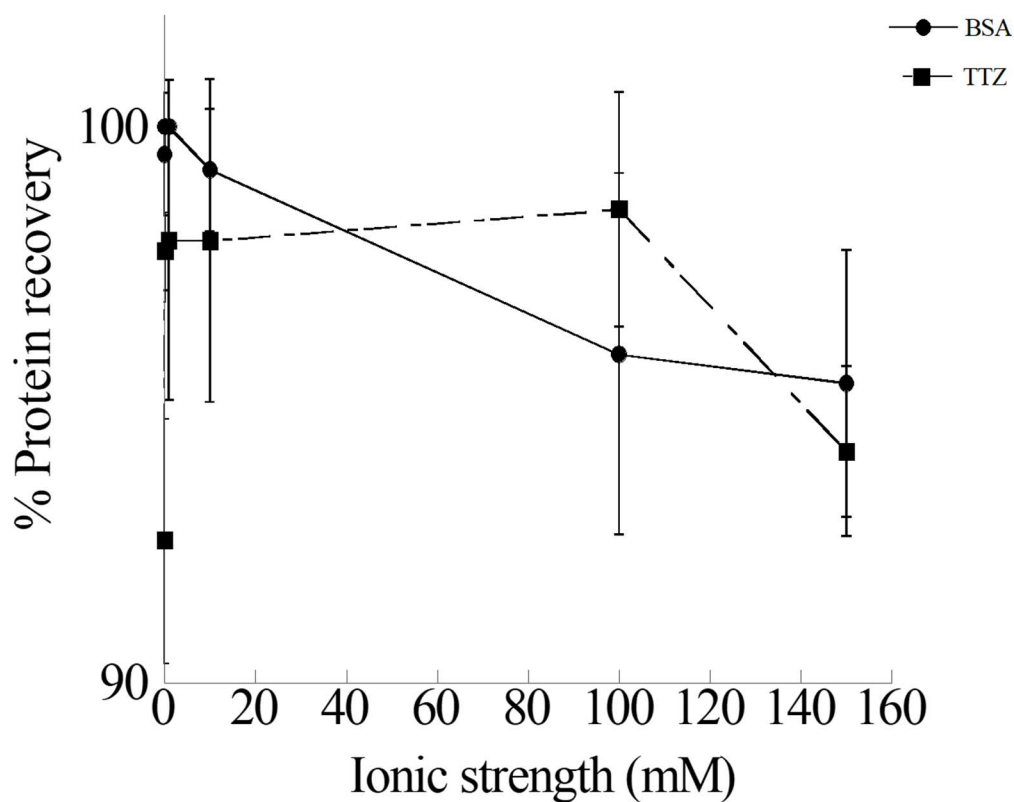


Figure 6. The effects of pH and salt concentrations on LPS removal by PCL NPs. (a) The effect of pH and buffers on the % LPS removal. Four different types of buffers (acetic acid, phosphate, PBS and sodium bicarbonate) covering pH range from 2.8-9.6 were used. (b) Dependence of protein recovery on salt concentrations in LPS and PCL NP systems. Solid line with filled, solid circles (●) represents BSA and the dotted line with filled, solid squares (■) indicates TTZ (cont.).

3.6. EFFECT OF SALT CONCENTRATION ON PROTEIN RECOVERY

Figure. 6b shows that the % protein recovery is almost linear that varies between 90 to 100% with the change in salt concentrations indicating that the ionic strength has a

little effect on protein recovery in our LPS-PCL NP system. At low salt concentrations extrapolated from zero salt concentration (water), the recovery was >90% for both BSA and TTZ which were increased further up to ~100% at higher salt concentrations (150 mM). These results indicate that the low affinity of proteins towards PCL NPs both in the absence and presence of solution ions. The mutual interactions between LPS and PCL NPs keep protein away in the bulk phase. At higher ionic strength, it is possible that free ions rearrange themselves into certain configuration around LPS-PCL NP complexes and proteins that promote increased retention of proteins in the mixture and thus slightly decrease the protein recovery to ~95%.

3.7. PCL NPs WERE REGENERATED TO REMOVE LPS

PCL NPs were regenerated by breaking LPS-PCL complexes in RO water which makes the LPS removal process more efficient and scalable (Figure. 7). NaOH was used to regenerate the PCL NPs that exchanged off LPS for the hydroxide (OH^{-1}) ion in the caustic solution which is well-known to desorb LPS from chromatography resins and particles quite effectively.⁸²⁻⁸⁴ The collected PCL NPs were re-dissolved off the (OH^{-1}), and this is facilitated by the 2 h contact time. A high LPS (EU/ml) recovery (~80%) was observed over the course of three regeneration cycles. An average LPS recovery of $> 2 \times 10^6$ EU/ml was obtained per regeneration cycle when LPS bound PCL particles were reacted with 0.2 N NaOH for 2 h and then washed using RO water before being reused for LPS binding again. Overall, the LPS removal efficiency of PCL NPs nearly had any change after three rounds of adsorption, elution, and reuse.

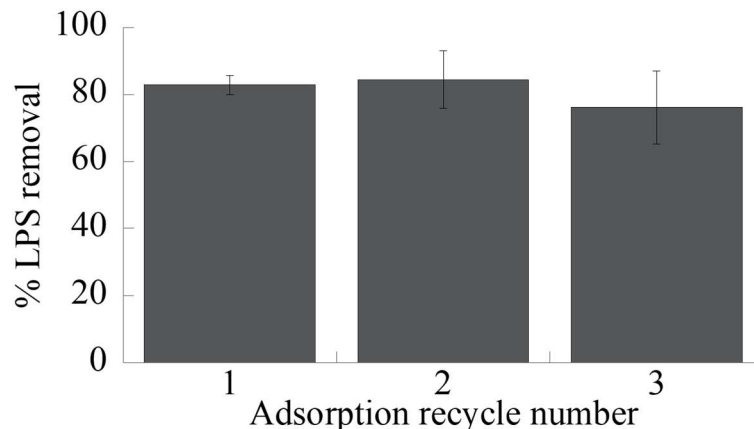


Figure 7. PCL NP regeneration. LPS removal efficiency after PCL NPs is regenerated three times by desorbing LPS from the NPs using 0.2 N NaOH and testing for LPS adsorption/removal.

3.8. PCL NPs WERE EMBEDDED IN CA MEMBRANES

The cross-sections of CA membranes were obtained by SEM (Figure. 8a) and compared with and without NPs. The original CA membrane exhibited a thickness of $116 \pm 2 \mu\text{m}$ and a relatively homogeneous macrostructure with a distinctive dense layer near the surface (Figure. 8a). Simply from the point of view of the ratio (~ 100) between the membrane thickness and the particle diameter, the presence of PCL NPs could be expected to have a great impact on the structural and transport properties of the membrane. Indeed, the CA membrane with PCL NPs showed a seemingly more uniform cross-sectional structure with no unique layer (Figure. 8b), which was revealed fluorescence microscopy to contain green dye-labeled spherical PCL particles on the flat surface of the membrane (Figure. 8c). The cavities in the PCL embedded membrane were found to be noticeably larger than those in the original CA membrane as visualized from the SEM images of their cross-sections (Figures. 8a and 8b). While the incorporation of

PCL NPs in the membrane appeared not to affect the pore opening size as there was only a slight change from $0.16 \pm 0.05 \mu\text{m}$ to $0.17 \pm 0.05 \mu\text{m}$ (Figure. S6), it has much greater impact on the membrane's macro-void cross-sectional morphology as it changed from a narrow, tortuous, and flaky pore structure (Figure. 8a) to a broad, straight, and finger-like pore structure (Figure. 8b).^{63,85-90} PCL NPs also increased the membrane thickness by more than 13%, from $116 \pm 403 \mu\text{m}$ to $132 \pm 12 \mu\text{m}$ (Table S8).

(a)

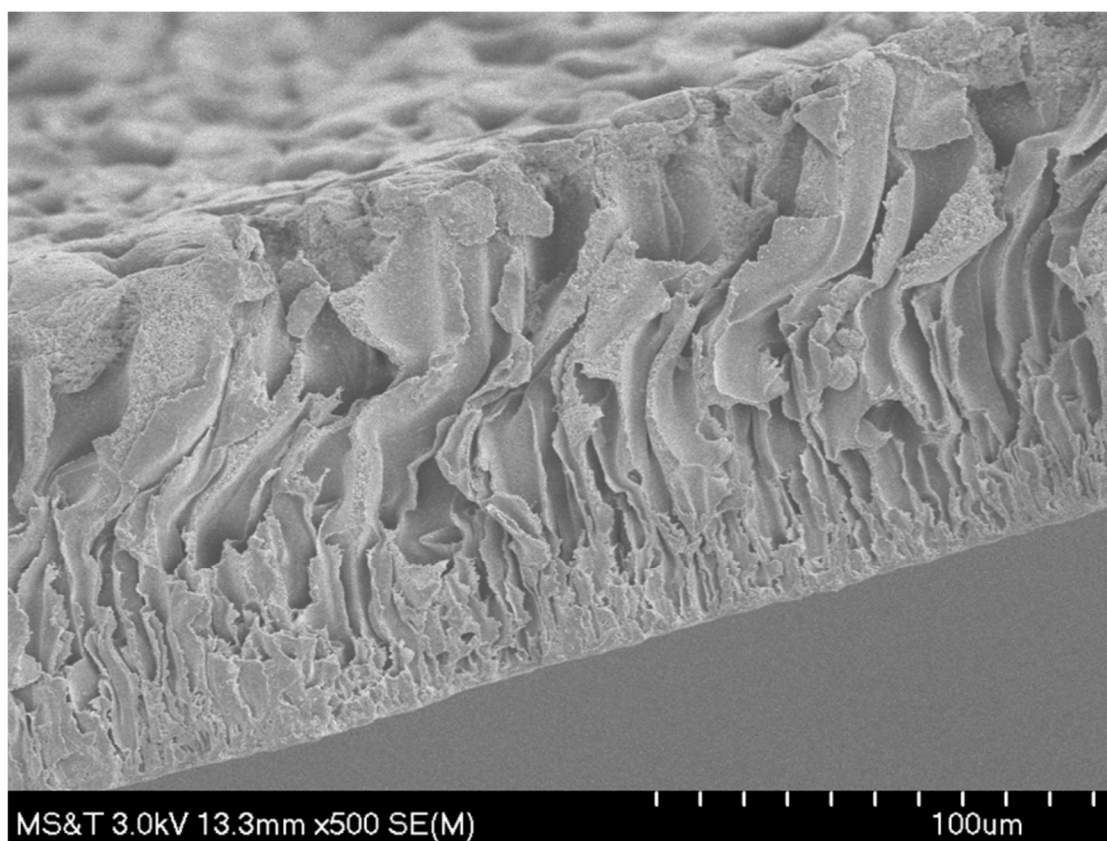
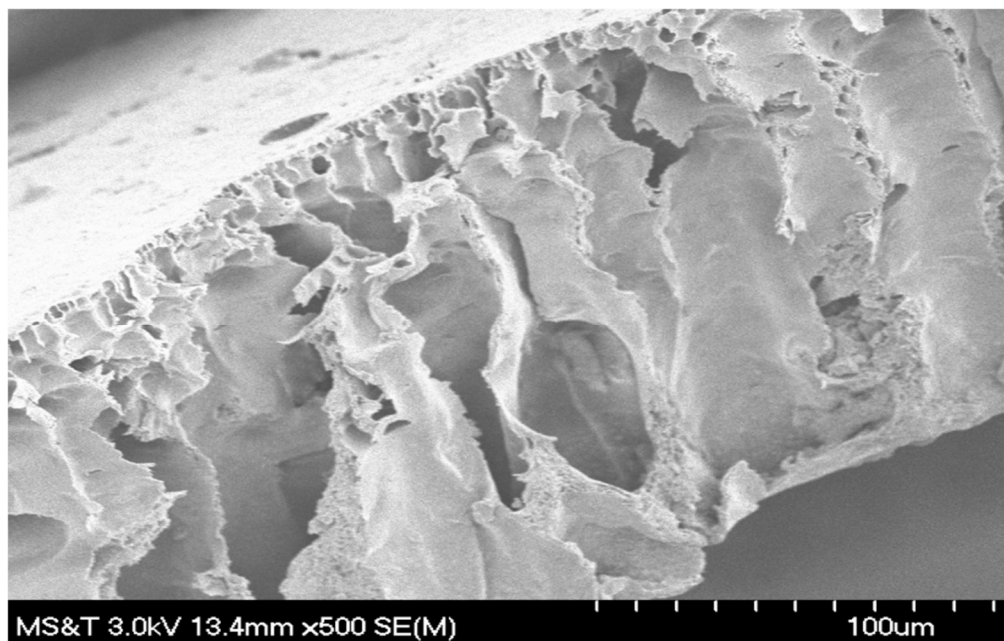


Figure 8. Characterization of PCL NP embedded filter. SEM images of the cross-sections of membranes prepared from (a) CA membrane, scale bar = $100 \mu\text{m}$, (b) CA membrane with PCL NPs in low magnification, scale bar = $100 \mu\text{m}$ and (c) Fluorescence microscopic images of fluorescein dye encapsulated PCL NPs in membranes in high magnification.

(b)



(c)

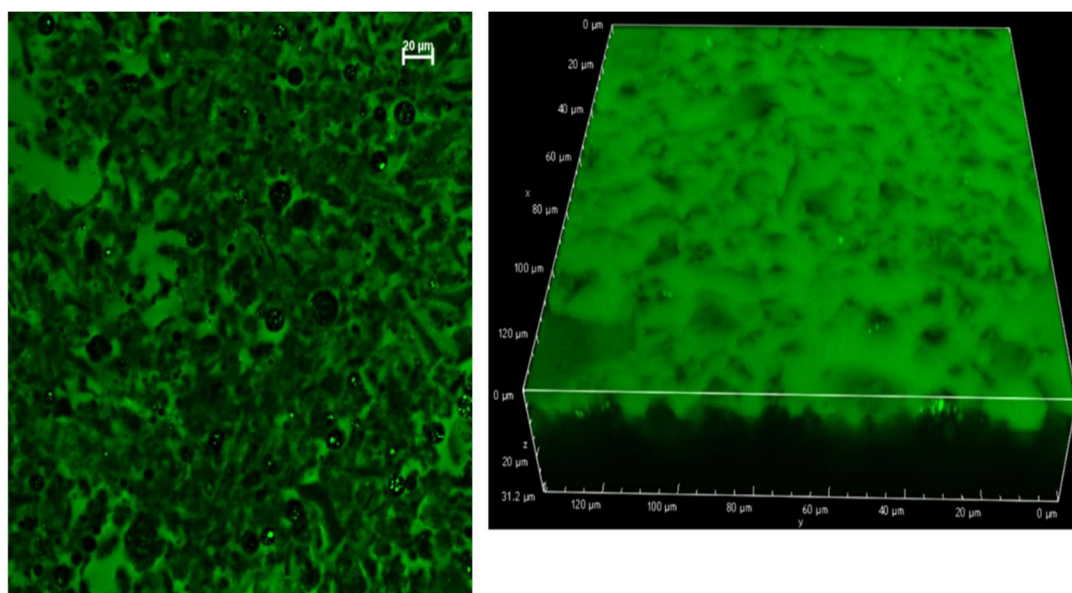


Figure 8. Characterization of PCL NP embedded filter. SEM images of the cross-sections of membranes prepared from (a) CA membrane, scale bar = 100 μm, (b) CA membrane with PCL NPs in low magnification, scale bar = 100 μm and (c) Fluorescence microscopic images of fluorescein dye encapsulated PCL NPs in membranes in high magnification (cont.).

3.9. PERMEATION OF WATER USING CA MEMBRANES WITHOUT AND WITH PCL NPs

The measurement of water flux driven by gravity-flow through CA membrane was illustrated in Figure. S4, which did not require any pumping equipment or any vacuum driven setup other than gravity. The permeation water fluxes were approximately 25 and $17 \frac{L}{m^2.h}$ at the end of 1 h through the CA membranes without and with PCL NPs, respectively, and reduced to 15 and $11 \frac{L}{m^2.h}$, respectively, at the end of 8 h of operation (Figure. 9a). These results were in agreement with previously reported values.⁹¹⁻⁹³ Although the incorporation of PCL NPs appeared to create larger in size pores in the membrane structure (Figures 9a and 9b) that could be favorable for water to flow through, it also increased the membrane thickness and hence the overall mass transfer resistance to water flow quite significantly, which may explain the resultant lower permeation fluxes. In addition, the presence of NPs occupying the pore space could also have a similar effect by resulting in significantly narrowed passageways for water flow. When LPS was mixed with water, the water fluxes were observed to be lowered as well (Figure. 9b). Specifically, the LPS containing water fluxes at the end of 1 h and 8 h were reduced to ~ 5.4 and $\sim 2.5 \frac{L}{m^2.h}$ using the original CA membrane, and ~ 4.2 and $\sim 2.2 \frac{L}{m^2.h}$ using the CA membrane embedded with PCL NPs. There could be a number of factors contributing to this phenomenon, which were considered not within the scope of this work but worthy of future studies. For example, the binding of LPS, being large elongated molecules, to the surfaces of the pores and PCL NPs could significantly reduce the pore sizes for water flow. The addition of LPS also changed the mass density of the solution which would certainly affect the gravity-driven flow through the membrane.

These factors can be pursued in the future in order to obtain a deeper understanding and enable further optimization of the membrane pore structure for achieving even greater processability of the LPS-containing solutions.

(a)

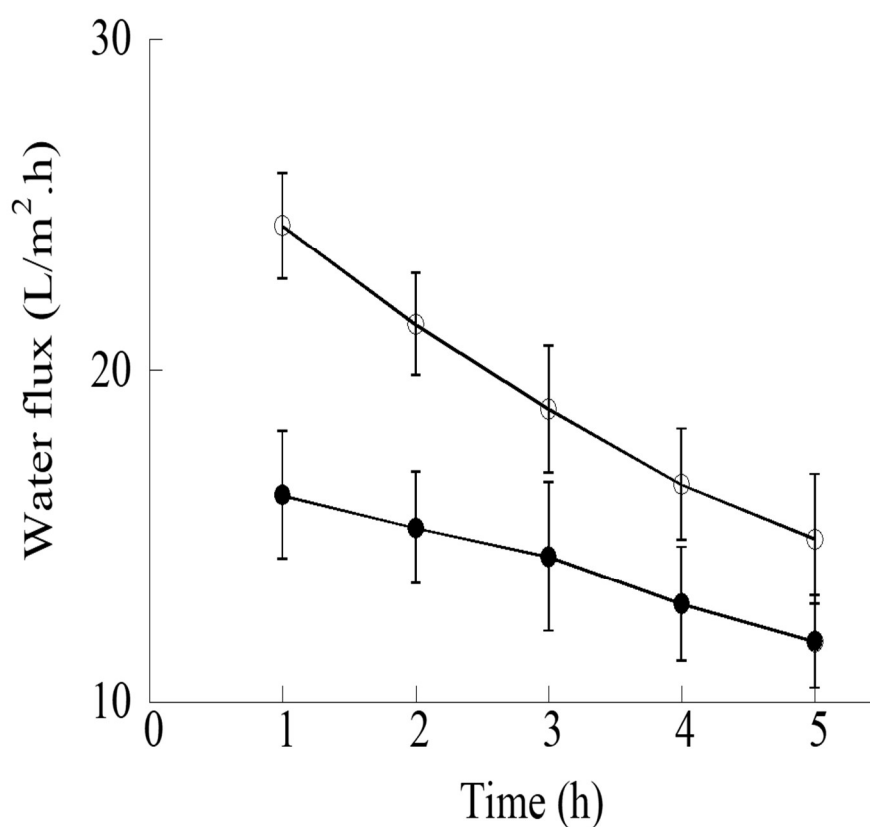


Figure 9. Water flux performance of CA and PCL impregnated CA membrane. The water flux performance of CA membrane (open circles; ○) and CA membrane impregnated with PCL NPs (filled, solid circles; ●) (a) in the absence of LPS and (b) in the presence of LPS. The flow rates were measured under gravity. Error bars represent standard deviations from three independent experiments. * and ** indicates p values of 0.03 and 0.01, respectively, representing statistically significant differences between the CA membrane and PCL NPs in CA membrane.

(b)

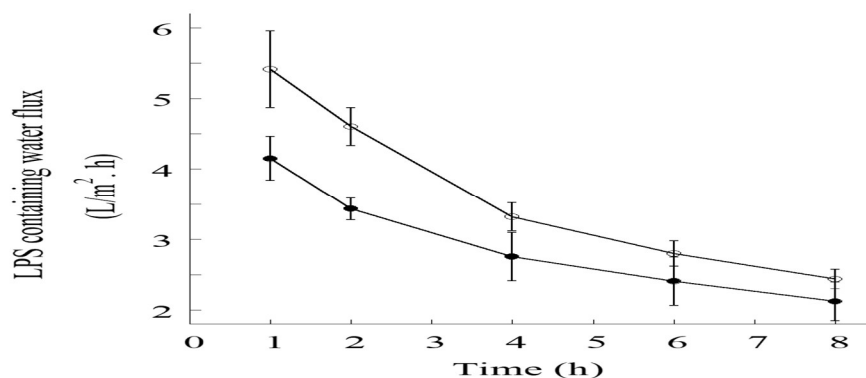


Figure 9. Water flux performance of CA and PCL impregnated CA membrane. The water flux performance of CA membrane (open circles; ○) and CA membrane impregnated with PCL NPs (filled, solid circles; ●) (a) in the absence of LPS and (b) in the presence of LPS. The flow rates were measured under gravity. Error bars represent standard deviations from three independent experiments. * and ** indicates p values of 0.03 and 0.01, respectively, representing statistically significant differences between the CA membrane and PCL NPs in CA membrane (cont.).

3.10. CA MEMBRANES WITHOUT AND WITH PCL NPs FOR REMOVING LPS FROM WATER

To confirm the adsorption capability of PCL NPs in a membrane form for potential application in larger scale operations, the LPS removal efficiencies by the CA membranes with or without PCL NPs were measured and compared. As can be seen in Figure. 10a, the incorporation of PCL NPs in membrane significantly boosted the LPS removal efficiency from ~48% to ~75% at the end of 1 h, and from 88% to near completion at the end of 8 h. The specific endotoxin units (EU) removed were further calculated and compared in Figure. 10b and Table S9, which clearly demonstrated the superior performance of PCL NPs in the membrane as compared to its pristine powder form. The removal efficiency per unit area was $\sim 4.3 \times 10^4$ EU/cm² ($\sim 2.8 \times 10^6$ EU/mg

of PCL NPs) which was 2-fold ($p < 0.005$) higher than that of NPs alone (Table S9). These results indicate a promising avenue for removing LPS without the requirement of any pumping devices or external power sources through the utilization of PCL NPs both in powder and membrane forms.

(a)

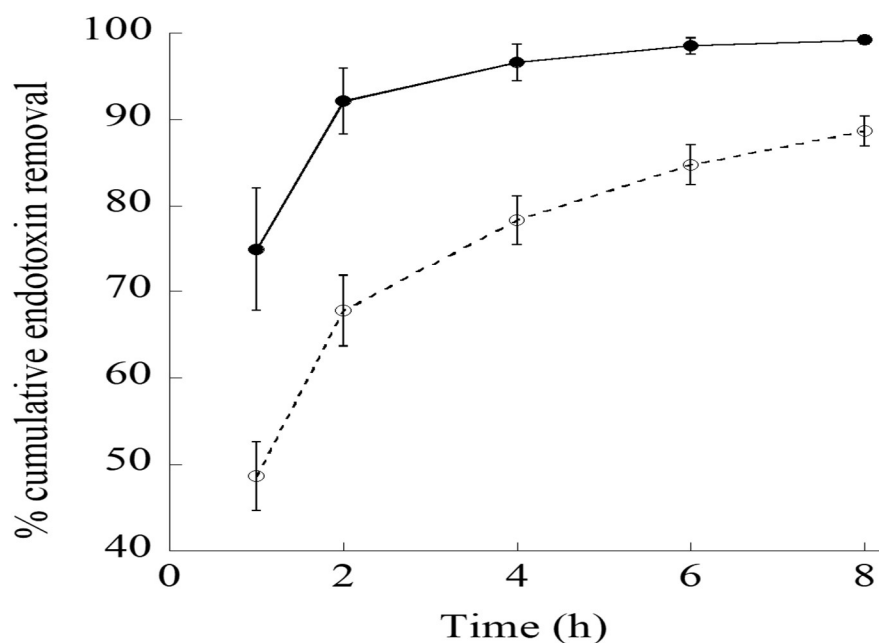


Figure 10. The LPS removal efficiency of PCL NP embedded filters. (a) Efficacy tests of CA membrane (open circles; \circ) and CA membrane with PCL NPs (filled, solid circles; \bullet) for the removal of LPS from the water. $C_0 = 270 \frac{\mu g}{ml}$ LPS and PCL dose $\approx 1670 \mu g/cm^2$ of membrane. *, ** and *** indicate p values of 0.03, 0.01 and less than 0.005 respectively, demonstrating statistically significant differences between PCL NPs in CA membrane and CA membrane. (b) Bar plot of LPS removed (EU) / mg of PCL NPs in powder form and also in CA membrane. The extent of error bar for PCL NPs in CA membrane is small due to the fact that the percentage LPS removal reached $\sim 100\%$. The difference between PCL NPs in powder and in the membrane is statistically significant ($p < 0.05$).

(b)

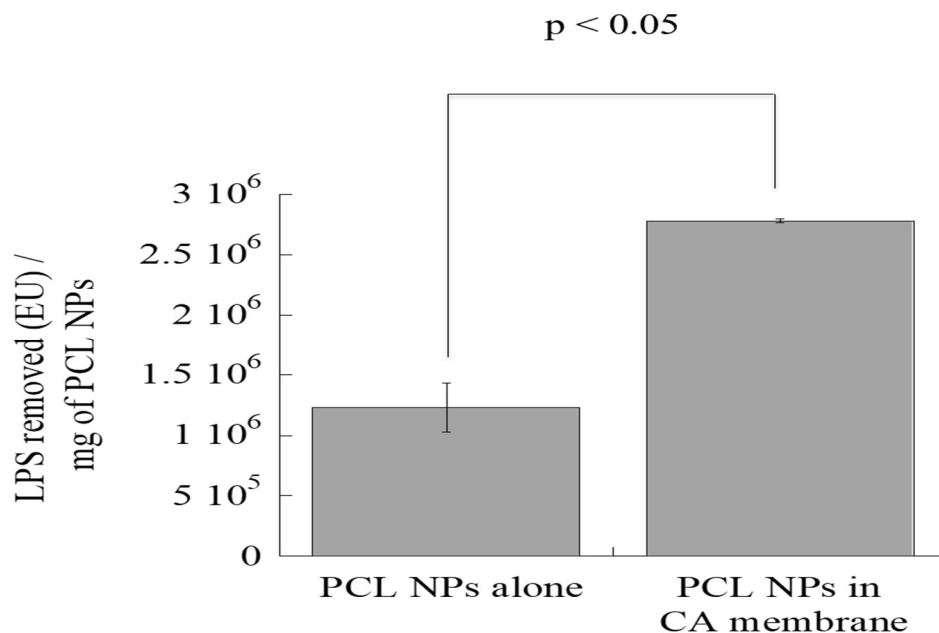


Figure 10. The LPS removal efficiency of PCL NP embedded filters. (a) Efficacy tests of CA membrane (open circles; ○) and CA membrane with PCL NPs (filled, solid circles; ●) for the removal of LPS from the water. $C_0 = 270 \frac{\mu g}{ml}$ LPS and PCL dose $\approx 1670 \mu g/cm^2$ of membrane. *, ** and *** indicate p values of 0.03, 0.01 and less than 0.005 respectively, demonstrating statistically significant differences between PCL NPs in CA membrane and CA membrane. (b) Bar plot of LPS removed (EU) / mg of PCL NPs in powder form and also in CA membrane. The extent of error bar for PCL NPs in CA membrane is small due to the fact that the percentage LPS removal reached $\sim 100\%$. The difference between PCL NPs in powder and in the membrane is statistically significant ($p < 0.05$) (cont.).

3.11. PRODUCT COMPARISON

PCL NPs and PCL NP retaining membranes were compared against five commercially available endotoxin removal products (Figure. 11 and Table I) following the manufacturers' instructions. A neutral pH 7.4 PBS solution containing $\sim 2.8 \times 10^6$ EU/ml of endotoxin was loaded in the presence of each product to determine the LPS

clearance and protein recovery. PCL NPs and membranes showed 1.25 to 30-fold higher efficiency than other commercially available products.

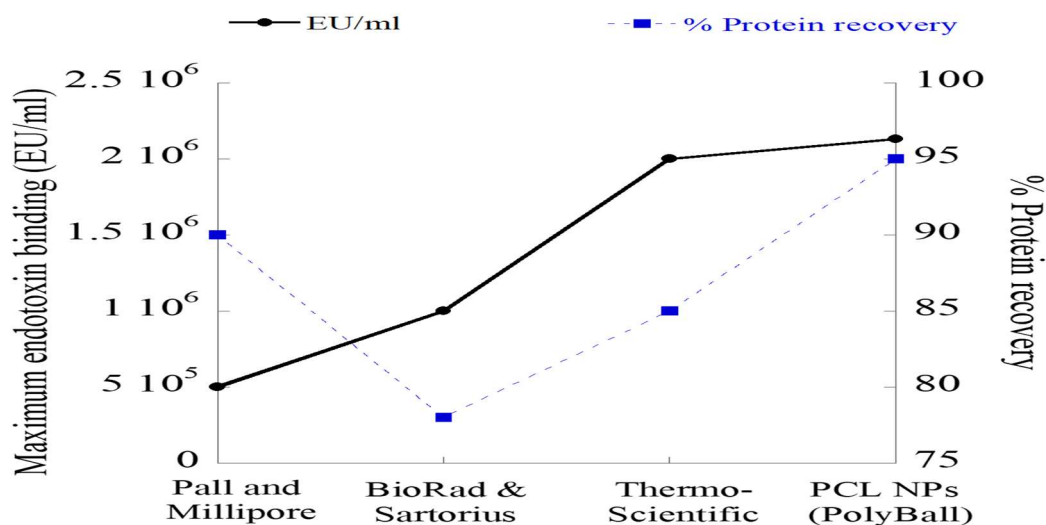


Figure 11. Endotoxin removal product comparison. PCL NPs show higher LPS binding capacity as well as higher protein recovery than five commercially available endotoxin removal products.

Table 1. Comparison of PCL NPs and the NP containing membrane versus four commercially available endotoxin removal products.

Product Name	Maximum Endotoxin Binding capacity (EU/ml)	Cost (\$)	Reusability
Pall Acrodisc Unit with Mustang E membrane	5.0×10^5	\$ 9.2 per 1 cm ² membrane area	Yes
Millipore charged Durapore cartridge membrane filters	$>5.0 \times 10^5$	\$ 2.7 per 1 cm ² membrane area	Yes
BioRad Proteus Endotoxin Removal Kits (Membrane based)	$5.0 \times 10^5 - 10^6$	\$ 12.4 per 1 cm ² membrane area	Yes
Sartobind Q100 membrane adsorbers (Sartorius)	1.0×10^6	NA	Yes
Thermo scientific Pierce High capacity endotoxin removal resins	2×10^6	\$ 20.2 per ml of resin slurry	Yes
PCL nanoparticles	1.45×10^6	\$2.4 per 1 g	Yes
PCL nanoparticles incorporated membrane	2.8×10^6	\$ 0.05 per 1 cm ² membrane area	Not tested yet

4. DISCUSSION

Relatively few polymers have been investigated for their potential to be synthesized into NP adsorbents for LPS removal. On a preparative scale, an important indicator of desirable properties from such NP adsorbents is the adsorption capacity per unit mass. In this work, the equilibrium adsorption capacity of PCL NPs in powder form and in the membrane was found to be more than $2.8 \times 10^6 \text{ EU/mg}$ of NPs as shown in Tables S2-S6 and Table S9. Previously, polymyxin B cross-linked cellulose porous microspheres of $\sim 150 \mu\text{m}$ in diameter have been shown to have a maximum adsorption capacity of $3.6 \times 10^6 \text{ EU/mg}$.⁷⁷ These porous beads, despite offering a high internal surface area for LPS adsorption, also present hindered intraparticle mass transport within their porous structure so that their use in a membrane or in a chromatographic column requires a large pressure drop.⁹⁴ One way to circumvent this challenging issue of high pressure drop associated with high internal adsorption capacity is to use a nonporous solid adsorbent particle that has sufficient capacity on the exterior surface to achieve high adsorption efficiency at short residence time and under low pressure drop. As a type of such desirable adsorbent particles, PCL NPs of $\sim 780 \text{ nm}$ in diameter have a BET specific area of $\approx 6.5 \text{ m}^2/\text{g}$ that provides 82–98% LPS removal efficiency in water and PBS. These data are comparable to other previously reported processes^{46,77,79} and indicative of the potential of PCL NPs to fill the gap as a suitable adsorbent for LPS removal.

The extent of LPS removal was found in previous studies to depend on the characteristics of the buffer solution, including salt concentration and pH. Increasing the ionic strength was found to enhance the LPS adsorption on Q-sepharose gel column.⁶⁷

The LPS adsorption levels were 10^2 and 10^3 EU/ml in 10 and 50 mM PBS, respectively.⁶⁷ Similar high LPS binding properties were shown by hydroxyapatite, polystyrene, Dowex 1-X2, activated charcoal, phenyl and octyl-sepharose in presence of a high concentration of ammonium sulfate salts.⁶⁹ Our PCL NPs were found to remove more than 10^6 EU/ml using 150 mM PBS containing 137 mM NaCl (Figures 2 –5), which represents an adsorption level almost 1000 fold higher than those of the previously published results. The effects of pH (protons) are also contingent on the electrostatic properties of the adsorbents.^{68,95} In this work, the adsorption driving forces between the generally hydrophobic PCL NPs (adsorbent) and LPS (adsorbate) are dominated by the van der Waals interactions and hydrophobic binding, which are further enhanced by increasing pH that weakens the repulsion between the adsorbent and the adsorbate as both possess partially negatively charged moieties. The enhancement in LPS binding to hydrophobic PCL surface can be attributed to the weakening of the shielding effect common with water molecules which cannot wet the hydrophobic surface and instead form highly ordered shell-like structure or shield around the hydrophobic surface due to its inability to form hydrogen bonds in all directions, thus enhancing the interaction between two hydrophobic surfaces (LPS and PCL).⁶⁶⁻⁷¹

Combinedly, our results suggest that the highly effective LPS separation could be due to synergistic van der Waals and hydrophobic-hydrophobic interactions driving the selective LPS binding with the PCL NP surface. The hydrophobic interaction of LPS lipid tails with PCL NPs allows recruitment and assembly of LPS molecules on the NP surface. This process is synergized further due to the hydration of LPS polar head groups by the partially positively charged hydrogen ions of water. When LPS and PCL NPs are

introduced to a protein solution, water molecules may rearrange by forming hydrogen bonds surrounding the LPS-PCL nanoparticle complex shell, thus effectively secluding the access of proteins to the particles. Because of this unstable nature of partial hydrogen ion plane surrounding the LPS-PCL NP complexes as well as individual observations, a wide variation in standard deviation was measured in water. In contrast, the presence of lyotropic salts like sodium chloride in PBS interacts strongly with these water molecules thus leaving less water available for the shielding effect to take place.

The effect of different buffers at variable pH's and constant ionic strength was investigated (Figure. 6). Isoelectric point for LPS is at pH 2, hence LPS is negatively charged at pH > 2.80 PCL NPs, on the other hand, has an isoelectric point at around pH 4⁹⁶ and thus are positively charged at pH < 4 and negatively charged for pHs > 4. At pH 2.8 (acetic acid buffer), LPS would be negatively charged and PCL will have a positive charge, hence in addition to strong hydrophobic and van der Waals interaction, ionic interaction contributes towards LPS binding on PCL and thus a high LPS removal of ~90% was observed. The presence of acetate ion (CH_3COO^-) which is a lyotrope also helps in enhancing or promoting the hydrophobic interaction even further. As the buffer pH increases greater than 4, both PCL NPs and LPS exhibit negative charges due to their carbonyl and phosphate groups respectively. Based on these results, it can be concluded that in case of phosphate buffer (pH 5.8-8) the repulsion between LPS and PCL NPs dominates the hydrophobic and van der Waals interactions and therefore results in reasonably low LPS removal efficiency varying between 30-75%. For sodium bicarbonate buffer (pH 9.6), there was a sharp rise in LPS removal efficiency up to ~90%, indicating that the hydrophobic and van der Waals interaction dominates the

repulsion action between PCL and LPS molecules at high pH. One major advantage of the biocompatible PCL particles is that they can be reused for LPS binding quite effectively without a major loss in binding efficiency (Figure. 7).

The LPS removal efficiency is further increased when PCL NPs were incorporated into a CA membrane, resulting in an adsorptive membrane that delivers a productivity flowrate of up to $25 \frac{L}{m^2.h}$ (Figure. 9a and 9b).⁹⁷ The porous CA membrane structure (Figure. 8a) has a small thickness (Table S6) and a favorable pore size distribution to not require high pressure drops for water flow across the membrane. Further insight in this respect can be obtained from an analogy using the Hagen-Poiseuille equation,

$$\Delta P = \frac{\mu L q}{2\pi a^2} \quad (7)$$

where the pressure difference (ΔP) can be related to $\mu = \text{viscosity of water} = 8.9 \times 10^{-4} Pa.s$, $L = \text{membrane thickness} = 130 \times 10^{-6} m$, $q = \text{volumetric flow rate} = 25 \frac{L}{m^2.h} = 6.9 \times 10^{-6} m/s$ and $a = \text{pore diameter} = 0.17 \times 10^{-6} m$. The resultant ΔP is equivalent to a low value of 63 Pa, which confirms the unnecessary of any pumping device for the solution to pass through the membrane to allow the adsorption removal of LPS to take place on the inside by the PCL NPs.

It is worth mentioning here that one direction for future study is to optimize the membrane pore structure to achieve higher productivity flowrates without sacrificing the loading and adsorption capability of PCL NPs. Some possibilities⁹⁸ in this regard could

result from using more branched cellulose polymers, additives or cross-linkers, and templated casting surface. In addition, a very preliminary cost analysis was performed (Table I) to get an idea of the costs associated with manufacturing the PCL NP embedded CA membrane. The result was acceptably less than a dollar per cm^2 . However, more extensive and rigorous analysis is needed when an actual process is being designed or in operation, which needs to take into account labor, utilities, storage, and other process variables including potentially pumping devices.

5. CONCLUSION

In this study, we report first the synthesis of polymeric PCL NPs by employing a solvent evaporation method and then the performances of PCL NPs for the adsorption and removal of LPS. It was found that PCL NPs in powder form removed around 88% of LPS from the water sample. The presence of salts via the addition of PBS increased the LPS removal efficiency further up to 100% by PCL NPs, while maintaining 100% protein recovery from solutions. This high removal efficiency of LPS from water and PBS attributed to strong hydrophobic and van der Waals interaction. Buffers of variable pH play a very important role in determining the LPS binding on PCL. Acidic (pH 2.8) and alkaline (pH 9.6) buffers give ~ 90% LPS removal whereas intermediate pHs from 5.8 to 8 give reasonably lower % LPS removal between 30-75%. The adsorption efficiency reached almost 100% when PCL NPs were incorporated into the CA membrane where the water flow through the porous structure was directly by gravity without the requirement of any pumping devices. The biocompatible PCL NPs can be reused by

desorbing majority of adsorbed LPS using 0.2 N NaOH solution. A preliminary cost analysis showed that the manufacturing cost of the PCL NP embedded CA membrane is quite affordable. These findings coupled with PCL NP's known biodegradability support the potential of hybrid NP-membrane system to be used in large-scale operations that remove LPS efficiently and reduce the downstream process costs in biotechnological industries.

ACKNOWLEDGMENTS

This work was supported by Technology Acceleration Grant, Missouri S&T's Innovation Fund, Missouri S&T's Center for Research in Energy and Environment, and the PI's start-up funds. The assistance from Alexandria E. Lore and Dibhya Barua (undergraduate researchers) for the research work related to BODIPY assay is also acknowledged.

SUPPLEMENTARY INFORMATION

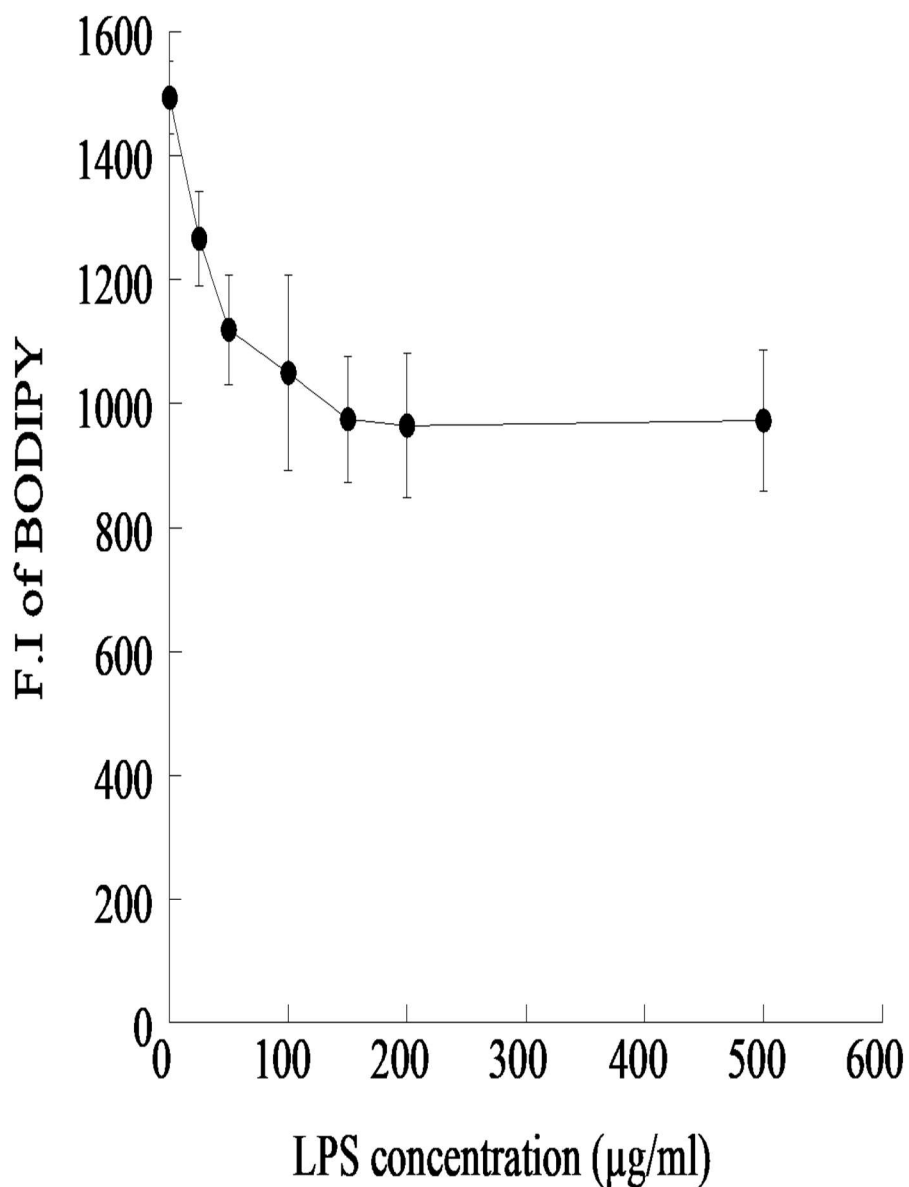


Figure S1. A standard curve to determine the optimum mass ratio of BODIPY : LPS interaction at different concentrations of LPS. BODIPY concentration was 262.11 µg/ml. Addition of LPS to BODIPY results in quenching due to binding of LPS to BODIPY sites. The binding saturates at 150 µg/ml endotoxin concentration. The optimum ratio of BOD: LPS was found to be 1.74.

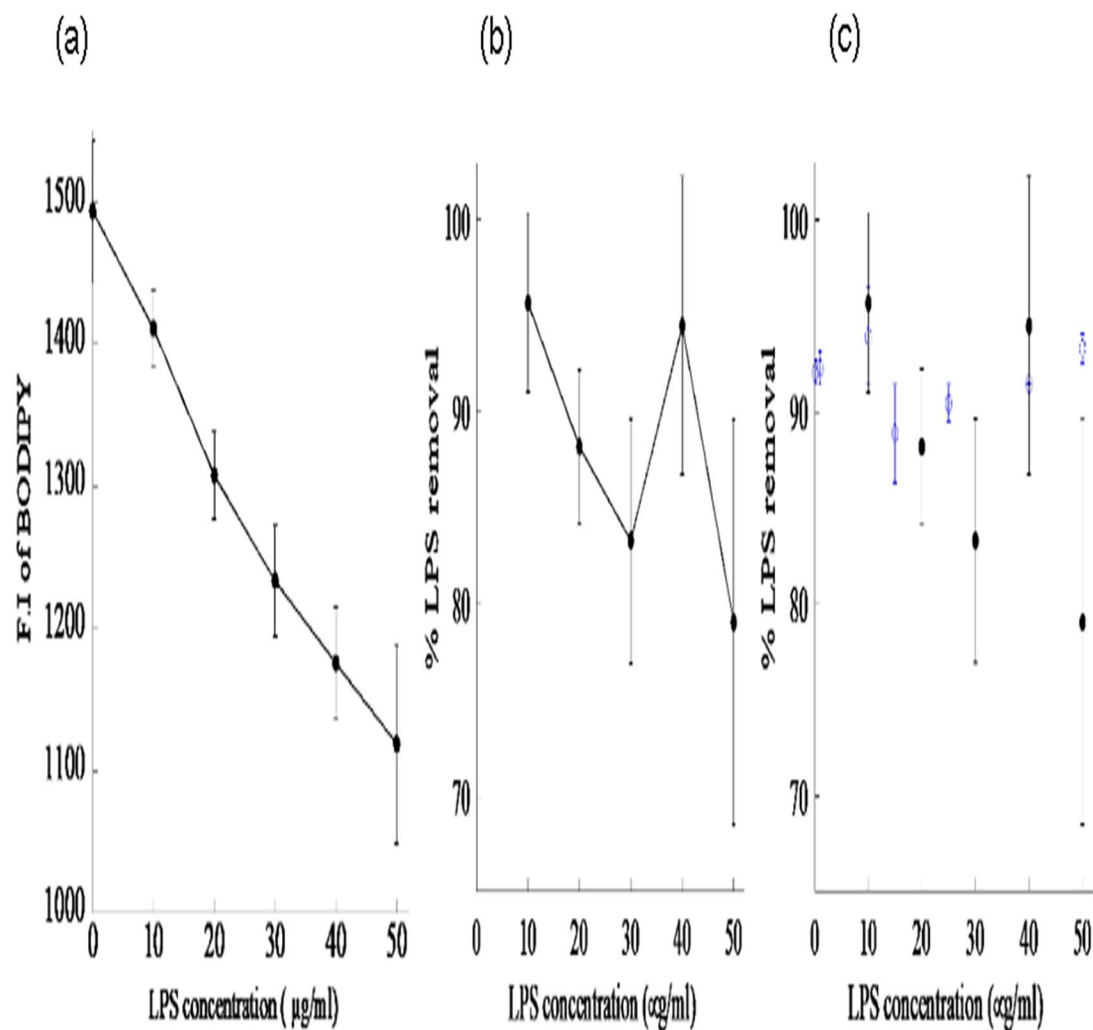


Figure S2. To confirm the linear correlation of the BODIPY assay standard curve for LPS detection (Figure S1) within the range of 0-50 $\mu\text{g/ml}$, the calibration curve was regenerated independently over the range of interest. (a) The BODIPY assay standard curve indeed shows a linear relationship at this low LPS concentration range. We further tested this new standard curve to calculate % LPS removal using LPS feed concentrations between 0-50 $\mu\text{g/ml}$. (b) The % LPS removal calculated using the correlation shown in (a). (c) The % LPS removal (solid circles) was compared with the values generated using Figure S1 (open circles) as shown in Figure 2 (b) in the main texts. The values from two independently generated standard curves were found to be evenly distributed and fit within the error range which ensured the preparation of the calibration standards.

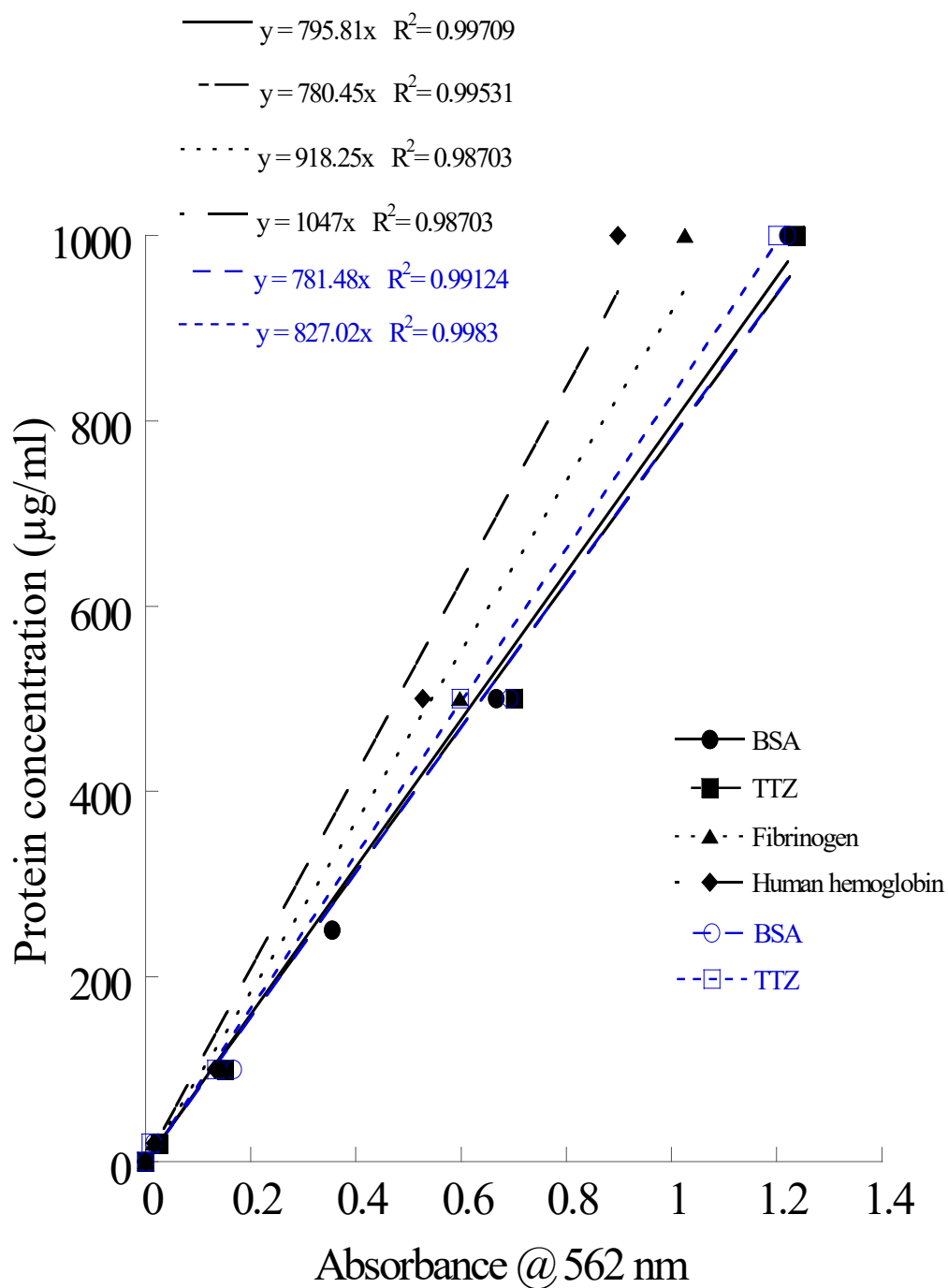


Figure S3. Protein standard curves of BSA and Trastuzumab (TTZ; Genentech) in water and PBS (pH 7.4) and Fibrinogen and Human hemoglobin in PBS (pH 7.4) were used to measure protein concentrations. R^2 represents the regression value.

Table S1. Buffer recipes of different pHs to study the effects of pH on LPS removal.

Buffer type (pH); ionic strength	Recipe
Glacial acetic acid buffer (2.8); 0.1M	Mix 5.72 ml of glacial acetic acid, 994.28 ml of DI water and 300 μ l of concentrated hydrochloric acid
Phosphate buffer (5.8); 0.1M	Mix 4 ml of 0.2 M sodium phosphate dibasic dihydrate ($\text{Na}_2\text{HPO}_4 \cdot 2\text{H}_2\text{O}$, FW=178.05) in water with 46 ml of 0.2 M sodium phosphate monobasic monohydrate ($\text{NaH}_2\text{PO}_4 \cdot \text{H}_2\text{O}$, FW=138.01) in water
Phosphate buffer (6.8); 0.1M	Mix 24.5 ml of 0.2 M sodium phosphate dibasic dihydrate ($\text{Na}_2\text{HPO}_4 \cdot 2\text{H}_2\text{O}$, FW=178.05) in water with 25.5 ml of 0.2 M sodium phosphate monobasic monohydrate ($\text{NaH}_2\text{PO}_4 \cdot \text{H}_2\text{O}$, FW=138.01) in water
Phosphate-buffered saline PBS (7.4); 0.1M	Mix 20 ml of 0.150 M PBS solution (137 mM NaCl, 10 mM phosphate, and 2.7 mM KCl) with 10 ml of DI water to obtain 30 ml 0.1 M PBS (91.4 mM NaCl, 6.7 mM phosphate, and 1.9 mM KCl)
Phosphate buffer (8.0); 0.1M	Mix 47.35 ml of 0.2 M sodium phosphate dibasic dihydrate ($\text{Na}_2\text{HPO}_4 \cdot 2\text{H}_2\text{O}$, FW=178.05) in water and 2.65 ml of 0.2 M sodium phosphate monobasic monohydrate ($\text{NaH}_2\text{PO}_4 \cdot \text{H}_2\text{O}$, FW=138.01) in water
Sodium bicarbonate buffer (9.6); 0.1M	Mix 8.4 g of sodium bicarbonate (NaHCO_3) with 991.6 ml of DI water



Figure S4. Experimental set up of a custom-made PVC column to sandwich CA membrane without and with PCL NPs in between two flow pipes. A piece of membrane was screw tightened between two flow pipes (top and bottom). Water and LPS containing water was fed on the top PVC pipe and let it flow by gravity. The permeability of membrane and % LPS removal were assessed using this set-up.

Table S2. The LPS binding capacity, endotoxin unit (EU) removed by per surface area and per milligram of PCL NPs in water. 1 EU \approx 0.1 – 0.2 ng of LPS.

LPS fed (endotoxin unit; EU)	PCL NP concentration (mg/ml)	PCL density (g/ml)	PCL NP diameter (μm)	# of PCL NPs/ml	PCL NPs ⁺ surface area/ml (cm ² /ml)	LPS removed (EU) /cm ² NPs	LPS removed (EU) /mg of PCL NPs
1.5×10^6	1	1.1	0.7	3.3×10^9	65	20.4×10^3	1.3×10^6
1.25×10^6						16.2×10^3	1.0×10^6
1.0×10^6						12.4×10^3	0.8×10^6
0.75×10^6						9.8×10^3	0.6×10^6
0.5×10^6						7.1×10^3	0.5×10^6
4.0×10^5						5.6×10^3	3.7×10^5
2.5×10^5						3.0×10^3	2.3×10^5
1.5×10^4						2.0×10^3	1.3×10^5
1.0×10^5						1.45×10^3	9.4×10^4
1.0×10^4						1.4×10^2	9.2×10^3
1.0×10^3						14.0	9.2×10^2

Table S3. The LPS binding capacity (EU/cm² and EU/mg) by PCL NPs from varying BSA concentrations in PBS (pH 7.4) when treated with a fixed concentration of LPS (150 µg/ml $\approx 1.5 \times 10^6$ EU/ml). 1 EU $\approx 0.1 - 0.2$ ng of LPS.

BSA concentration (µg/ml)	PCL NP concentration (mg/ml)	PCL density (g/ml)	PCL NP diameter (µm)	# of PCL NPs/ml	PCL NPs' surface area/ml (cm ² /ml)	LPS removed (EU) /cm ² NPs	LPS removed (EU) /mg of PCL NPs
250	1	1.1	0.7	3.2×10^9	65	21.0×10^3	1.4×10^6
500						21.5×10^3	1.4×10^6
1000						22.0×10^3	1.4×10^6

Table S4. LPS binding capacity (EU/cm² and EU/mg) by PCL NPs from varying Trastuzumab concentrations in PBS (pH 7.4) when treated with a fixed concentration of LPS (150 µg/ml $\approx 1.5 \times 10^6$ EU/ml).

TTZ concentration (µg/ml)	PCL NP concentration (mg/ml)	PCL density (g/ml)	PCL NP diameter (µm)	# of PCL NPs/ml	PCL NPs' surface area/ml (cm ² /ml)	LPS removed (EU) /cm ² NPs	LPS removed (EU) /mg of PCL NPs
250	1	1.1	0.7	3.2×10^9	65	22×10^3	1.4×10^6
500						22×10^3	1.4×10^6
1000						22×10^3	1.4×10^6

Table S5. LPS binding capacity (EU/cm² and EU/mg) by PCL NPs from varying Fibrinogen concentrations in PBS (pH 7.4) when treated with a fixed concentration of LPS (150 µg/ml \approx 1.5 \times 10⁶ EU/ml).

Fibrinogen concentration (µg/ml)	PCL NP concentration (mg/ml)	PCL density (g/ml)	PCL NP diameter (µm)	# of PCL NPs/ml	PCL NPs' surface area/ml (cm ² /ml)	LPS removed (EU)/cm ² NPs	LPS removed (EU)/mg of PCL NPs
250	1	1.1	0.7	3.2 \times 10 ⁹	65	21 \times 10 ³	1.4 \times 10 ⁶
500						20 \times 10 ³	1.3 \times 10 ⁶
1000						21 \times 10 ³	1.4 \times 10 ⁶

Table S6. LPS binding capacity (EU/cm² and EU/mg) by PCL NPs from varying Human hemoglobin concentrations in PBS (pH 7.4) when treated with a fixed concentration of LPS (150 µg/ml \approx 1.5 \times 10⁶ EU/ml).

Human Hemoglobin concentration (µg/ml)	PCL NP concentration (mg/ml)	PCL density (g/ml)	PCL NP diameter (µm)	# of PCL NPs/ml	PCL NPs' surface area/ml (cm ² /ml)	LPS removed (EU)/cm ² NPs	LPS removed (EU)/mg of PCL NPs
250	1	1.1	0.7	3.2 \times 10 ⁹	65	21 \times 10 ³	1.3 \times 10 ⁶
500						19 \times 10 ³	1.2 \times 10 ⁶
1000						19 \times 10 ³	1.2 \times 10 ⁶

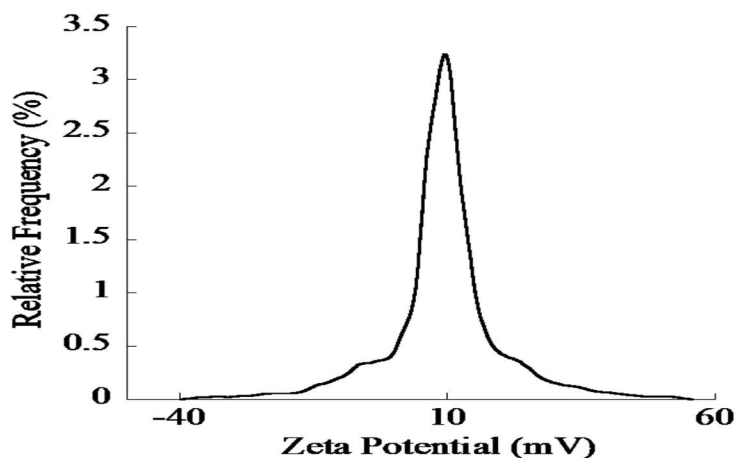
Table S7. Comparison of adsorption isotherms of LPS removal with literature values.

LPS binding material	LPS Feed range (EU/ml)	Langmuir isotherm parameters			Freundlich isotherm parameters		
		q _s (μg LPS/mg)	K (ml solution/mg)	R ²	K (μg LPS/mg PCL NPs)	n	R ²
PCL NPs	10 ³ – 5 × 10 ⁶ (in water)	-	-	-	9.5	1.1	0.95
PCL NPs	10 ⁴ – 1.5 × 10 ⁶ (BSA in water)	-	-	-	7.6	1.3	0.99
PCL NPs	10 ⁴ – 1.5 × 10 ⁶ (IgG in water)	-	-	-	8.7	1.4	0.93
PCL NPs	10 ⁴ – 1.5 × 10 ⁶ (BSA in PBS)	-	-	-	13	1.2	0.99
PCL NPs	10 ⁴ – 1.5 × 10 ⁶ (IgG in PBS)	-	-	-	11.7	1.3	0.98
PMB-CL-CMs	1–100	3.6 × 10 ⁻⁴	6.5 × 10 ⁶	0.99	-	-	-
Si gel-His	10 ³ – 6 × 10 ⁴	1.2	740	0.90	-	-	-
Agarose	10 – 1.8 × 10 ⁷	3300	56	0.99	-	-	-
Bone Char	1–100	2.9 × 10 ⁻⁶	9.0 × 10 ⁻¹¹	0.99	-	-	-

PMB-CL-CMs= Polymyxin B immobilized cross-linked cellulose microspheres

Si gel-His= Histidine immobilized silica gel

(a)



(b)

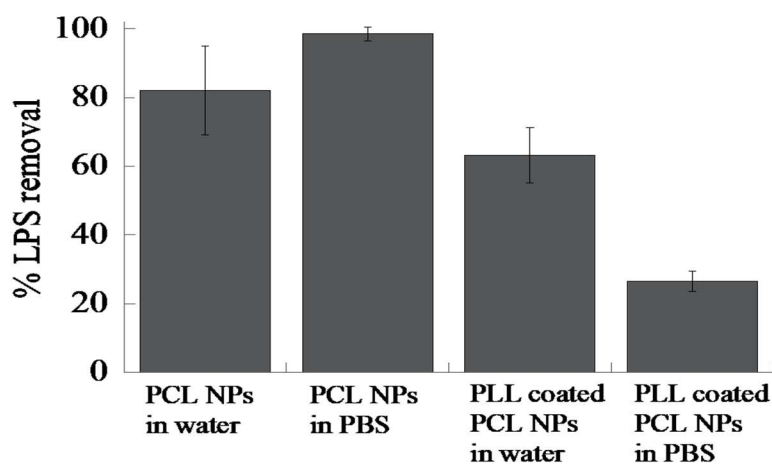


Figure S5. Zeta potential and LPS removal efficiency of poly-l-lysine (PLL) coated PCL NPs. (a) The surface zeta potential of positively charged PLL coated PCL NPs which confirmed the clear shift in surface charge towards (10 ± 0.3) mV from (-20 ± 5) mV of bare PCL NPs (Figure 1(c)). (b) The PLL coated PCL NPs showed ~20 and 80% reduction in % LPS removal in water and PBS, respectively compared to bare PCL NPs indicating the cationic charges on the surface of PCL NPs decreased the interaction of LPS with the NP surface.

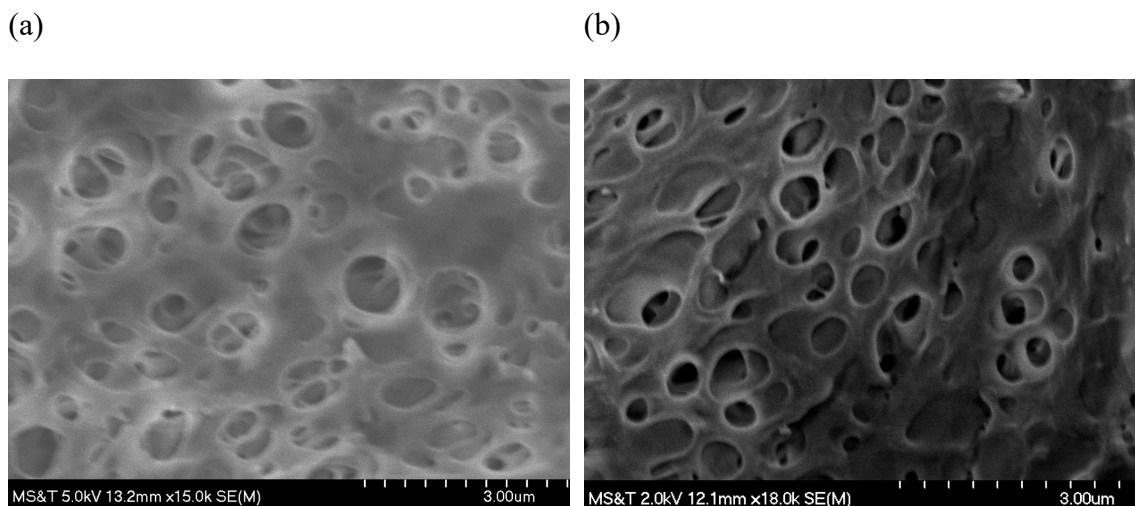


Figure S6. Surface SEM morphology of CA membrane (a) without and (b) with PCL NPs.

Table S8. Calculations of CA membrane thickness and pore size with and without PCL NPs.

Membrane type	Membrane thickness ($\mu\text{m} \pm \text{S.D.}$)	Surface pore diameter ($\mu\text{m} \pm \text{S.D.}$)
CA Membrane	116 ± 2	0.16 ± 0.05
CA Membrane with PCL NPs	132 ± 12	0.17 ± 0.05

Table S9. Detailed calculations of EU removed by PCL NPs impregnated in CA membrane.

PCL NPs present in the membrane (mg)/membrane	Endotoxins fed (endotoxin unit; EU)	LPS removed (EU)/cm ²	LPS removed (EU)/mg of PCL NPs
3.0 ± 1.2	8.5×10^6	42.6×10^3	2.8×10^6

REFERENCES

1. Walsh, G. Biopharmaceutical benchmarks 2010. *Nature Biotechnology* 28, 917 (2010).
2. Overton, T.W. Recombinant protein production in bacterial hosts. *Drug Discovery Today* 19, 590-601 (2014).
3. Huang, C.-J., Lin, H. & Yang, X. Industrial production of recombinant therapeutics in *Escherichia coli* and its recent advancements. *Journal of Industrial Microbiology & Biotechnology* 39, 383-399 (2012).
4. Terpe, K. Overview of bacterial expression systems for heterologous protein production: from molecular and biochemical fundamentals to commercial systems. *Applied Microbiology and Biotechnology* 72, 211 (2006).
5. Van Belleghem, J.D., Merabishvili, M., Vergauwen, B., Lavigne, R. & Vanechoutte, M. A comparative study of different strategies for removal of endotoxins from bacteriophage preparations. *Journal of Microbiological Methods* 132, 153-159 (2017).
6. Johnson, I.S. Human insulin from recombinant DNA technology. *Science* 219, 632-637 (1983).
7. Gorbet, M.B. & Sefton, M.V. Endotoxin: the uninvited guest. *Biomaterials* 26, 6811-6817 (2005).
8. Magalhães, P.O., *et al.* Methods of endotoxin removal from biological preparations: a review. *J Pharm Pharm Sci* 10, 388-404 (2007).
9. Bosshart, H. & Heinzelmann, M. Targeting bacterial endotoxin. *Annals of the New York Academy of Sciences* 1096, 1-17 (2007).
10. Frattari, A., *et al.* Recurring septic shock in a patient with blunt abdominal and pelvic trauma: How mandatory is source control surgery?: A case report. *Journal of Medical Case Reports* 11(2017).
11. Stasi, A., *et al.* Emerging role of Lipopolysaccharide binding protein in sepsis-induced acute kidney injury. *Nephrology Dialysis Transplantation* 32, 24-31 (2017).

12. London, A.S., Mackay, K., Lihon, M., He, Y. & Alabi, B.R. Gel filtration chromatography as a method for removing bacterial endotoxin from antibody preparations. *Biotechnology Progress* 30, 1497-1501 (2014).
13. Saraswat, M., *et al.* Preparative Purification of Recombinant Proteins: Current Status and Future Trends. *BioMed Research International* 2013, 18 (2013).
14. Diogo, M.M., Queiroz, J.A. & Prazeres, D.M.F. Chromatography of plasmid DNA. *Journal of Chromatography A* 1069, 3-22 (2005).
15. Mohammadian-Mosaabadi, J., *et al.* Improving purification of recombinant human interferon γ expressed in *Escherichia coli*; effect of removal of impurity on the process yield. *Protein Expression and Purification* 51, 147-156 (2007).
16. Anne, S.L., Brendan, K., R., T.W. & Kasey, M. Endotoxin removal and prevention for pre-clinical biologics production. *Biotechnology Journal* 7, 1509-1516 (2012).
17. Lowe, A.J., Bardliving, C.L. & Batt, C.A. Methods for chromatographic removal of endotoxin. in *Methods in Molecular Biology*, Vol. 899 265-275 (2012).
18. Ghose, S., Hubbard, B. & Cramer, S.M. Binding capacity differences for antibodies and Fc-fusion proteins on protein A chromatographic materials. *Biotechnology and Bioengineering* 96, 768-779 (2007).
19. Hou, Y., Jiang, C., Shukla, A.A. & Cramer, S.M. Improved process analytical technology for protein a chromatography using predictive principal component analysis tools. *Biotechnology and Bioengineering* 108, 59-68 (2011).
20. Naik, A.D., *et al.* Silica resins and peptide ligands to develop disposable affinity adsorbents for antibody purification. *Biochemical Engineering Journal*, 53-61 (2019).
21. Zeman, L.J. & Zydney, A.L. *Microfiltration and ultrafiltration: principles and applications*, (CRC Press, 2017).
22. Van Reis, R. & Zydney, A. Membrane separations in biotechnology. *Current Opinion in Biotechnology* 12, 208-211 (2001).
23. Wu, Q., *et al.* Fabrication of membrane absorbers based on amphiphilic carbonaceous derivatives for selective endotoxin clearance. *Journal of Materials Chemistry B* 5, 8219-8227 (2017).

24. Zong, W., *et al.* Preparation of PVA/amino multi-walled carbon nanotubes nanocomposite microspheres for endotoxin adsorption. *Artificial cells, nanomedicine, and biotechnology* 46, 185-191 (2018).
25. Kish, W.S., *et al.* Purification of human erythropoietin by affinity chromatography using cyclic peptide ligands. *Journal of Chromatography B: Analytical Technologies in the Biomedical and Life Sciences* 1085, 1-12 (2018).
26. Liu, Z., Gurgel, P.V. & Carbonell, R.G. Purification of human immunoglobulins A, G and M from Cohn fraction II/III by small peptide affinity chromatography. *Journal of Chromatography A* 1262, 169-179 (2012).
27. Menegatti, S., Naik, A.D., Gurgel, P.V. & Carbonell, R.G. Purification of polyclonal antibodies from Cohn fraction II + III, skim milk, and whey by affinity chromatography using a hexamer peptide ligand. *Journal of Separation Science* 35, 3139-3148 (2012).
28. Zhang, Y., Rojas, O.J. & Carbonell, R.G. Nanofibrillated cellulose as carrier for short peptides assemblies for human IgG detection and affinity separation. in *TAPPI International Conference on Nanotechnology 2013* 802-811 (2013).
29. Romaschin, A.D., Obiezu-Forster, C.V., Shoji, H. & Klein, D.J. Novel Insights into the Direct Removal of Endotoxin by Polymyxin B Hemoperfusion. *Blood Purification* 44, 193-197 (2017).
30. Saito, H., Tagawa, M., Takahashi, Y., Morimoto, T. & Takahashi, S. Efficacy of polymyxin B-immobilized fiber column direct hemoperfusion for non-endotoxin-associated severe septic shock. *Pediatrics International* 58, 1346-1347 (2016).
31. Ryder, M.P., Wu, X., McKelvey, G.R., McGuire, J. & Schilke, K.F. Binding interactions of bacterial lipopolysaccharide and the cationic amphiphilic peptides polymyxin B and WLBU2. *Colloids and Surfaces B: Biointerfaces* 120, 81-87 (2014).
32. Mitaka, C., *et al.* Polymyxin B-immobilized fiber column hemoperfusion removes endotoxin throughout a 24-hour treatment period. *Journal of Critical Care* 29, 728-732 (2014).
33. Zhang, J., Zhu, C. & Fan, D. Endotoxin removal from recombinant human-like collagen preparations by triton X-114 two-phase extraction. *Biotechnology* 12, 135-139 (2014).
34. Gun'ko, V.M., Betz, W.R., Patel, S., Murphy, M.C. & Mikhalovsky, S.V. Adsorption of lipopolysaccharide on carbon sieves. *Carbon* 44, 1258-1262 (2006).

35. Rapala, J., *et al.* Endotoxins associated with cyanobacteria and their removal during drinking water treatment. *Water Research* 36, 2627-2635 (2002).
36. Mendiola, L.R., *et al.* Purification of bacterial endotoxins by zonal centrifugation. *Infection and immunity* 6, 27-31 (1972).
37. Hobb, R.I., Fields, J.A., Burns, C.M. & Thompson, S.A. Evaluation of procedures for outer membrane isolation from *Campylobacter jejuni*. *Microbiology (Reading, England)* 155, 979-988 (2009).
38. Klimentová, J. & Stulík, J. Methods of isolation and purification of outer membrane vesicles from gram-negative bacteria. *Microbiological Research* 170, 1-9 (2015).
39. Branston, S.D., Wright, J. & Keshavarz-Moore, E. A non-chromatographic method for the removal of endotoxins from bacteriophages. *Biotechnology and Bioengineering* 112, 1714-1719 (2015).
40. Ma, R., Zhao, J., Du, H.C., Tian, S. & Li, L.W. Removing endotoxin from plasmid samples by Triton X-114 isothermal extraction. *Analytical Biochemistry* 424, 124-126 (2012).
41. Teodorowicz, M., *et al.* Optimized Triton X-114 assisted lipopolysaccharide (LPS) removal method reveals the immunomodulatory effect of food proteins. *PloS one* 12, e0173778 (2017).
42. de Almeida, K.M., Almeida, M.M., Fingola, F.F. & Ferraz, H.C. Membrane adsorber for endotoxin removal. *Brazilian Journal of Pharmaceutical Sciences* 52, 171-177 (2016).
43. Kontana, A., Papadimitriou, C.A., Samaras, P., Zdragas, A. & Yiangou, M. Effectiveness of ozonation and chlorination on municipal wastewater treatment evaluated by a battery of bioassays and biomarkers. *Water Science and Technology* 60, 1497-1505 (2009).
44. Lambadi, P.R., *et al.* Facile biofunctionalization of silver nanoparticles for enhanced antibacterial properties, endotoxin removal, and biofilm control. *International Journal of Nanomedicine* 10, 2155-2171 (2015).
45. Lee, J.J., *et al.* Synthetic ligand-coated magnetic nanoparticles for microfluidic bacterial separation from blood. *Nano Letters* 14, 1-5 (2014).
46. Darkow, R., Groth, T., Albrecht, W., Lützow, K. & Paul, D. Functionalized nanoparticles for endotoxin binding in aqueous solutions. *Biomaterials* 20, 1277-1283 (1999).

47. Prasad, P., Sachan, S., Suman, S., Swayambhu, G. & Gupta, S. Regenerative Core–Shell Nanoparticles for Simultaneous Removal and Detection of Endotoxins. *Langmuir* 34, 7396-7403 (2018).
48. Ghosh, R. Protein separation using membrane chromatography: opportunities and challenges. *Journal of Chromatography A* 952, 13-27 (2002).
49. Orr, V., Zhong, L., Moo-Young, M. & Chou, C.P. Recent advances in bioprocessing application of membrane chromatography. *Biotechnol Adv* 31, 450-465 (2013).
50. Muthukumar, S., Muralikrishnan, T., Mendhe, R. & Rathore, A.S. Economic benefits of membrane chromatography versus packed bed column purification of therapeutic proteins expressed in microbial and mammalian hosts. *Journal of Chemical Technology & Biotechnology* 92, 59-68 (2017).
51. Danafar, H. & Schumacher, U. MPEG-PCL copolymeric nanoparticles in drug delivery systems. *Cogent Medicine* 3(2016).
52. Jia, W., *et al.* Preparation of biodegradable polycaprolactone/poly (ethylene glycol)/polycaprolactone (PCEC) nanoparticles. *Drug Deliv* 15, 409-416 (2008).
53. Malikmammadov, E., Tanir, T.E., Kiziltay, A., Hasirci, V. & Hasirci, N. PCL and PCL-based materials in biomedical applications. *J Biomater Sci Polym Ed*, 1-31 (2017).
54. Rao, J.P. & Geckeler, K.E. Polymer nanoparticles: preparation techniques and size-control parameters. *Progress in polymer science* 36, 887-913 (2011).
55. Mendoza-Muñoz, N., Alcalá-Alcalá, S. & Quintanar-Guerrero, D. Preparation of Polymer Nanoparticles by the Emulsification-Solvent Evaporation Method: From Vanderhoff's Pioneer Approach to Recent Adaptations. in *Polymer Nanoparticles for Nanomedicines* 87-121 (Springer, 2016).
56. Badri, W., Miladi, K., Nazari, Q.A., Fessi, H. & Elaissari, A. Effect of process and formulation parameters on polycaprolactone nanoparticles prepared by solvent displacement. *Colloids and Surfaces A: Physicochemical and Engineering Aspects* 516, 238-244 (2017).
57. Vauthier, C. & Ponchel, G. *Polymer Nanoparticles for Nanomedicines*, (Springer, 2017).
58. Donnell, M.L., Lyon, A.J., Mormile, M.R. & Barua, S. Endotoxin hitchhiking on polymer nanoparticles. *Nanotechnology* 27, 285601 (2016).

59. Stewart J. Wood, K.A.M., and Sunil A. David. Anti-Endotoxin Agents. 1. Development of a Fluorescent Probe displacement method optimized for high throughput identification of Lipopolysaccharide-Binding Agents. *Combinatorial Chemistry & High Throughput Screening* 7(2004).
60. Stoll, V.S. & Blanchard, J.S. [4] Buffers: Principles and practice. in *Methods in enzymology*, Vol. 182 24-38 (Elsevier, 1990).
61. Ferguson, W.J., *et al.* Hydrogen ion buffers for biological research. *Analytical biochemistry* 104, 300-310 (1980).
62. Good, N.E., *et al.* Hydrogen ion buffers for biological research. *Biochemistry* 5, 467-477 (1966).
63. Lv, C., *et al.* Enhanced permeation performance of cellulose acetate ultrafiltration membrane by incorporation of Pluronic F127. *Journal of membrane science* 294, 68-74 (2007).
64. Vos, K.D. & Burris Jr, F. Drying cellulose acetate reverse osmosis membranes. *Industrial & Engineering Chemistry Product Research and Development* 8, 84-89 (1969).
65. Ferlita, R.R., Phipps, D., Safarik, J. & Yeh, D.H. Cryo-snap: A simple modified freeze-fracture method for SEM imaging of membrane cross-sections. *Environmental Progress* 27, 204-209 (2008).
66. McCue, J.T. Theory and use of hydrophobic interaction chromatography in protein purification applications. in *Methods in enzymology*, Vol. 463 405-414 (Elsevier, 2009).
67. Lee, S.-H., Kim, J.-S. & Kim, C.-W. Optimization of buffer conditions for the removal of endotoxins using Q-sepharose. *Process Biochemistry* 38, 1091-1098 (2003).
68. Luey, J.K., McGuire, J. & Sproull, R.D. The effect of pH and NaCl concentration on adsorption of beta-lactoglobulin at hydrophilic and hydrophobic silicon surfaces *Journal of Colloid and Interface Science* 143, 489-500 (1991).
69. Maitra, S.K., Yoshikawa, T.T., Guze, L. & Schotz, M. Properties of binding of Escherichia coli endotoxin to various matrices. *Journal of clinical microbiology* 13, 49-53 (1981).
70. Tomaz, C.T. Hydrophobic interaction chromatography. in *Liquid Chromatography (Second Edition)* 171-190 (Elsevier, 2017).

71. Blitz, J.P. & Gun'ko, V.M. *Surface chemistry in biomedical and environmental science*, (Springer Science & Business Media, 2006).
72. Webb, S.D., Cleland, J.L., Carpenter, J.F. & Randolph, T.W. A new mechanism for decreasing aggregation of recombinant human interferon- γ by a surfactant: Slowed dissolution of lyophilized formulations in a solution containing 0.03% polysorbate 20. *Journal of Pharmaceutical Sciences* 91, 543-558 (2002).
73. Foo, K.Y. & Hameed, B.H. Insights into the modeling of adsorption isotherm systems. *Chemical engineering journal* 156, 2-10 (2010).
74. Chen, X. Modeling of experimental adsorption isotherm data. *Information* 6, 14-22 (2015).
75. Liu, D., *et al.* Adsorption behavior of heavy metal ions from aqueous solution by soy protein hollow microspheres. *Industrial & Engineering Chemistry Research* 52, 11036-11044 (2013).
76. Zhang, Y., Yang, H., Zhou, K. & Ping, Z. Synthesis of an affinity adsorbent based on silica gel and its application in endotoxin removal. *Reactive and Functional Polymers* 67, 728-736 (2007).
77. Cao, X., Zhu, B., Zhang, X. & Dong, H. Polymyxin B immobilized on cross-linked cellulose microspheres for endotoxin adsorption. *Carbohydrate Polymers* 136, 12-18 (2016).
78. Wei, Z., Huang, W., Hou, G., Yuan, Z. & Fang, J. Studies on adsorption isotherms of endotoxin and BSA using an affinity column. *Process Biochemistry* 42, 285-288 (2007).
79. Rezaee, A., Ghanizadeh, G., Behzadiyannejad, G., Yazdanbakhsh, A. & Siyadat, S.D. Adsorption of Endotoxin from Aqueous Solution Using Bone Char. *Bulletin of Environmental Contamination and Toxicology* 82, 732-737 (2009).
80. Shi, Y., HogenEsch, H., Regnier, F.E. & Hem, S.L. Detoxification of endotoxin by aluminum hydroxide adjuvant. *Vaccine* 19, 1747-1752 (2001).
81. Chandler, D. Interfaces and the driving force of hydrophobic assembly. *Nature* 437, 640 (2005).
82. Fung, E.S., Unice, K.M., Paustenbach, D.J., Finley, B.L. & Kovoichich, M. Methods for Sterilizing Clinically Relevant Wear Particles Isolated from Metal-on-Metal Hip Implants. *Scientific reports* 8, 2384 (2018).

83. Healthcare, G. Use of sodium hydroxide for cleaning and sanitizing chromatography media and systems. (Application note 18-1124-57 AE, 2006).
84. Ng, P.K. & McLaughlin, V. Regeneration studies of anion-exchange chromatography resins. *BioProcess International* 5, 52 (2007).
85. Abedini, R., Mousavi, S.M. & Aminzadeh, R. A novel cellulose acetate (CA) membrane using TiO₂ nanoparticles: preparation, characterization and permeation study. *Desalination* 277, 40-45 (2011).
86. Mansourpanah, Y., *et al.* Fabrication new PES-based mixed matrix nanocomposite membranes using polycaprolactone modified carbon nanotubes as the additive: property changes and morphological studies. *Desalination* 277, 171-177 (2011).
87. El Badawi, N., Ramadan, A.R., Esawi, A.M. & El-Morsi, M. Novel carbon nanotube–cellulose acetate nanocomposite membranes for water filtration applications. *Desalination* 344, 79-85 (2014).
88. Liao, Y., *et al.* Highly dispersible polypyrrole nanospheres for advanced nanocomposite ultrafiltration membranes. *Materials Horizons* 1, 58-64 (2014).
89. Guo, J. & Kim, J. Modifications of polyethersulfone membrane by doping sulfated-TiO₂ nanoparticles for improving anti-fouling property in wastewater treatment. *RSC Advances* 7, 33822-33828 (2017).
90. Saljoughi, E., Sadrzadeh, M. & Mohammadi, T. Effect of preparation variables on morphology and pure water permeation flux through asymmetric cellulose acetate membranes. *Journal of Membrane Science* 326, 627-634 (2009).
91. Su, J., Yang, Q., Teo, J.F. & Chung, T.-S. Cellulose acetate nanofiltration hollow fiber membranes for forward osmosis processes. *Journal of Membrane Science* 355, 36-44 (2010).
92. Gasemloo, S., Khosravi, M., Sohrabi, M.R., Dastmalchi, S. & Gharbani, P. Fabrication of sulfated nanofilter membrane based on carboxymethyl cellulose. *Water Science and Technology* (2016).
93. Krason, J. & Pietrzak, R. Membranes obtained on the basis of cellulose acetate and their use in removal of metal ions from liquid phase. in *Polish Journal of Chemical Technology*, Vol. 18 104 (2016).
94. Tallarek, U., Vergeldt, F.J. & As, H.V. Stagnant Mobile Phase Mass Transfer in Chromatographic Media: Intraparticle Diffusion and Exchange Kinetics. *The Journal of Physical Chemistry B* 103, 7654-7664 (1999).

95. Zhang, H., *et al.* Fabrication of hydrophilic and hydrophobic site on polypropylene nonwoven for removal of bisphenol a from water: explorations on adsorption behaviors, mechanisms and configurational influence. *Journal of Polymer Research* 24, 171 (2017).
96. Jesus, S., Borchard, G. & Borges, O. Freeze dried chitosan/poly- ϵ -caprolactone and poly- ϵ -caprolactone nanoparticles: evaluation of their potential as DNA and antigen delivery systems. *J Genet Syndr Gene Ther* 4, 2 (2013).
97. Sakata, M., *et al.* Aminated Cellulose Nanofibers for Selective Removal of Endotoxins from Protein Solutions. *Chemistry Letters* 46, 194-196 (2017).
98. Wang, J.C., Bruttini, R. & Liapis, A.I. Molecular Dynamics Modeling and Simulation Studies of the Effects of Additive Solutes on the Dehydration and Rehydration of Polymeric Porous Media. *Industrial & Engineering Chemistry Research* 55, 6649-6660 (2016).

II. UNDERSTANDING THE MECHANISM OF INTERACTION BETWEEN ENDOTOXIN AND POLYMER NANOPARTICLE

Sidharth Razdan, Justin Adler, Jee-Ching Wang and Sutapa Barua

Department of Chemical and Biochemical Engineering, Missouri University of Science
and Technology, Rolla, MO 65409

Tel: 573-341-7551

Email: baruas@mst.edu

ABSTRACT

Endotoxin removal from therapeutic solutions is a challenging task for the biopharmaceutical industries. Currently, approximately one- third of all therapeutics are produced from biological sources like *Escherichia coli* and *Salmonella*. In addition to the useful bio therapeutics these *E. coli* cells also release endotoxins in the surrounding media thus contaminating the life-saving therapeutics. Hence, these therapeutic products need to be thoroughly purified before being used for any parenteral applications. It was demonstrated that biocompatible polymeric PCL NPs ($d_p \sim 800 \text{ nm}$) were effective in removing endotoxins from aqueous solutions with a removal efficiency $\sim 98 \%$ in phosphate buffer saline (PBS) and protein recovery of $\sim 100 \%$. The goal of this work was to test the validity of the hypothesis that synergistic combination of van der Waals and hydrophobic interactions were responsible for endotoxin binding on polycaprolactone (PCL) nanoparticle's (NPs) surface. This hypothesis was tested by evaluating endotoxin removal efficiency of a material which shows surface hydrophobicity similar to that of PCL NPs. Polystyrene (PS) nanoparticles, $\sim 800 \text{ nm}$,

with surface properties similar to PCL NPs were used as a control to test the hypothesis. Additionally, this work demonstrated that acidic (pH 2.8) and basic (pH 11.5) conditions do not have a major impact on protein recovery using PCL NPs. Six different types of proteins with molecular weights varying from 14 kDa - 341 kDa and isoelectric points (pI) from 4.5-10.7 showed protein recovery > 92 % under extreme operating pH. Finally, in order to increase the throughput and address the mass transfer limitations, the PCL NPs incorporated cellulose acetate (CA) biofilter were synthesized and applied to different protein solutions with a maximum endotoxin removal efficiency ~ 99 % and protein recovery >92 %.

1. INTRODUCTION

The source of one-third of all biotherapeutics, presently, is gram-negative bacteria^[1, 2] for example, *Escherichia coli* and *Salmonella*. Endotoxins are the primary and most toxic components located on the outer cell membrane of these gram-negative bacteria.^[3-8] As a result, while extracting biotherapeutics from these bacteria, endotoxins also get tagged along. It, therefore, requires thorough purification and polishing steps before being used for parenteral applications.^[2,9-11] Endotoxin structure comprises polar heteropolysaccharide chains that are covalently bonded to the non-polar lipid-A moiety.^[3-8, 12] Lipid-A tail is responsible for anchoring and providing mechanical stability to the endotoxin molecule in the cell membrane.^[3, 8, 12] Removing undesirable contaminants like endotoxins from biologically derived therapeutic products thus is a challenging task for biopharmaceutical engineers. Isoelectric point (pI) of endotoxin molecules is at pH 2,

thus in most biological solutions endotoxin structure comprises a hydrophobic lipid tail and a negatively charged phosphate group. Therefore, both ionic^[7, 13-17] (ion exchange chromatography) and hydrophobic interactions^[18, 19] (hydrophobic interaction chromatography) are widely utilized to bind and remove endotoxins from biological solutions. Endotoxin binding mechanism on the ligand surface is dependent on the ionic strength of the liquid media. In liquid media with low high ionic strength binding is mainly dominated by charge based ionic interaction which weakens in presence of salt ions. On the other hand, in conditions of higher ionic strength (PBS; 150 mM), interactions driven by hydrophobicity and van der Waals binding are more impactful.^[20]

In literature different types of interactions have been highlighted to remove endotoxins from biological solutions. For example, bare polymeric nanoparticles and adsorbent crystals like polycaprolactone nanoparticles (PCL NPs)^[21] and allantoin^[22] (2,5-dioxo-4-imidazolidinyl urea) have shown high endotoxin removal efficiency of > 98 %. These adsorbents also provide high protein recovery of > 92 % and ~ 80 % respectively, hence making these a viable alternative to remove endotoxins from protein solutions. PCL NPs have been reported to utilize van der Waals and hydrophobic interactions^[21] to bind endotoxins whereas endotoxin binding on allantoin surface is mediated by hydrogen bonding.^[22] In addition to the bare particles, different types of endotoxin-selective ligands have been grafted, immobilized or coated on the surface of metallic or polymeric matrices to devise a viable endotoxin binding material. For example, chitosan-iron oxide nanocomposites have also been very effective at binding negatively charged endotoxins from various protein solutions due to their positive charge from chitosan.^[12] It provides an endotoxin removal of > 99 % and a protein recovery > 90

%.^[12] Polymyxin-B is another such ligand which finds widespread application in endotoxin binding. Polymyxin-B coated silver nanoparticles have been shown to remove > 97 % endotoxins from aqueous solutions.^[23] These coated silver particles utilize ionic interaction between the phosphate ion on endotoxin and cationic peptide on polymyxin-B. Polymyxin-B with other ligands like polyethyleneimine (PEI), histamine and tetracaine have been used to modify surface of polystyrene core and polyglycidyl methacrylate shell based polymeric nanoparticles to use these as an endotoxin binding material.^[20] The modified nanoparticles have been shown to have an endotoxin removal efficiency of around 90 % from water and salt solutions. They utilize van der Waals, hydrophobic and ionic interactions to bind endotoxin on their surface. Additionally, grafting of long carbon chain on nanoparticle surface to induce hydrophobicity has also been utilized in many cases. One such system comprised of long C18 acyl chains attached to Fe₃O₄/Au/Fe₃O₄ nanoflowers (NFs). These NFs utilize hydrophobic interaction between the lipid-A part and C-18 chains to carry out endotoxin removal effectively.^[24]

Even though porous resins (with or without ligands) based techniques are effective at binding and removing endotoxin from biological solutions they suffer from various drawbacks like, high pressure drop, poor mass transfer, clogging and pore structure damage.^[25, 26] Hence, downstream purification operation with these materials is expensive and inconvenient. Also, Polymyxin-B and histamine immobilized resins can lead to neurotoxicity and nephrotoxicity.^[3, 6-8, 27] To address these drawbacks, non-porous and biocompatible PCL NPs ($d_p \sim 800 \text{ nm}$) were synthesized for binding endotoxin on their surface.^[21] The present work attempts to test the validity of the hypothesis that van

der Waals and hydrophobic interactions are responsible for endotoxin binding on the hydrophobic surface. To test the hypothesis, a model polymer, polystyrene nanoparticles with hydrophobic surface similar to that of PCL NPs are used as a control. In addition, the effect of extreme pH conditions on protein recoveries has also been investigated. Also, the paper extends the application of PCL NPs incorporated cellulose acetate (CA) biofilter in removing endotoxins from protein solutions. The biofilter combine the advantages of both PCL NPs and thin sheet flat filters for improved binding and flow properties at a reduced cost with higher throughput.

2. MATERIALS AND METHODS

2.1. SYNTHESIS OF BARE PCL AND MODIFIED PCL NANOPARTICLES

Bare PCL NPs were synthesized using the solvent evaporation technique which utilized high-speed homogenization and sonication, followed by solvent evaporation, centrifugation to remove surfactants, and finally freeze-drying to remove water.^[21, 28-32] A preformed polycaprolactone (PCL) polymer solution in ethyl acetate at a concentration of 10 mg/ml was injected using a syringe pump to a 1% w/v polyvinyl alcohol (PVA) solution prepared with reverse osmosis (RO) water. The mixture was homogenized by using a homogenizer rotating at 3000 rpm while being placed in a sonication bath. Ethyl acetate was removed by stirring the mixture at 300 rpm for two days. The obtained particle suspension was washed five times using RO water and centrifugation for 30 minutes at 10,000 rcf. The resulting products were freeze-dried, weighed, and stored at 4°C until further use. PCL NPs surface was coated with three different cationic ligands.

The three ligands used were poly-L-Lysine (PLL; Sigma Aldrich), polyethylenimine (PEI; Sigma Aldrich) and chitosan (MP Biomedicals).^[33] To coat the surface of bare PCL NPs, 10 mg of freeze dried PCL NPs were incubated with 1 ml of 50 $\mu\text{g/ml}$ solution of these ligands for 1 h. Post incubation the particle suspension was centrifuged for 30 min at 16,000 ref and the supernatant was separated. Subsequently, the ligand-coated nanoparticles were washed with RO water five times and the particles freeze-dried to obtain positively charged and modified PCL NPs.

2.2. CHARACTERIZATION OF BARE PCL AND MODIFIED PCL NANOPARTICLES

The surface morphology, topology and geometry of PCL NPs were observed using Hitachi S-4700 scanning electron microscope (SEM) at an accelerating voltage of 15 kV. Samples were sputter coated with Denton Au/Pd coater before being inserted into the microscope. The average PCL NP size was measured by analyzing the SEM images using the ImageJ software (version 1.51w). The average particle size was reported as mean \pm standard deviation (SD) based on the diameters of 200 randomly selected particles. The hydrodynamic size and surface charge of NPs were characterized by dynamic light scattering (DLS) and zeta potential (ζ) measurements, respectively using Malvern NanoZS90 Zetasizer. The hydrodynamic diameter of PCL NPs was measured at 25°C using He-Ne Lasers at 90° scattering angle. The size distribution was obtained based on three independent experiments utilizing 100 successive runs. Zeta potential values were reported based on three independent experiments; each experiment utilizing 15 successive runs, and the results were reported as millivolts (mV) \pm SD.

2.3. EFFECTS OF pH ON PROTEIN RECOVERIES

BCA assay (Thermo fisher scientific) was employed to calculate the amount of protein recovered after endotoxin was removed from the solution using polymeric particles. Six different proteins were used in the experiments, namely, ovalbumin (pI 4.5; Thermo fisher scientific), bovine serum albumin (BSA; pI 4.7; Thermo fisher scientific), fibrinogen (pI 5.8; Alfa Aesar), bovine hemoglobin (pI 7.1; Sigma Aldrich), trastuzumab (TTZ; pI 8.5; Genentech) and lysozyme (pI 10.7; Thermo fisher scientific). A suspension of PCL NPs (1000 $\mu\text{g/ml}$) and protein (1000 $\mu\text{g/ml}$) at three different pH: acidic (pH 2.8), pI (protein) and basic (pH 11.5) was incubated for 30 minutes under room conditions. Subsequently, the suspension was centrifuged for 30 min at 16,000 rcf and the supernatant was treated with BCA assay reagents to estimate the protein recoveries. This was done by comparing absorbance values at 562 nm after and before introducing PCL NPs using the standard curves for each protein at the given pH values (Figures. S1, S2 and S3). The different pH values are based on recipes in (Table S1).

2.4. EVALUATION OF CONJUGATION EFFICIENCY OF MODIFIED PCL NANOPARTICLES

Conjugation efficiency of PLL, PEI and chitosan on PCL NPs was evaluated using the ninhydrin assay.^[34, 35] To begin with, 4 M sodium hydroxide buffer with pH 5.2 was prepared using glacial acetic acid, sodium hydroxide and water. Ninhydrin reagent (125 mg/ml) was prepared using dimethyl sulfoxide (DMSO) and sodium hydroxide buffer in 1:3 ratio. Next, to 100 μL of known standard PLL, PEI and chitosan ligand concentrations added 100 μL of ninhydrin reagent (Sigma Aldrich) and placed the centrifuge tubes in water bath at 80° C for 30 minutes. Post water bath treatment cooled

the tubes down to room temperature and added 300 μL of stabilizing agent (water). Subsequently, poured 150 μL in triplicates from each tube into the 96 well plates and measured the absorbance at 570 nm for each ligand concentration. To evaluate the conjugation efficiency post incubation for each of the three cationic ligands (50 $\mu\text{g}/\text{ml}$), centrifuged the tubes at 16,000 rcf for 30 minutes and then repeated the above steps with 100 μL of the supernatant. Percent (%) conjugation efficiency of each of the ligands can be evaluated using the standard curves (Figure. S4).

2.5. EVALUATION OF ENDOTOXIN REMOVAL EFFICIENCY OF PARTICLES (IN RO WATER AND PBS)

Endotoxin (*Escherichia coli* O111 : B4 LPS; Sigma Aldrich) removal efficiency of bare Polycaprolactone (PCL), modified PCL and Polystyrene (PS) NPs (Magsphere, Inc) of ~ 800 nm was evaluated using the Bodipy (BOD; Invitrogen) fluorescence displacement assay technique.^[21, 32, 36] BOD is a fluorescent dye which acts as a lipid biomarker and quenches its fluorescence intensity (F.I) on interaction with endotoxin.^[21, 32] The evaluation of endotoxin binding on polymeric particle surface was evaluated by indirectly calculating the amount of endotoxin present in the supernatant after incubating the endotoxin spiked aqueous solution with known PCL NPs concentration.^[20] In these experiments, known polymer particle (PCL, modified PCL and PS NPs) concentration of 1000 $\mu\text{g}/\text{ml}$ was incubated for 30 minutes under room conditions with known endotoxin concentration of 150 $\mu\text{g}/\text{ml}$ in a centrifuge tube. Subsequently, the suspension was centrifuged for 30 min at 16,000 rcf and the supernatant was treated with BOD to estimate the endotoxin removal efficiency. Separate sets of experiments were performed in both RO water (pH ~ 7) and phosphate buffered

saline (PBS; 150 mM, pH ~7.4). The composition of PBS is as follows: 137 mM NaCl, 10 mM phosphate, and 2.7 mM KCl at 25°C. Endotoxin removal efficiency of polystyrene NPs was also calculated at 10X and 100X dilutions of PBS in addition to the PBS alone to study the effect of salt ionic strength on endotoxin removal.

The F.I. of BOD was used to determine the endotoxin concentration in solution. The F.I. measurements were carried out using a microplate reader (BioTek). Excitation and emission wavelengths for BOD were 485/20 and 528/20 nm, respectively. RO water was used as a negative control. The background fluorescence intensities were subtracted to avoid any interferences. The percentage (%) endotoxin removal by polymeric NPs from water and PBS was calculated using equation (1):

$$\% \text{Endotoxin removal} = \frac{FI_{BOD.End.Pol} - FI_{BOD.End}}{FI_{BOD} - FI_{BOD.End}} \times 100 \quad (1)$$

where FI_{BOD} , $FI_{BOD.End}$, and $FI_{BOD.End.Pol}$ represent the F.I. of BOD alone, BOD mixed with endotoxin, and BOD mixed with supernatant of polymeric NPs and endotoxin suspension, respectively.

2.6. SYNTHESIS OF CELLULOSE ACETATE (CA) BIOFILTER

Blank CA biofilter without any PCL NPs were prepared by a non-solvent induced phase separation process.^[21, 37, 38] A casting solution was prepared by dissolving 10 wt.% each of CA and 5 wt.% glycerol in dimethyl sulfoxide (DMSO). For biofilter with NPs, 1 wt.% of PCL NPs was dispersed in the casting solution under vigorous stirring (1100

rpm) at 50°C for 1 h to allow homogenous mixing and then left overnight to allow complete release of bubbles. The final solution was cast on a casting plate and then immersed in RO water coagulation bath for 30 min. Finally, the water wet biofilter was immersed in 30% glycerol (plasticizer) for 15 min, which in addition to improving the mechanical properties also helped in dry storage of the membrane for at least 300 days with no major loss in membrane flux and removal properties.^[21, 39]

2.7. MICROSCOPY AND MICROANALYSIS

The CA biofilter with or without PCL NPs was dried using the freeze–fracture method.^[40] Samples were attached to a SEM stub and sputter coated with Denton Au/Pd coater. The biofilter surface and cross sections were imaged using the Hitachi S-4700 SEM operated at 3 kV. The biofilter surface and cross-sectional morphology, pore size, and thickness were analyzed using ImageJ software (version 1.51w). The average biofilter pore size and thickness were based on 100 randomly selected pores and locations from different images. The results were reported as average \pm standard deviation (SD). The incorporation of PCL NPs in the biofilter were further validated by magnifying the surface and cross-section of the membrane sample under consideration.

2.8. WATER FLUX STUDIES

The flux measurements were carried out using custom-made biofilter testing experimental set-up. The apparatus comprised of two polyvinyl chloride (PVC) pipes attached to blocks that sandwich the biofilter between them. Each of the PVC pipes had a diameter of 1.5 cm. The top half of the experimental set-up consisted of PVC pipe which

was 20 cm long whereas bottom half had a PVC pipe that was 10 cm long. The biofilter area coming in contact with the water or endotoxin spiked protein solution was 1.8 cm². For each experiment the feed volume (water or endotoxin spiked protein solution) was kept constant at 20 ml and then allowed to pass through the biofilter under the influence of gravity. For endotoxin spiked protein solution the concentration of protein was kept constant at 1000 µg/ml and that of endotoxin was fixed at 57.4 µg/ml. The permeate volumes were measured at 15 minute intervals for 90 minutes duration to estimate the change in flux.

The water flux was calculated based on the following equation (2):

$$J = \frac{V}{A \times t} \quad (2)$$

where J ($\frac{L}{m^2h}$) is the water flux of the samples, V (L) is the volume of permeate collected at specific time interval, A (m²) is the biofilter contact area and t (h) is the time.

2.9. QUANTIFICATION OF ENDOTOXIN REMOVAL USING PCL NPS IN CA BIOFILTER

The determination of endotoxin removal by CA biofilter with or without PCL NPs was also carried out by BOD fluorescence displacement assay technique [32, 41] in the apparatus described above. A volume of 20 ml protein solution (1000 µg/ml) spiked with 57.4 µg/ml of endotoxin was fed to the top flow pipe to flow through a sandwiched biofilter by gravity. A fixed volume 460 µL of the endotoxin spiked protein feed and permeate was collected every 15 minutes until 90 minutes. The samples were mixed with

BOD (99.99 $\mu\text{g/ml}$) and the F.I. of BOD was measured using a plate reader (BioTek).

The percent (%) endotoxin removal was calculated using equation (3),

$$\% \text{ Endotoxin removal} = \left(1 - \frac{FI_{BOD,Protein} - FI_{BOD,Protein,End \text{ in permeate}}}{FI_{BOD,Protein} - FI_{BOD,Protein,End \text{ in feed}}}\right) \times 100 \quad (3)$$

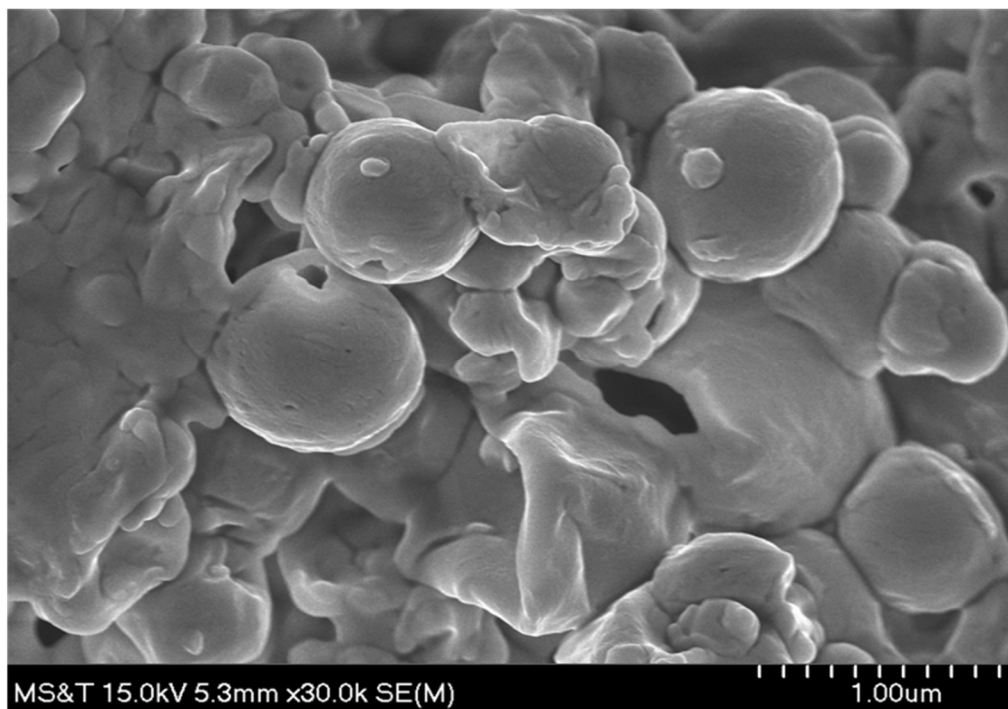
where FI_{BOD} , $FI_{BOD,End \text{ in permeate}}$, and $FI_{BOD,End \text{ in feed}}$ are the F.I.s of BOD alone, BOD mixed with endotoxin in permeate, and BOD mixed with endotoxin in the feed solution, respectively. Each value used here were based on triplicate measurements from three independent experiments. The mean differences and standard deviations were also evaluated.

3. RESULTS

3.1. SYNTHESIS OF POLYCAPROLACTONE NANOPARTICLES

The spherical PCL NPs were successfully prepared using the solvent evaporation technique. From the SEM image (Figure. 1a) and dynamic light scattering (DLS) plot (Figure. 1b) it is apparent that the particles were spherical and non-porous with smooth surface. The particle size was $760 \pm 345 \text{ nm}$. Zeta potential (ζ), of PCL NPs in water was $-17 \pm 4 \text{ mV}$ (Figure. 1c) suggesting that the particles were reasonably stable in suspension form and would resist agglomeration.

(a)



(b)

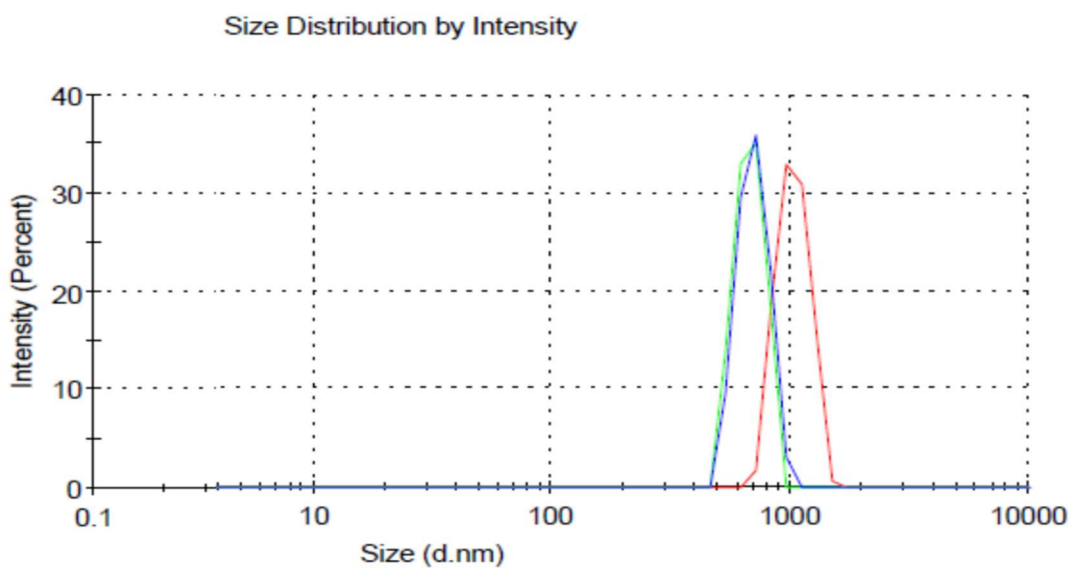


Figure 1. Characterization of PCL NPs. (a) SEM image of PCL NPs at 30,000 X magnification. (b) Plot showing size distribution of PCL NPs. (c) Zeta potential of PCL NPs in water. Multiple colors indicate different independent runs.

(c)

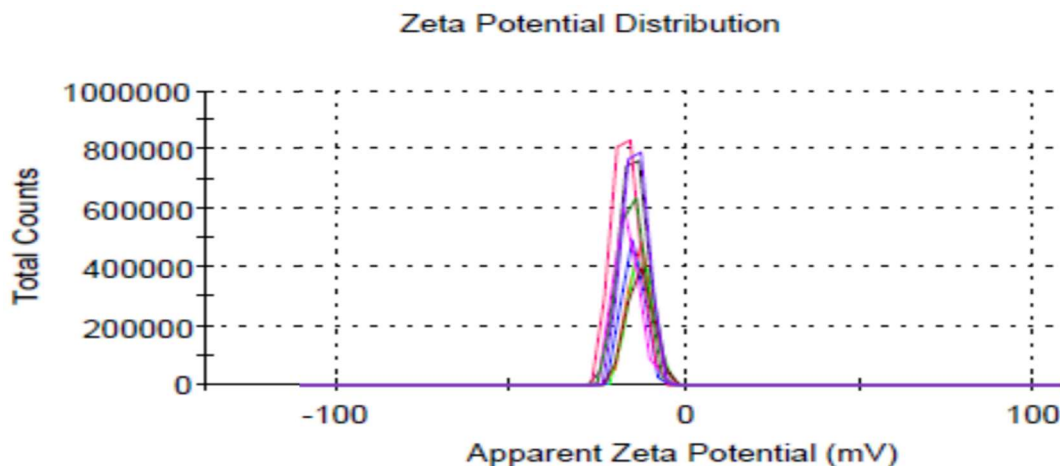


Figure 1. Characterization of PCL NPs. (a) SEM image of PCL NPs at 30,000 X magnification. (b) Plot showing size distribution of PCL NPs. (c) Zeta potential of PCL NPs in water. Multiple colors indicate different independent runs (cont.).

3.2. EFFECT OF pH ON PROTEIN RECOVERIES

The effect of pH on protein recovery were also investigated for six different proteins in presence of PCL NPs. Proteins used in the experiments were: ovalbumin (M.W- 42.7 kDa; pI 4.5), bovine serum albumin (M.W- 66.5 kDa; BSA; pI 4.7), fibrinogen (M.W- 341 kDa; pI 5.8), bovine hemoglobin (M.W- 64.5 kDa; pI 7.1), trastuzumab (M.W- 148 kDa; TTZ; pI 8.5) and lysozyme (M.W- 14.3 kDa; pI 10.7). Protein recovery for each samples were evaluated at three different pH conditions: pH 2.8, pH= isoelectric point (pI) and pH 11.5. In each set of experiments the proteins were water based and a fixed concentration of 1000 $\mu\text{g}/\text{ml}$ was used for proteins and PCL NPs. At pH 2.8, all the protein samples except TTZ gave high protein recoveries > 96 % (Figure. 2). The protein recoveries varied between 94% for TTZ to 100 % for lysozyme. At pH 11.5, all the protein samples except lysozyme saw protein recoveries > 97 %

(Figure. 2). The protein recoveries varied between 93% for lysozyme to 100 % for fibrinogen and bovine hemoglobin. On performing the experiment at the pI, protein recoveries ~ 100 % (98-100 %) were seen for all protein samples (Figure. 2). The recipes to obtain the mentioned pH's can be found in the supplementary information section (Table S1).

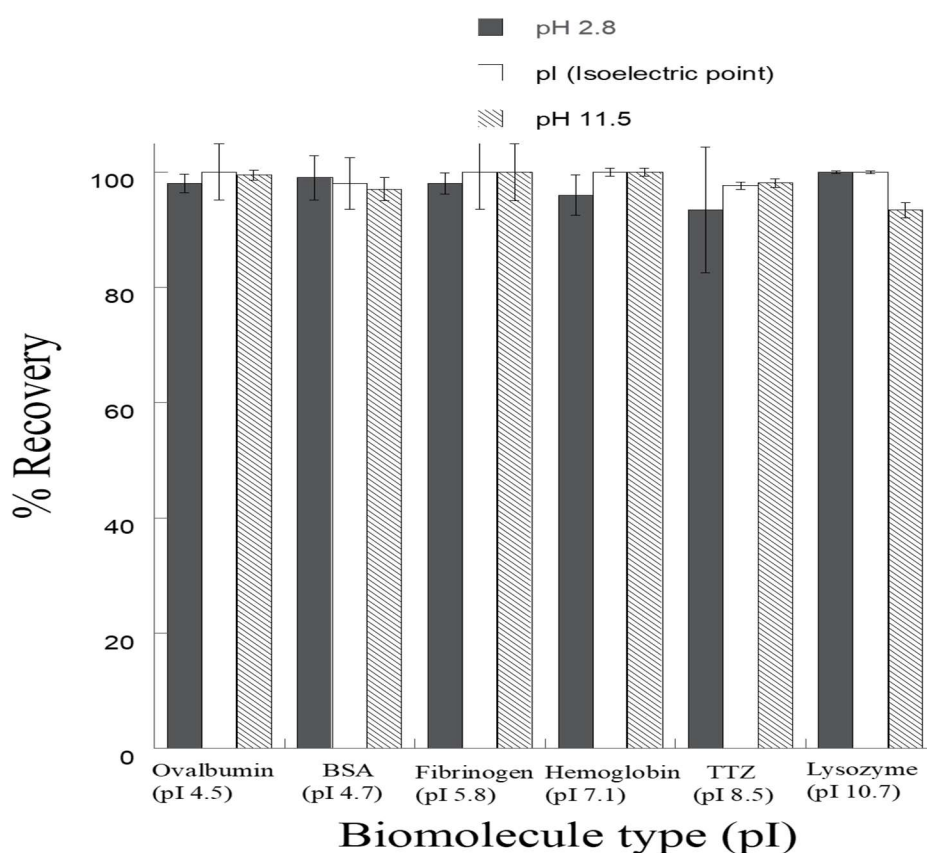


Figure 2. The effects of pH on protein recovery using PCL NPs. The effect of pH on protein recoveries was evaluated at three different values: pH 2.8, isoelectric point (pI) and 11.5. Six different types of proteins with different pI's and molecular weights were used: Ovalbumin (M.W- 42.7 kDa; pI 4.5), Bovine Serum Albumin (BSA; M.W- 66.5 kDa; pI 4.7), Fibrinogen (Fib; M.W- 341 kDa; pI 5.8), Bovine Hemoglobin (M.W- 64.5 kDa; pI 7.1), Trastuzumab (TTZ; M.W- 148 kDa; pI 8.5) and Lysozyme (M.W- 14.3 kDa; pI 10.7) Particle and protein concentration were kept constant at 1000 $\mu\text{g/ml}$.

3.3. ENDOTOXIN REMOVAL EFFICIENCY COMPARISON FROM WATER AND PBS USING PCL NPs AND POLYSTYRENE NPs

As stated before PCL NPs were hypothesized to utilize synergistic combination of van der Waals and hydrophobic interactions to bind and remove endotoxin from biological solutions effectively. Similar to PCL NPs, PS NPs also possess a hydrophobic surface and show binding affinity towards endotoxin, but not as high as PCL NPs. Endotoxin binding efficiency of PS NPs ($d_p \sim 800 \text{ nm}$) was investigated in water and PBS at different dilutions. PS NPs ($d_p \sim 800 \text{ nm}$) and endotoxin concentrations were fixed at $1000 \mu\text{g/ml}$ and $150 \mu\text{g/ml}$ ($1.5 \times 10^6 \text{ EU/ml}$). The endotoxin binding experiments were carried out in RO water, PBS and PBS at different dilutions (10X and 100X). PS NPs endotoxin removal efficiency was $\sim 31 \%$ ($4.6 \times 10^5 \text{ EU/ml}$) from water which increased to $\sim 75 \%$ ($1.1 \times 10^6 \text{ EU/ml}$) in presence of PBS (Figures. 3 and S5; Table S2). On diluting PBS to 10X and 100X the endotoxin binding efficiency reduced to 45% ($6.7 \times 10^5 \text{ EU/ml}$) and 35% ($5.2 \times 10^5 \text{ EU/ml}$) respectively (Figures. 3 and S5; Table S2).

3.4. CONJUGATION EFFICIENCY OF CATIONIC LIGAND ON PCL NPs SURFACE

Bare PCL NPs were coated with cationic ligands to modify the surface of the PCL NPs. In these experiments three different cationic ligands were used to coat the PCL surface. Poly-L-Lysine (PLL), polyethylenimine (PEI) and chitosan solutions ($50 \mu\text{g/ml}$) were incubated with 10 mg PCL NPs. Conjugation efficiency for each ligand was evaluated using the ninhydrin assay.

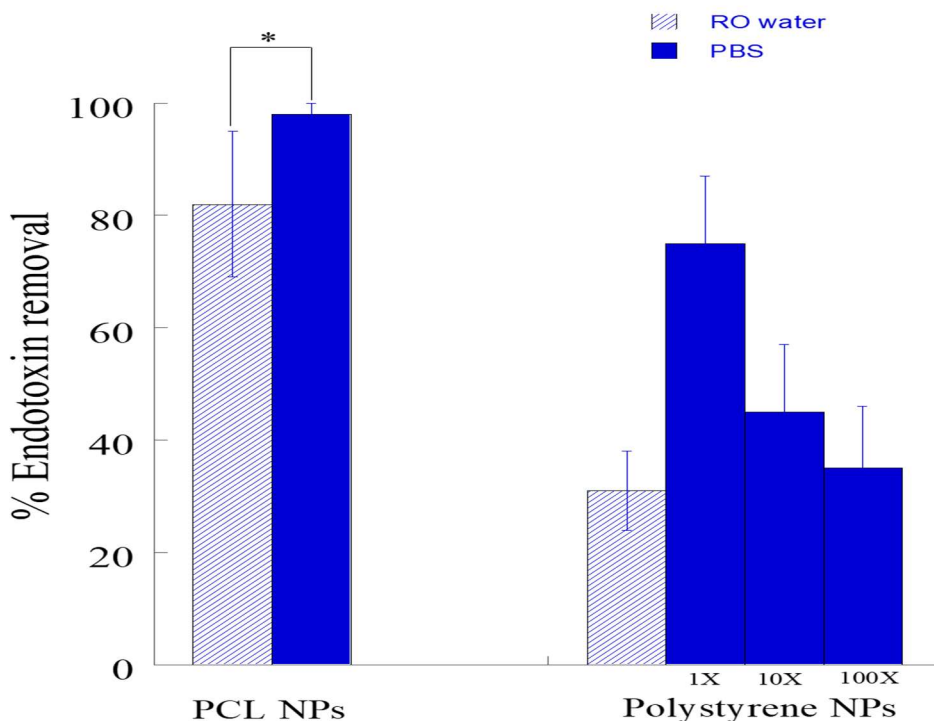
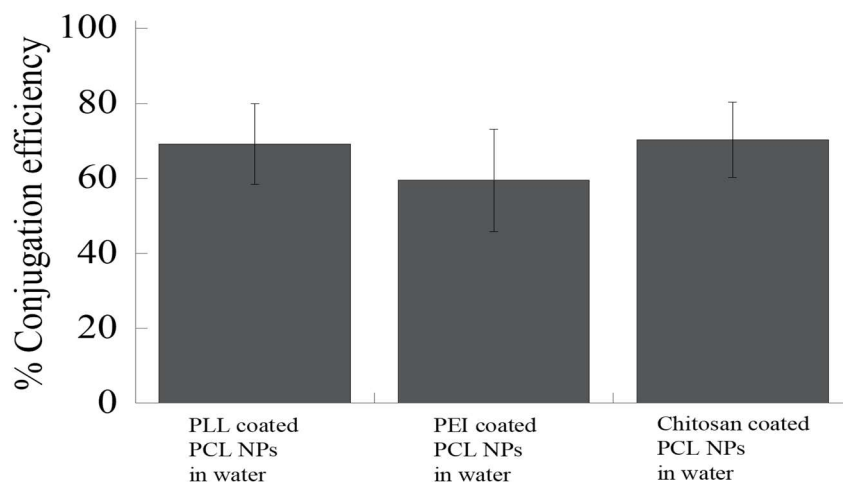


Figure 3. Comparison of endotoxin removal and binding efficiency of bare PCL NPs with Polystyrene NPs in water and PBS. % endotoxin removal efficiency comparison of PCL NPs ($d_p \sim 800 \text{ nm}$) with Polystyrene NPs ($d_p \sim 800 \text{ nm}$) in RO water and PBS at different dilutions. Particle concentration was maintained constant at $1000 \mu\text{g/ml}$ and endotoxin concentration at $150 \mu\text{g/ml}$. * indicates the p-value < 0.1 showing a statistically significant difference between % endotoxin removal in water and PBS.

The % conjugation efficiency for PLL, PEI and chitosan ligands was 70 %, 60 % and 71 % respectively (Figure. 4a). Subsequently, the zeta potential of modified PCL NPs was measured. PLL, PEI and chitosan coated PCL NPs showed a zeta potential value of $8 \pm 4 \text{ mV}$, $12.6 \pm 3 \text{ mV}$ and $1.4 \pm 2 \text{ mV}$ respectively (Figures. 4b, 4c and 4d). The change in zeta potential values of PCL NPs ($-17 \pm 4 \text{ mV}$) post incubation with the cationic ligands indicated successful coating of the PCL surface with the desired cationic ligand.

(a)



(b)

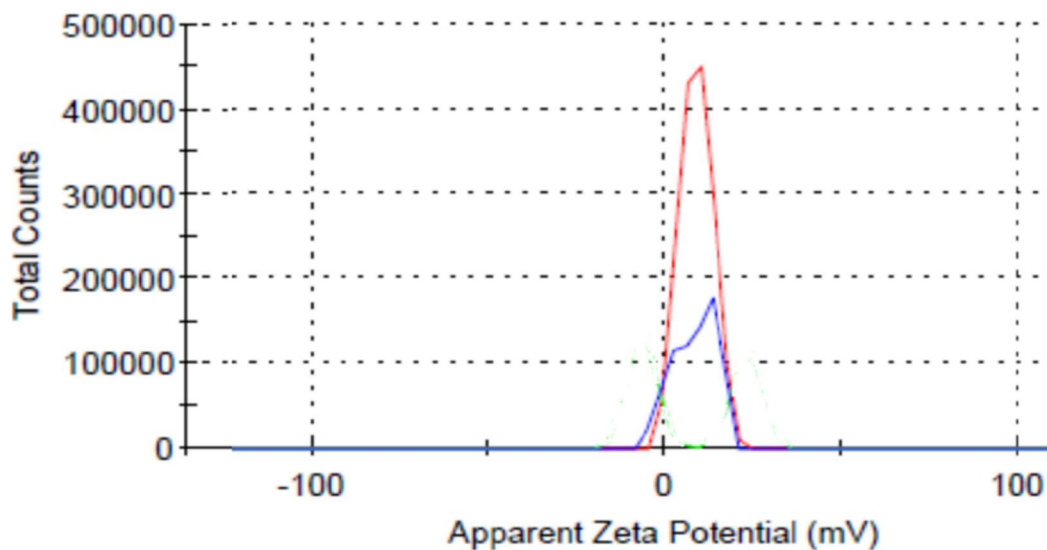
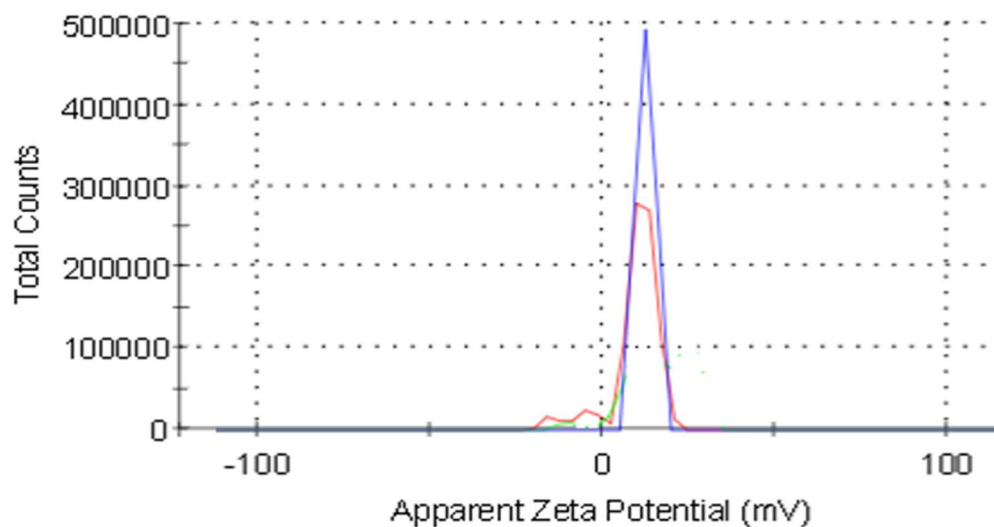


Figure 4. % Conjugation efficiency and zeta potential of PLL, PEI and chitosan ligands coated PCL NPs. (a) PCL NPs were coated with cationic ligands like, PLL, PEI and chitosan by incubating 10 mg of particles with 1 ml of 50 $\mu\text{g}/\text{ml}$ ligand solution for 1 hour. Conjugation efficiency of the ligands was evaluated using the ninhydrin assay. (b) Zeta potential of PLL coated PCL NPs. (c) Zeta potential of PEI coated PCL NPs. (d) Zeta potential of chitosan coated PCL NPs. Different colors indicate independent runs.

(c)



(d)

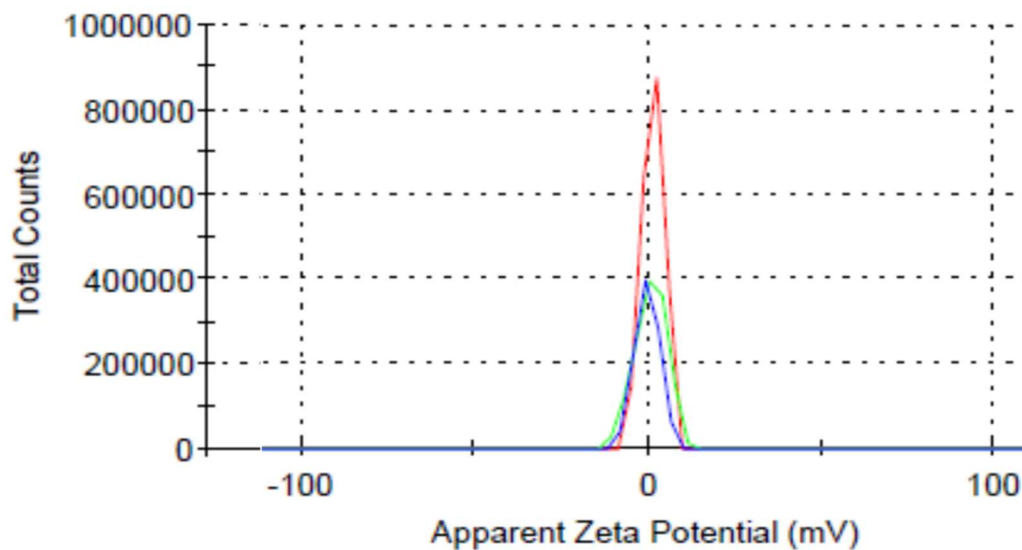


Figure 4. % Conjugation efficiency and zeta potential of PLL, PEI and chitosan ligands coated PCL NPs. (a) PCL NPs were coated with cationic ligands like, PLL, PEI and chitosan by incubating 10 mg of particles with 1 ml of 50 $\mu\text{g}/\text{ml}$ ligand solution for 1 hour. Conjugation efficiency of the ligands was evaluated using the ninhydrin assay. (b) Zeta potential of PLL coated PCL NPs. (c) Zeta potential of PEI coated PCL NPs. (d) Zeta potential of chitosan coated PCL NPs. Different colors indicate independent runs (cont.).

3.5. ENDOTOXIN REMOVAL EFFICIENCY COMPARISON FROM WATER AND PBS USING PCL NPs AND CATIONIC LIGAND MODIFIED PCL NPs

Endotoxin removal performance of cationic ligand modified PCL NPs was investigated from water and PBS (pH 7.4). For these experiments the polymer particle and endotoxin concentrations were maintained constant at 1000 $\mu\text{g/ml}$ and 150 $\mu\text{g/ml}$ (1.5×10^6 EU/ml). The endotoxin removal efficiency varied from 10 - 32 % (1.5×10^5 – 4.8×10^5 EU/ml) for cationic ligand modified PCL NPs in water (Figures. 5 and S6; Table S3). Under the same conditions PCL NPs showed an endotoxin removal efficiency of ~ 82 % (1.2×10^6 EU/ml) which was much higher than cationic ligand coated particles (Figures. 5 and S6; Table S3). In presence of PBS endotoxin binding due to ionic interaction further weakened (Figures. 5 and S6; Table S4) as the removal performance of cationic ligand coated particles dropped further to 8 - 10 % (1.2×10^5 – 1.4×10^5 EU/ml). On comparison, PCL NPs (Figures. 5 and S6; Table S4) saw an upward increasing trend with a removal efficiency of ~ 98 % ($\sim 1.4 \times 10^6$ EU/ml) in PBS solution.

3.6. ENDOTOXIN REMOVAL FROM PROTEIN SAMPLES USING PCL NPs INCORPORATED CA BIOFILTER

PCL NPs showed good endotoxin binding efficiency from water, phosphate buffer saline (PBS) and therapeutics. Thus, in this work cellulose acetate (CA) biofilter with PCL NPs incorporated in the matrix were used to bind and remove endotoxin from various protein solutions. The biofilter were prepared using the non-solvent induced phase separation technique (NIPS).

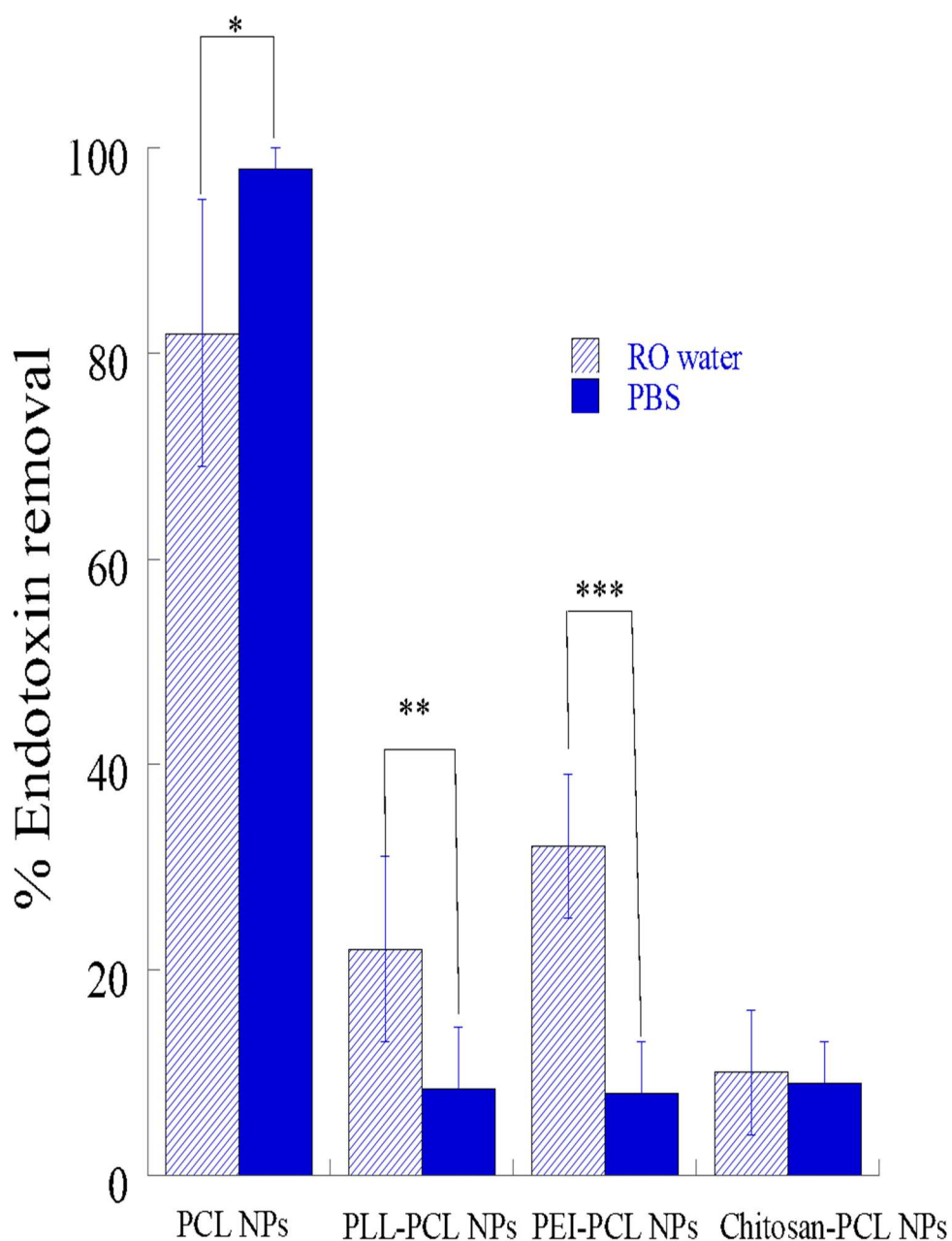


Figure 5. Comparison of endotoxin removal and binding efficiency of bare PCL NPs with cationic ligand modified PCL NPs in RO water and PBS. % endotoxin removal efficiency comparison of PCL NPs , PLL, PEI and chitosan coated PCL NPs in RO water and PBS.

Particle concentration was maintained constant at 1000 $\mu\text{g/ml}$ and endotoxin concentration at 150 $\mu\text{g/ml}$. ***, ** and * indicates the p-value < 0.01 , < 0.05 and < 0.1 showing a statistically significant difference between % endotoxin removal in water and PBS.

Figures 6a and 6b represent the SEM image of CA biofilter and PCL incorporated CA biofilter. From the images it can be seen that the surface pore size of CA and PCL incorporated CA biofilter is $0.37 \pm 0.13 \mu\text{m}$ and $0.40 \pm 0.12 \mu\text{m}$ respectively. CA and PCL incorporated CA biofilter had a thickness of $117 \pm 4 \mu\text{m}$ and $120 \pm 3 \mu\text{m}$ respectively. Presence of PCL NPs in the biofilter can be confirmed from Figure. 6b.

(a)

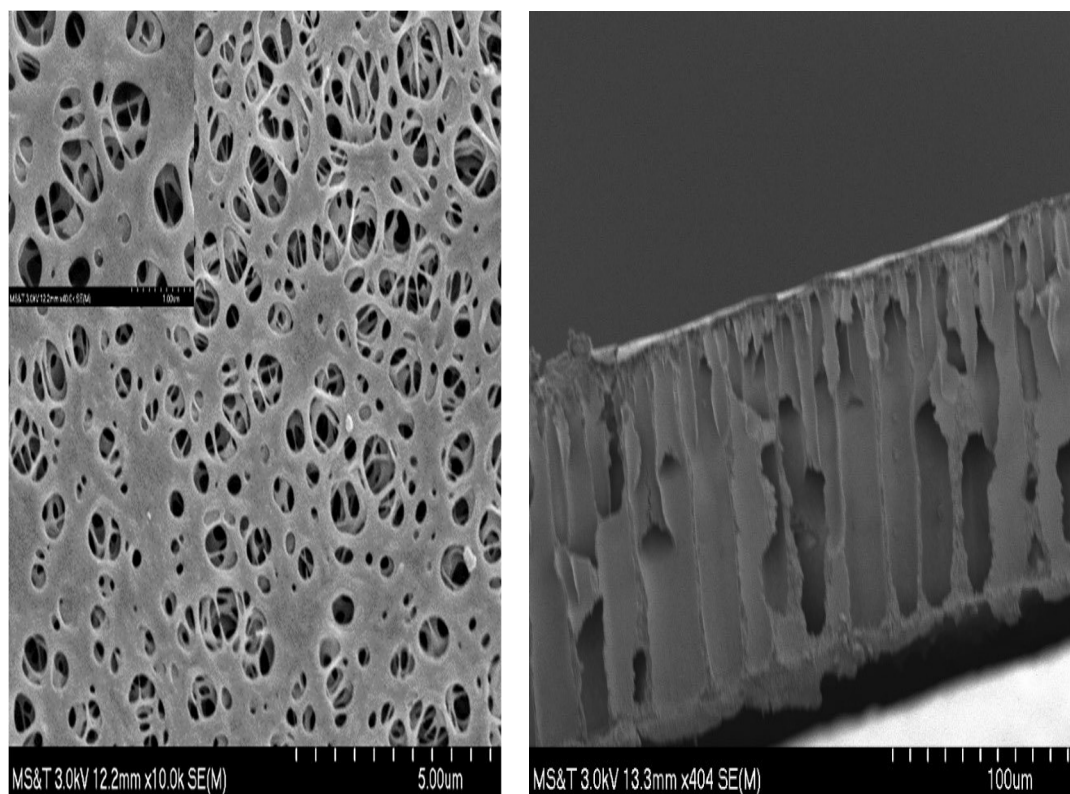


Figure 6. Surface and cross-section morphology of biofilter. The SEM images represent the surface and cross-section morphology of two different types of biofilter: (a). Surface and cross-sectional morphology of cellulose acetate (CA) biofilter. Pore size and thickness of the biofilter were estimated based on 100 random measurements and is $0.37 \pm 0.13 \mu\text{m}$ and $117 \pm 4 \mu\text{m}$ respectively. (b). Surface and cross-sectional morphology of PCL NPs incorporated CA biofilter. Pore size and thickness of the biofilter were estimated based on 100 random measurements and is $0.40 \pm 0.12 \mu\text{m}$ and $120 \pm 3 \mu\text{m}$ respectively.

(b)

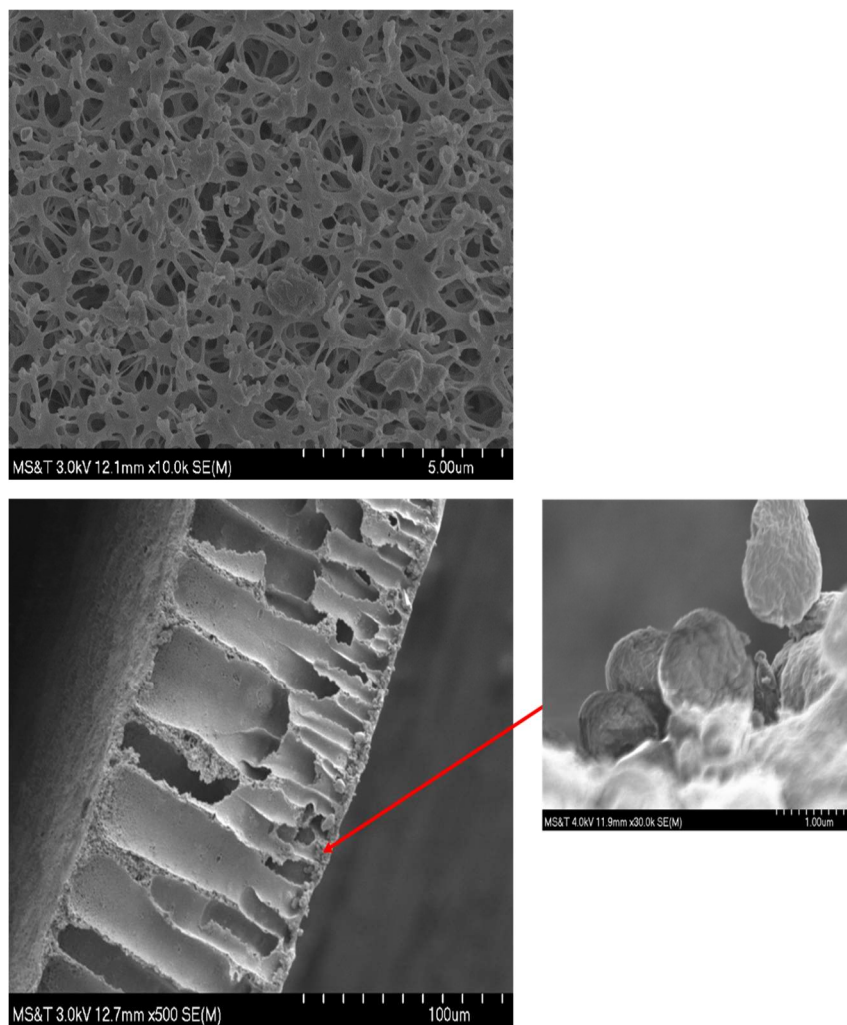


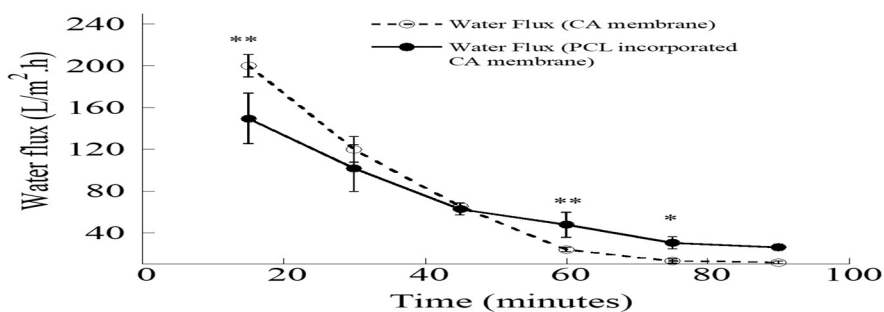
Figure 6. Surface and cross-section morphology of biofilter. The SEM images represent the surface and cross-section morphology of two different types of biofilter: (a). Surface and cross-sectional morphology of cellulose acetate (CA) biofilter. Pore size and thickness of the biofilter were estimated based on 100 random measurements and is $0.37 \pm 0.13 \mu\text{m}$ and $117 \pm 4 \mu\text{m}$ respectively. (b). Surface and cross-sectional morphology of PCL NPs incorporated CA biofilter. Pore size and thickness of the biofilter were estimated based on 100 random measurements and is $0.40 \pm 0.12 \mu\text{m}$ and $120 \pm 3 \mu\text{m}$ respectively (cont.).

Water flux experiments with gravity as the driving force were carried out for both biofilter, with and without PCL NPs. As shown in Figure. 7a the pure water flux of CA (open circles; dotted lines) and PCL NPs incorporated CA biofilter (solid circles; solid

lines) was approximately 200 and $150 \frac{L}{m^2.h}$ to begin with at the end of 15 minutes which reduced to 12 and $26 \frac{L}{m^2.h}$, respectively, at the end of 90 minutes of operation. When water flux measurements of protein samples spiked with endotoxins were carried out a drop in water flux was observed with both CA (dotted lines) and PCL incorporated CA biofilter (solid lines). Average water flux at the end of 15 minutes was $90 \frac{L}{m^2.h}$ for BSA (●), ovalbumin (■), bovine hemoglobin (▲), lysozyme (○) and trastuzumab (□) proteins when passed through the CA biofilter (Figure. 7b). The water flux value dropped to $60 \frac{L}{m^2.h}$ at the end of 90 minutes. On the other hand for PCL NPs incorporated CA biofilter the average water flux at the end of 15 minutes was $41 \frac{L}{m^2.h}$ (Figure. 7b) which dropped to $15 \frac{L}{m^2.h}$ at the end of 90 minutes.

The drop in pure water, protein and endotoxin spiked water flux in biofilter with PCL NPs can be attributed to the resistance offered by PCL NPs incorporated within the matrix of the filter thus slowing down the flow. Also, resistance offered by endotoxin micelles (elongated structure) attached to the PCL surface within the membranes could be another possible reason for the drop in flux. In terms of endotoxin removal from proteins, we noticed a reasonably high endotoxin removal capability of CA biofilter with PCL NPs. During the experiment five different proteins were considered namely, bovine serum albumin (BSA), ovalbumin, bovine hemoglobin, trastuzumab (TTZ) and lysozyme. The average maximum endotoxin removal efficiency varied from 95 % (5.5×10^5 EU/ml) for TTZ to 99% (5.7×10^5 EU/ml) for ovalbumin at the end of 15 minutes (Figure. 8a and S8).

(a)



(b)

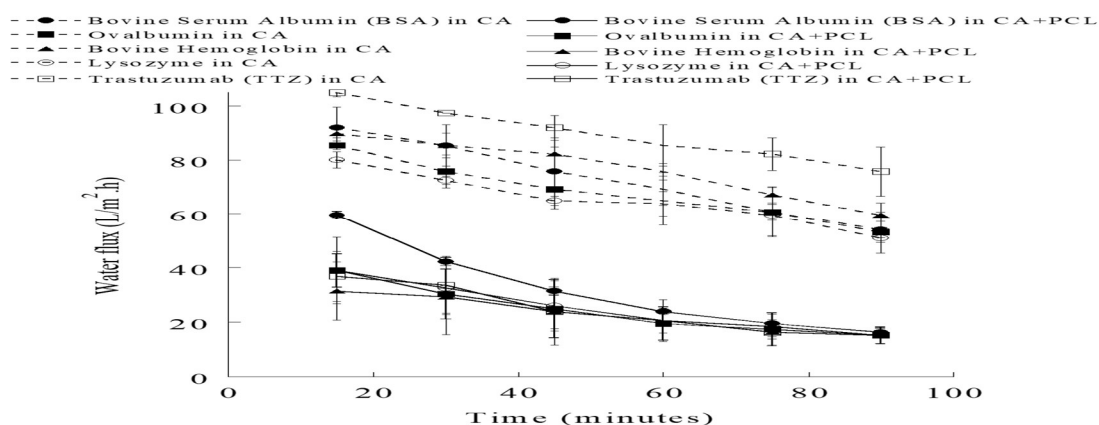


Figure 7. Water flux through CA and PCL incorporated CA biofilter. (a) Water flux plot for 90 minute duration using CA (open circles, \circ ; dotted line) and PCL incorporated CA biofilter (filled, solid circles, \bullet ; solid line). * and ** indicates p values of < 0.1 and < 0.05 , respectively, representing statistically significant differences between the water flux of CA biofilter and PCL NPs incorporated CA biofilter. (b) Water flux for Bovine Serum Albumin (BSA, \bullet), Ovalbumin (\blacksquare), Bovine Hemoglobin (\blacktriangle), Lysozyme (\circ) and Trastuzumab (TTZ, \square) spiked endotoxin solution in water through CA (dotted lines) and PCL incorporated CA biofilter (solid lines). Protein and endotoxin concentration during the experiments were kept constant at $1000 \mu\text{g/ml}$ and $57.4 \mu\text{g/ml}$. CA (open shape; dotted line) and PCL incorporated CA biofilter (Solid shape; solid line).

At the end of 90 minutes the average removal efficiency values varied from 75 % (4.3×10^5 EU/ml) for TTZ to 92% (5.3×10^5 EU/ml) for BSA (Figure. 8a and S8). In terms of protein recovery, the values varied from 92 % for ovalbumin to 100 % for BSA

and TTZ at the end of 15 minutes (Figure. 8b). At the end of 90 minutes duration the recovery values varied between 98 and 100 % for all proteins under consideration (Figure. 8b). The high recovery values suggest that there is minimal non-specific binding between the protein and the PCL NPs located in the CA biofilter. For blank CA biofilter without PCL NPs, at the end of 15 minutes the endotoxin removal values were low and varied between 6% (3.4×10^4 EU/ml) and 30 % (1.7×10^5 EU/ml) (Figure. 8a and S8). After 90 minutes, the endotoxin removal varied between 0 and 25 % (1.4×10^5 EU/ml) (Figure. 8a and S8). The protein recoveries were >96 % during the whole duration.

(a)

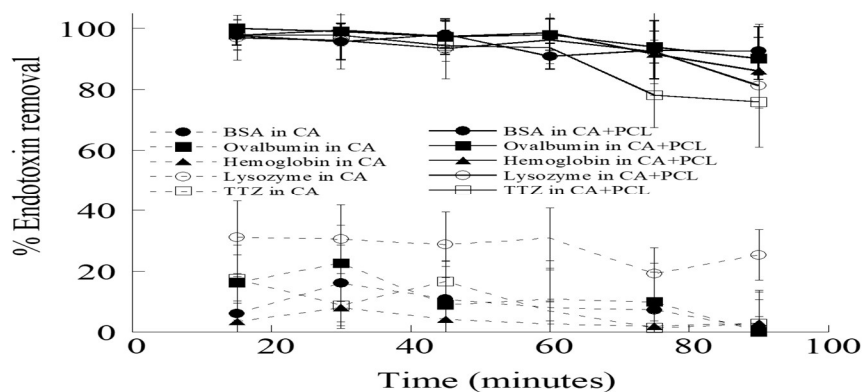


Figure 8. The endotoxin removal efficiency and protein recovery of different proteins using CA and PCL incorporated CA biofilter. (a) Endotoxin removal efficiency from Bovine Serum Albumin (BSA, ●), Ovalbumin (■), Bovine Hemoglobin (▲), Lysozyme (○) and Trastuzumab (TTZ, □) spiked endotoxin solution in water using CA (dotted lines) and PCL incorporated CA biofilter (solid lines). Protein and endotoxin concentration during the experiments were kept constant at 1000 $\mu\text{g/ml}$ and 57.4 $\mu\text{g/ml}$. (b) Protein recovery for Bovine Serum Albumin (BSA, ●), Ovalbumin (■), Bovine Hemoglobin (▲), Lysozyme (○) and Trastuzumab (TTZ, □) spiked endotoxin solution in water using CA and PCL incorporated CA biofilter. Protein concentration during the experiments were kept constant at 1000 $\mu\text{g/ml}$.

(b)

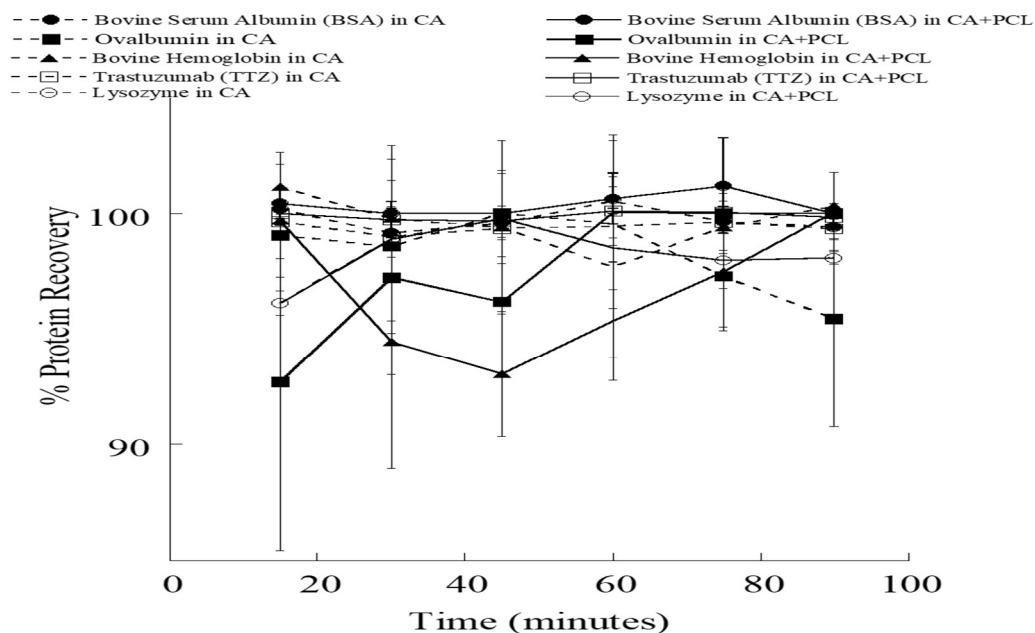


Figure 8. The endotoxin removal efficiency and protein recovery of different proteins using CA and PCL incorporated CA biofilter. (a) Endotoxin removal efficiency from Bovine Serum Albumin (BSA, ●), Ovalbumin (■), Bovine Hemoglobin (▲), Lysozyme (○) and Trastuzumab (TTZ, □) spiked endotoxin solution in water using CA (dotted lines) and PCL incorporated CA biofilter (solid lines). Protein and endotoxin concentration during the experiments were kept constant at 1000 $\mu\text{g}/\text{ml}$ and 57.4 $\mu\text{g}/\text{ml}$. (b) Protein recovery for Bovine Serum Albumin (BSA, ●), Ovalbumin (■), Bovine Hemoglobin (▲), Lysozyme (○) and Trastuzumab (TTZ, □) spiked endotoxin solution in water using CA and PCL incorporated CA biofilter. Protein concentration during the experiments were kept constant at 1000 $\mu\text{g}/\text{ml}$ (cont.).

4. DISCUSSION

In this work, bare PCL NPs (~ 800 nm) were synthesized using the solvent evaporation technique.^[21] PCL NPs were effective in binding endotoxins from biological solutions thus decontaminating the solution for parenteral application. To begin with, the effect of different pH conditions on protein recovery using PCL NPs was investigated.

For the experiments, three types of pH conditions were considered: pH 2.8 (acidic), pH = pI (isoelectric point of protein) and pH 11.5 (basic). Isoelectric points of PCL used in the experiments was at pH 4 and for that of endotoxin was at pH 2.^[3, 8, 42] Thus, at any pH < 4, PCL would be positively charged and negatively charged at any pH > 4. Similarly, at any pH < 2, endotoxins would be positively charged and negatively charged at any pH > 2. Isoelectric points for proteins investigated are: Ovalbumin (pI 4.5), BSA (pI 4.7), fibrinogen (pI 5.8), bovine hemoglobin (pI 7.1), TTZ (pI 8.5) and lysozyme (pI 10.7). At pH 2.8, all the proteins and PCL NPs surface would possess a positive charge and endotoxin would be negatively charged. Protein recovery varied between 93 and 100 %. Van der Waals, hydrophobic and ionic interaction would be responsible for endotoxin binding on PCL surface. PCL and proteins have same type of charges thus ionic interaction would not cause any protein binding on PCL surface. Hence, the loss of protein would be due to protein binding on endotoxin surface due to ionic, affinity and hydrophobic interaction.^[3, 8, 43] Subsequently, the protein laden endotoxin binds to the PCL surface. Also, possibility of interaction between the PCL surface and proteins cannot be neglected. In the past, lysozyme and hemoglobin have been reported to show strong interaction with endotoxin thus corroborating the possibility of interaction between proteins and endotoxins.^[3, 8, 43] At isoelectric point, the surface of proteins are neutral, both endotoxins and PCL NPs possess a negative charge due to their phosphate and carbonyl groups respectively. Protein recovery varied between 98 and 100 % thus indicating almost no interaction either between the protein and the PCL NPs or the protein and the endotoxin. At pH 11.5, the surface of proteins, PCL NPs and endotoxins possess a negative charge respectively. Protein recovery varies between 94 and 100 %.

Due to similar charges on all the surfaces, ionic interaction would not contribute towards any loss in protein after endotoxin removal. Hence, the loss in protein would be due to affinity, van der Waals and hydrophobic interaction between PCL surface and proteins or endotoxin and proteins.^[3, 8, 43] To sum up, pH does play a role in protein recovery but in almost all cases the protein recovery was > 93 % which is considered reasonably high.

Further, PCL NPs binding experiments were carried out by suspending PCL NPs in the endotoxin spiked solution and then centrifuged to separate out the endotoxin laden PCL NPs from the solution. From literature, it has been suggested that the synergistic combination of van der Waals and hydrophobic interaction are driving the binding of endotoxin on PCL NPs surface.^[21]

The aim of this paper was to test the validity of the hypothesis. To begin with polystyrene nanoparticles (PS NPs) of $d_p \sim 800 \text{ nm}$ with hydrophobic nature similar to that of PCL NPs were taken as a control. Subsequently, the endotoxin binding experiments were carried out to evaluate PS NPs endotoxin removal efficiency. PS NPs had an endotoxin removal efficiency of $\sim 31 \%$ ($4.6 \times 10^5 \text{ EU/ml}$) in water (Figures. 3 and S5; Table S2). The binding efficiency increased to 75% ($1.1 \times 10^6 \text{ EU/ml}$) in PBS (Figures. 3 and S5; Table S2). Unlike PCL NPs, PS NPs endotoxin binding performance was not very impressive. These results suggests that endotoxin binding on the surface of PCL NPs is not solely due to van der Waals and hydrophobic interaction but there are other forces that are contributing towards the endotoxin adsorption on PCL surface and need further investigation. Even though, van der Waals and hydrophobic forces are contributing towards endotoxin binding but that is just a small part of large group of forces as evident from low removal efficiency by PS's hydrophobic surface.

The presence of water and salt molecules also play an important role in strengthening the binding interaction between endotoxin and PCL molecules. Endotoxin structure comprises a negative charge due to the presence of phosphate group (PO_4^{3-}) in its polar head chain. On the other hand, PCL NPs also possess negative charge due to the carbonyl group (CO^-) in its structure. The presence of negative charges on both the surfaces should have induced a strong electrostatic repulsive action and thus should have acted as a barrier and impeded the binding on endotoxin on PCL surface. However, the presence of water and salt (NaCl) molecules result in ion hydration through H^+ and Na^+ ions and thus stabilize the charged surfaces (endotoxin and PCL) and strengthen the attractive binding forces between endotoxin and PCL NPs surface.^[21, 44, 45]

Study was also carried out to evaluate the endotoxin binding efficiency due to ionic interaction. This was done by coating the surface of the PCL NPs with three different cationic ligands, PLL, PEI and chitosan to make the surface cationic.^[33] Subsequently, after coating the PCL NPs with the cationic ligands the zeta potential (surface charge) of the particles increased from ~ -17 mV (Figure. 1c) to 8, 12.6 and 1.4 mV (Figures. 3b, 3c and 3d) confirming the surface modification. The % conjugation efficiency of the three ligands on PCL surface varied between 60 and 70 %. (Figure. 3a). On comparing the endotoxin removal efficiency of the bare PCL NPs with the positively charged cationic NPs in water, it was observed that PCL NPs possessed a much higher ~ 82 % (1.2×10^6 EU/ml) endotoxin removal efficiency than modified NPs with values varying between 10 and 32 % ($1.5 \times 10^5 - 5 \times 10^5$ EU/ml) (Figures. 4 and S5; Table S2). In presence of PBS the endotoxin binding efficiency of modified cationic NPs reduced further to ~ 8 -10 % ($1.2 \times 10^5 - 1.4 \times 10^5$ EU/ml) (Figures. 4 and S5; Table

S3). Thus, suggesting that in case of binding due to ionic interaction taking place in water, salt ions are used to modulate the binding capacity.^[46] The role of positively charged NPs is to bind endotoxin through its negatively charged phosphate group in water but in presence of salt (NaCl; 137 mM) in PBS, charge shielding effect comes into play as in addition to negatively charged endotoxin molecules, chloride ions are also competing for the same binding site thus reducing the particle's endotoxin binding efficiency even further.^[46-49] Even though, porous resins or particle based chromatographic separation techniques were quite mature and effective but they suffered from various limitations like poor mass transfer, high pressure drop and in some cases low purification efficiency as seen in the case of polymyxin B cross-linked cellulose microspheres.^[25, 26, 50, 51] The porous microspheres ~ 150 μm in size possessed high endotoxin binding capacity of $\sim 3.6 \times 10^6$ EU/mg but suffered from poor mass transfer and large pressure drop.^[51] To address these drawbacks the non-porous particle (PCL NPs) loaded biofilter were synthesized which combined the advantages of high binding capacity of the particles with improved flow properties and reduced pressure drop of the flat-sheet filter.^[21, 25, 26] From literature, it has been shown that PCL NPs (~ 800 nm) incorporated CA biofilter were effective in removing endotoxins from water.^[21] Here we applied that biofilter to protein solutions and demonstrated the effectiveness of the biofilter in removing endotoxin from protein solutions. Non-porous PCL NPs (~ 800 nm) with a BET specific area of $\approx 6.5 \text{ m}^2/\text{g}$ are very effective in removing endotoxins from water, biological and protein solutions.^[21] Hence, on incorporating these in the biofilter matrix the combined advantages of both the particles and filters can be utilized for cost effective and efficient downstream purification with higher throughput.^[25]

Non-porous PCL NPs loaded biofilter used in the experiments were fed with five types of endotoxin spiked proteins, namely, ovalbumin, BSA, bovine hemoglobin, TTZ and lysozyme. The biofilter possessed a high maximum endotoxin removal efficiency varying between 95 and 99 % (TTZ-ovalbumin; $5.5 \times 10^5 - 5.7 \times 10^5$) (Figure. 8a and S8). Thus suggesting that PCL NPs loaded biofilter were quite effective in providing binding sites for removing endotoxin from protein solutions. In addition to the high endotoxin removal efficiency the protein recovery after endotoxin removal varied between 92 and 100 % (Figure. 8b) , thus suggesting that the majority of binding sites within the biofilter were being utilized for endotoxin binding and most of the protein was allowed to pass through. In comparison, CA biofilter without any PCL NPs showed low endotoxin removal efficiency between 0 % and 30 %. Another advantage associated with the biofilter was the flux at which the removal took place. PCL NPs loaded CA biofilter possessed a maximum pure water flux of $\sim 150 \frac{L}{m^2.h}$ (Figure. 7a) and an average protein and endotoxin spiked water flux of $\sim 41 \frac{L}{m^2.h}$, thus highlighting the rapidness of the separation (Figure. 7b). It is worth mentioning here that the CA biofilter used for the endotoxin removal from protein solutions were gravity driven (Figure. S7) thus cutting costs associated with pumping devices.

5. CONCLUSIONS

In this work, the goal was to test the validity of the hypothesis that endotoxin binding on PCL NP surface was due to van der Waals and hydrophobic interaction occurring between lipid-A tail of endotoxins and hydrophobic surface of PCL. This was

evaluated by taking polystyrene nanoparticles, which have similar hydrophobic nature as polycaprolactone nanoparticles used as control. Subsequently, PS NPs did not show as high endotoxin removal (31%-75 %) efficiency as PCL NPs thus suggesting that in case of PCL NPs there were attractive forces other than van der Waals and hydrophobic interaction that resulted in high endotoxin binding efficiency and need further investigation. Further, the effect of pH on protein recovery for PCL NPs were also evaluated. Six different types of proteins with molecular weights varying from 14 kDa - 341 kDa and isoelectric points (pI) from 4.5- 10.7 were selected. pH values of 2.8, isoelectric point of protein and 11.5 were selected for the experiments and it was observed that protein recovery irrespective of conditions were > 93 %, which is reasonably high. Thus suggesting that pH does not have a major effect on protein recovery when using PCL NPs. It has also been shown that PCL NPs incorporated CA biofilter are effective in removing endotoxins from various protein solutions with improved flow properties and higher throughput. The maximum endotoxin removal efficiency was ~ 99 % and a protein recovery > 92 % thus indicating that majority of endotoxin binding sites within the biofilter were being utilized for endotoxin binding and very less amount of protein was getting lost during the purification operation.

ACKNOWLEDGMENTS

This work was supported by EPA grant, Technology Acceleration Grant, Missouri S&T's Innovation Fund, Missouri S&T's Center for Research in Energy and Environment, and the PI's start-up funds.

SUPPLEMENTARY INFORMATION

Table S1. Buffer recipes of different pHs to study the effects of pH on protein recovery.

Buffer type (pH); ionic strength	Recipe
Glacial acetic acid buffer (2.8); 0.1M	Mix 5.72 ml of glacial acetic acid, 994.28 ml of DI water and 300 μ l of concentrated hydrochloric acid
Phosphate buffer (4.5); 0.1M	Mix 2 ml of 0.2 M sodium phosphate dibasic dihydrate ($\text{Na}_2\text{HPO}_4 \cdot 2\text{H}_2\text{O}$, FW=178.05) in water with 23 ml of 0.2 M sodium phosphate monobasic monohydrate ($\text{NaH}_2\text{PO}_4 \cdot \text{H}_2\text{O}$, FW=138.01) in water. To the final mixture add 365 μ l of 1N hydrochloric acid (HCl)
Phosphate buffer (4.7); 0.1M	Mix 2 ml of 0.2 M sodium phosphate dibasic dihydrate ($\text{Na}_2\text{HPO}_4 \cdot 2\text{H}_2\text{O}$, FW=178.05) in water with 23 ml of 0.2 M sodium phosphate monobasic monohydrate ($\text{NaH}_2\text{PO}_4 \cdot \text{H}_2\text{O}$, FW=138.01) in water. To the final mixture add 340 μ l of 1N hydrochloric acid (HCl)
Phosphate buffer (5.8); 0.1M	Mix 4 ml of 0.2 M sodium phosphate dibasic dihydrate ($\text{Na}_2\text{HPO}_4 \cdot 2\text{H}_2\text{O}$, FW=178.05) in water with 46 ml of 0.2 M sodium phosphate monobasic monohydrate ($\text{NaH}_2\text{PO}_4 \cdot \text{H}_2\text{O}$, FW=138.01) in water

Table S1. Buffer recipes of different pHs to study the effects of pH on protein recovery (cont.).

Phosphate buffer (7.1) ; 0.1M	Mix 12.25 ml of 0.2 M sodium phosphate dibasic dihydrate ($\text{Na}_2\text{HPO}_4 \cdot 2\text{H}_2\text{O}$, FW=178.05) in water with 12.75 ml of 0.2 M sodium phosphate monobasic monohydrate ($\text{NaH}_2\text{PO}_4 \cdot \text{H}_2\text{O}$, FW=138.01) in water. To the final mixture add 80 μl of 10N sodium hydroxide (NaOH)
Phosphate buffer (8.5) ; 0.1M	Mix 23.675 ml of 0.2 M sodium phosphate dibasic dihydrate ($\text{Na}_2\text{HPO}_4 \cdot 2\text{H}_2\text{O}$, FW=178.05) in water and 1.325 ml of 0.2 M sodium phosphate monobasic monohydrate ($\text{NaH}_2\text{PO}_4 \cdot \text{H}_2\text{O}$, FW=138.01) in water. To the final mixture add 20 μl of 10N sodium hydroxide (NaOH)
Sodium bicarbonate buffer (10.7) ; 0.1M	Mix 8.4 g of sodium bicarbonate (NaHCO_3) with 991.6 ml of DI water. To 25 ml of sodium bicarbonate buffer add 210 μl of 10N sodium hydroxide (NaOH)
Carbonate-Bicarbonate buffer (11.5) ; 0.1M	Mix 0.525 g of sodium bicarbonate (NaHCO_3) and 4.638 g of sodium carbonate (Na_2CO_3) with 500 ml of DI water. To the final mixture add 850 μl of 10N sodium hydroxide (NaOH)

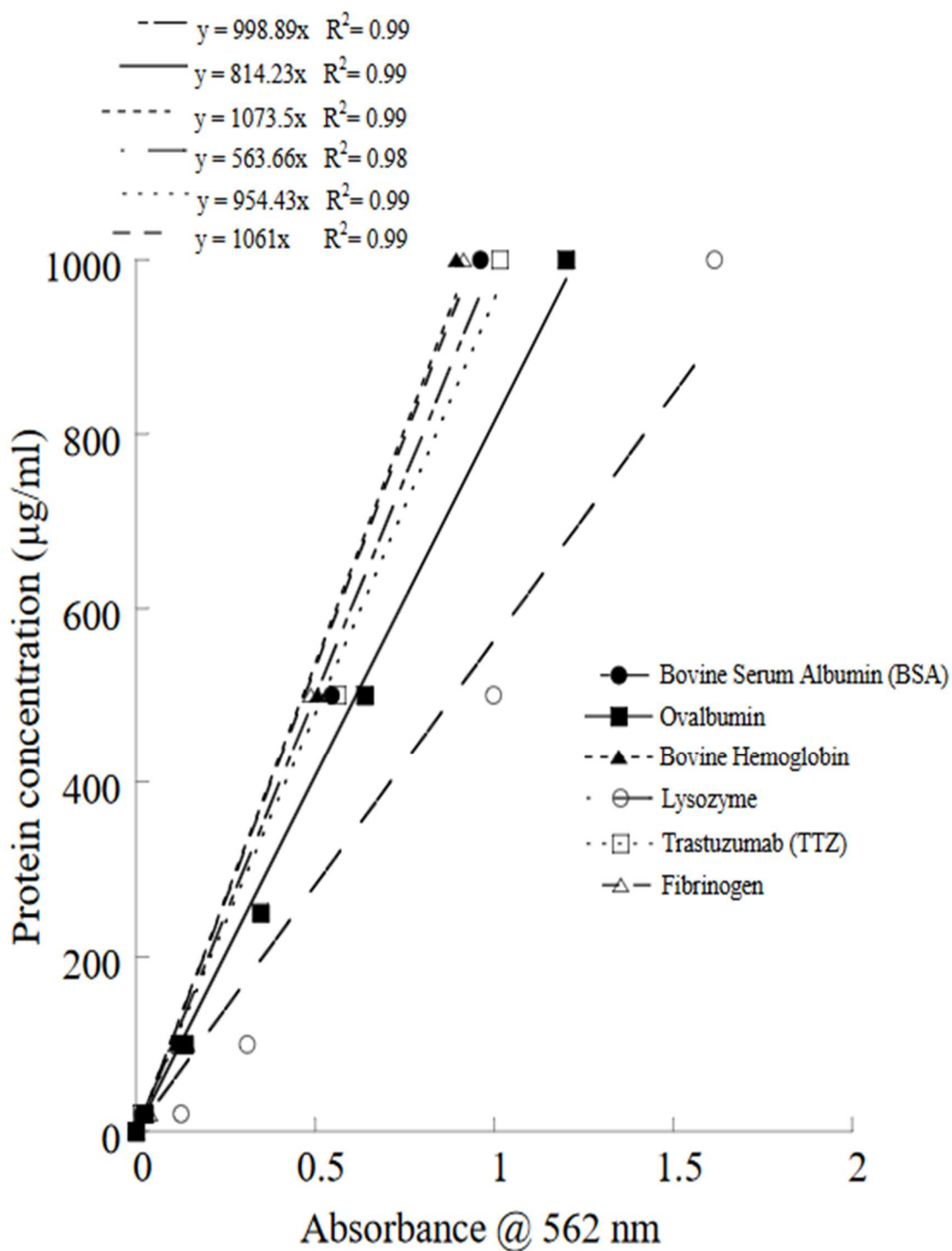


Figure S1. Protein standard curves of Ovalbumin, Bovine Serum Albumin (BSA), Fibrinogen, Bovine Hemoglobin, Trastuzumab (TTZ; Genentech) and Lysozyme at isoelectric points (pI) and were used to measure protein concentrations. R^2 represents the regression value.

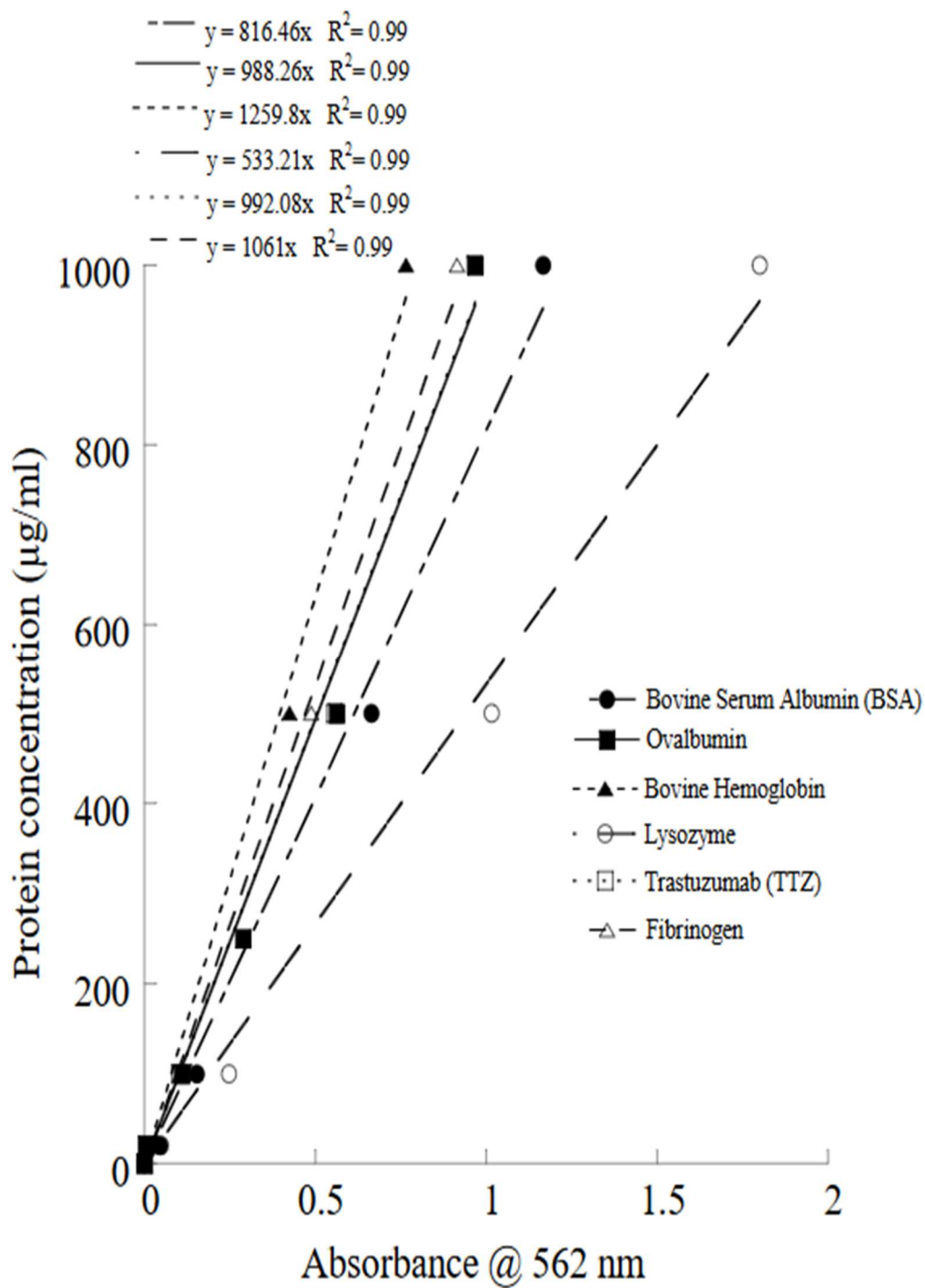


Figure S2. Protein standard curves of Ovalbumin, Bovine Serum Albumin (BSA), Fibrinogen, Bovine Hemoglobin, Trastuzumab (TTZ; Genentech) and Lysozyme at pH 2.8 and were used to measure protein concentrations. R^2 represents the regression value.

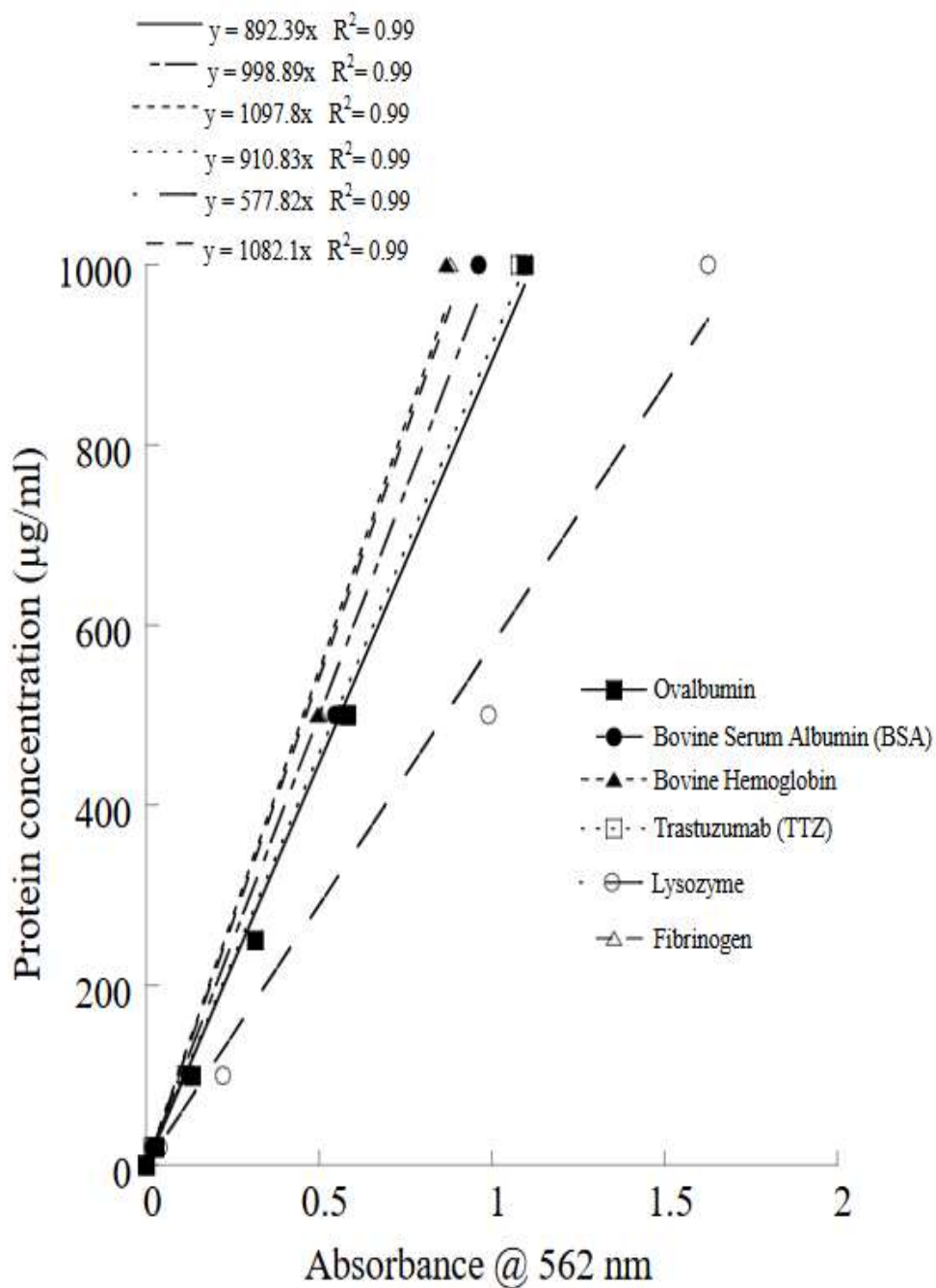


Figure S3. Protein standard curves of Ovalbumin, Bovine Serum Albumin (BSA), Fibrinogen, Bovine Hemoglobin, Trastuzumab (TTZ; Genentech) and Lysozyme at pH 11.5 and were used to measure protein concentrations. R^2 represents the regression value.

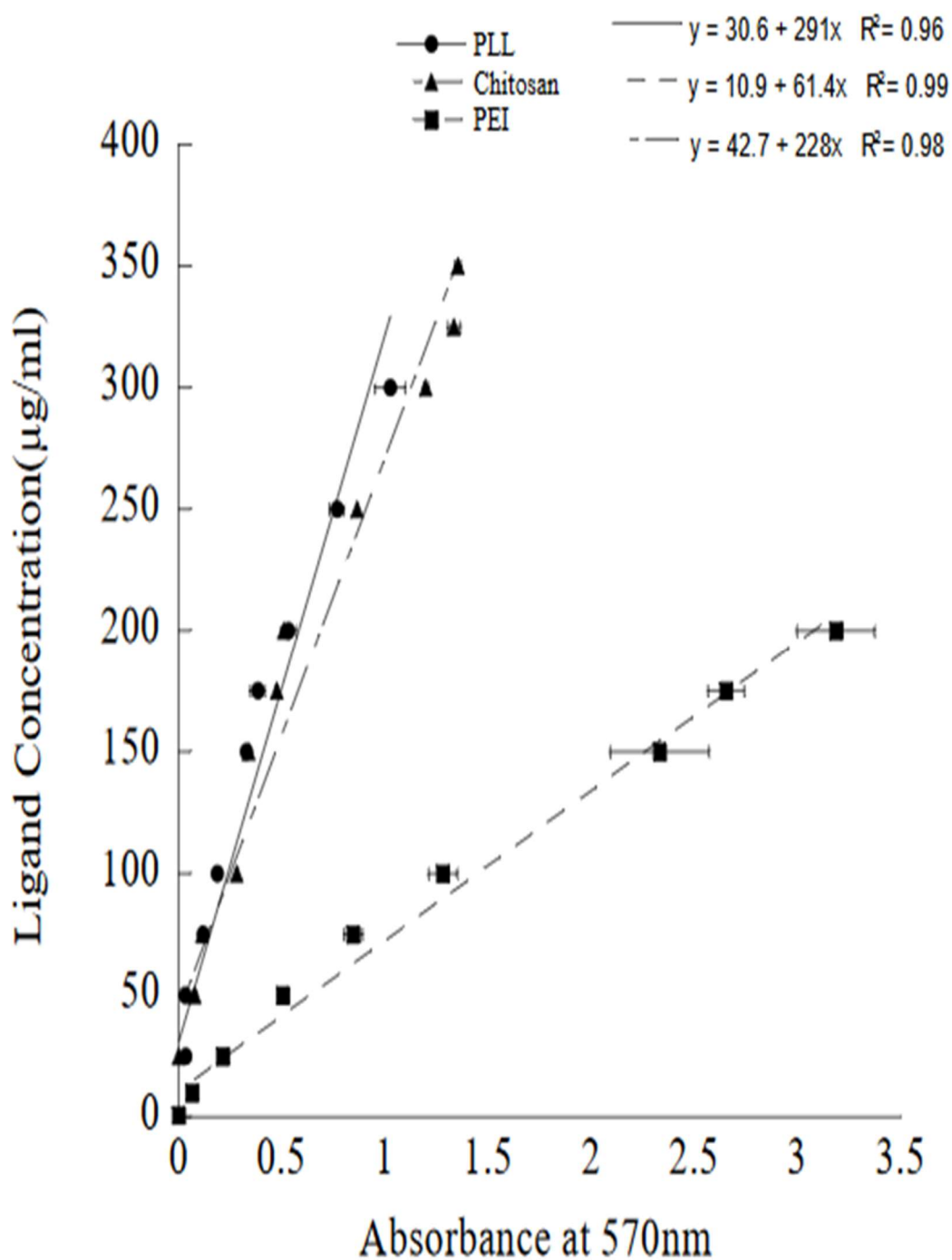


Figure S4. Poly-L-Lysine (PLL), Polyethylenimine (PEI) and chitosan standard curves for conjugation efficiency calculation using ninhydrin assay. The curves were used to measure the ligand concentrations. R^2 represents the regression value.

Table S2. The endotoxin unit (EU) bound per ml of endotoxin-spiked solution using PCL NPs and Polystyrene (PS) NPs in water and PBS at different dilutions. 1 EU \approx 0.1 – 0.2 ng of endotoxin.

Endotoxin fed (endotoxin unit; EU/ml)	Polymeric NP type	Liquid media	Polymeric NPs concentration (mg/ml)	Polymeric NPs diameter (μm)	Endotoxin bound to particle surface (endotoxin unit; EU/ml)
1.5×10^6	PCL NPs	DI water	1	0.8	1.2×10^6
1.5×10^6	PCL NPs	PBS	1	0.8	1.4×10^6
1.5×10^6	PS NPs	DI water	1	0.8	4.6×10^5
1.5×10^6	PS NPs	PBS	1	0.8	1.1×10^6
1.5×10^6	PS NPs	10X PBS	1	0.8	0.6×10^6
1.5×10^6	PS NPs	100X PBS	1	0.8	0.5×10^6

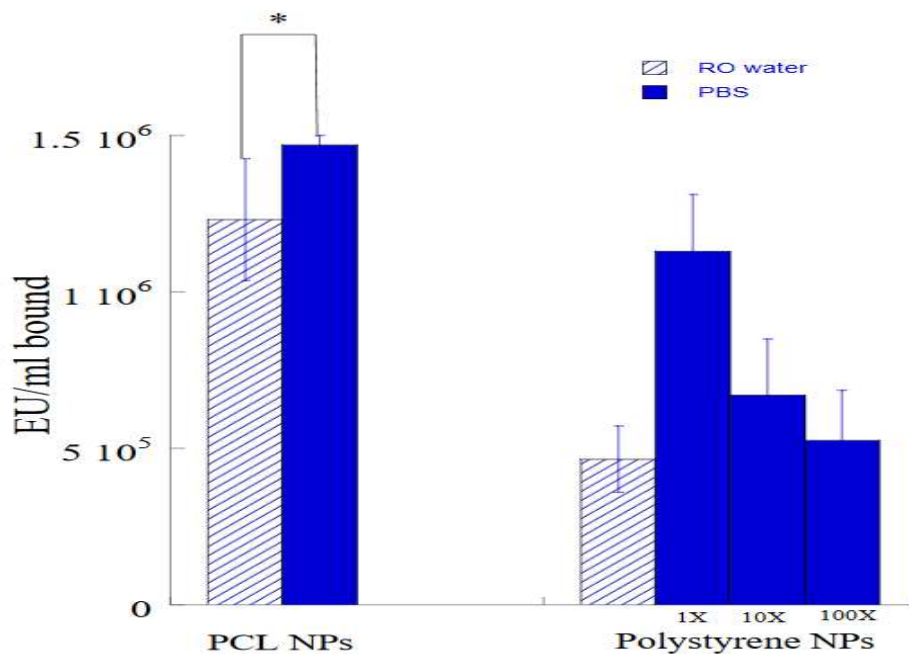


Figure S5. Comparison of Endotoxin unit (EU) per ml bound to the surface of PCL NPs with Polystyrene NPs ($d_p \sim 800 \text{ nm}$) in water and PBS at different dilutions. EU/ml fed was kept constant at 1.5×10^6 and particle concentration at $1000 \mu\text{g/ml}$. * indicates the p-value < 0.1 showing a statistically significant difference between % endotoxin removal in water and PBS.

Table S3. The endotoxin unit (EU) bound per ml of endotoxin-spiked solution using PCL NPs and modified PCL NPs in water. 1 EU \approx 0.1 – 0.2 ng of endotoxin.

Endotoxin fed (endotoxin unit; EU/ml)	Polymeric NP type	Polymeric NPs concentration (mg/ml)	Polymeric NPs diameter (μ m)	Endotoxin bound to particle surface (endotoxin unit; EU/ml)
1.5×10^6	PCL NPs	1	0.8	1.2×10^6
1.5×10^6	PLL-PCL NPs	1	0.8	3.2×10^5
1.5×10^6	PEI-PCL NPs	1	0.8	4.8×10^5
1.5×10^6	Chitosan-PCL NPs	1	0.8	1.5×10^5

Table S4. The endotoxin unit (EU) bound per ml of endotoxin-spiked solution using PCL NPs and modified PCL NPs in PBS. 1 EU \approx 0.1 – 0.2 ng of endotoxin.

Endotoxin fed (endotoxin unit; EU/ml)	Polymeric NP type	Polymeric NPs concentration (mg/ml)	Polymeric NPs diameter (μ m)	Endotoxin bound to particle surface (endotoxin unit; EU/ml)
1.5×10^6	PCL NPs	1	0.8	1.4×10^6
1.5×10^6	PLL-PCL NPs	1	0.8	1.3×10^5
1.5×10^6	PEI-PCL NPs	1	0.8	1.2×10^5
1.5×10^6	Chitosan-PCL NPs	1	0.8	1.4×10^5

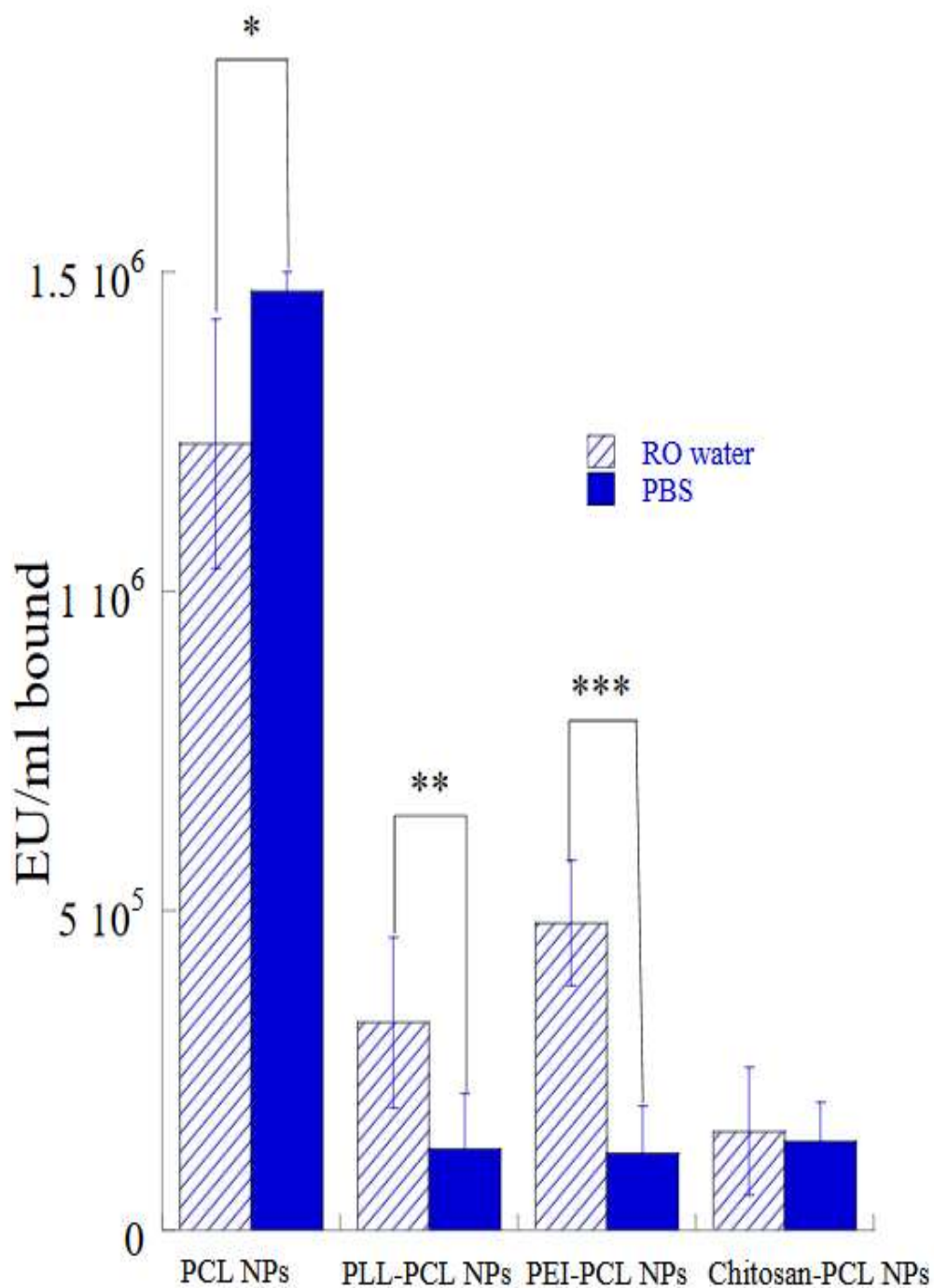


Figure S6. Endotoxin unit (EU) per ml bound to the surface of PCL NPs, PLL, PEI and chitosan coated PCL NPs in RO water and PBS. EU/ml fed was kept constant at 1.5×10^6 and particle concentration at $1000 \mu\text{g/ml}$. ***, ** and * indicates the p-value < 0.01 , < 0.05 and < 0.1 showing a statistically significant difference between % endotoxin removal in water and PBS.



Figure S7. Custom-made membrane filtration set up made out of PVC. CA biofilter without and with PCL NPs are sandwiched between two blocks and butterfly screws are used to tighten the biofilter. Endotoxin spiked protein solution is fed from the top part of the pipe and permeate is collected from the bottom half of the pipe.

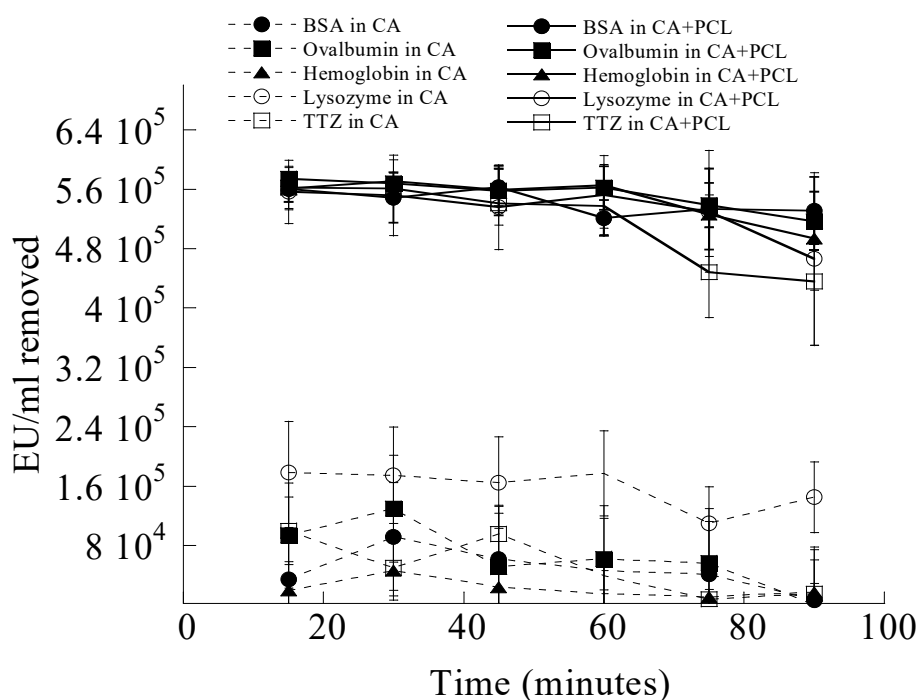


Figure S8. Endotoxin units (EU) per ml removed from Bovine Serum Albumin (BSA, ●), Ovalbumin (■), Bovine Hemoglobin (▲), Lysozyme (○) and Trastuzumab (TTZ, □) spiked endotoxin solution in water using PCL incorporated CA biofilter (solid lines). Protein and endotoxin concentration during the experiments were kept constant at 1000 $\mu\text{g}/\text{ml}$ and 57.4 $\mu\text{g}/\text{ml}$ (5.7×10^5 EU/ml).

REFERENCES

1. Wilding, K.M., et al., *Endotoxin-Free E. coli-Based Cell-Free Protein Synthesis: Pre-Expression Endotoxin Removal Approaches for on-Demand Cancer Therapeutic Production*. Biotechnology Journal, 2019. 14(3): p. 1800271.
2. Metzger, K.F.J., et al., *Adsorptive filtration: A case study for early impurity reduction in an Escherichia coli production process*. Biotechnol Prog, 2019: p. e2948.
3. Anspach, F.B., *Endotoxin removal by affinity sorbents*. Journal of biochemical and biophysical methods, 2001. 49(1-3): p. 665-681.
4. Aida, Y. and M.J. Pabst, *Removal of endotoxin from protein solutions by phase separation using Triton X-114*. Journal of immunological methods, 1990. 132(2): p. 191-195.
5. Gorbet, M.B. and M.V. Sefton, *Endotoxin: the uninvited guest*. Biomaterials, 2005. 26(34): p. 6811-7.
6. Magalhães, P.O., et al., *Methods of endotoxin removal from biological preparations: a review*. J Pharm Pharm Sci, 2007. 10(3): p. 388-404.
7. Ongkudon, C.M., et al., *Chromatographic removal of endotoxins: a bioprocess engineer's perspective*. ISRN Chromatography, 2012. 2012.
8. Petsch, D. and F.B. Anspach, *Endotoxin removal from protein solutions*. Journal of biotechnology, 2000. 76(2-3): p. 97-119.
9. Gronemeyer, P., R. Ditz, and J. Strube, *Trends in Upstream and Downstream Process Development for Antibody Manufacturing*. Bioengineering (Basel), 2014. 1(4): p. 188-212.
10. Hanke, A.T. and M. Ottens, *Purifying biopharmaceuticals: knowledge-based chromatographic process development*. Trends Biotechnol, 2014. 32(4): p. 210-20.
11. Jozala, A.F., et al., *Biopharmaceuticals from microorganisms: from production to purification*. Braz J Microbiol, 2016. 47 Suppl 1: p. 51-63.
12. Konwar, A., D. Chowdhury, and A. Dan, *Chitosan based in situ and ex situ magnetic iron oxide nanoparticles for rapid endotoxin removal from protein solutions*. Materials Chemistry Frontiers, 2019. 3(4): p. 716-725.

13. Chen, R.H., et al., *Factors affecting endotoxin removal from recombinant therapeutic proteins by anion exchange chromatography*. Protein Expression and Purification, 2009. 64(1): p. 76-81.
14. Hou, K.C. and R. Zaniewski, *Endotoxin removal by anion-exchange polymeric matrix*. Biotechnology and applied biochemistry, 1990. 12(3): p. 315-324.
15. Van Belleghem, J.D., et al., *A comparative study of different strategies for removal of endotoxins from bacteriophage preparations*. Journal of microbiological methods, 2017. 132: p. 153-159.
16. Fekete, S., et al., *Ion-exchange chromatography for the characterization of biopharmaceuticals*. Journal of pharmaceutical and biomedical analysis, 2015. 113: p. 43-55.
17. Diogo, M., J. Queiroz, and D. Prazeres, *Chromatography of plasmid DNA*. Journal of Chromatography A, 2005. 1069(1): p. 3-22.
18. Freitas, S.S., J.A. Santos, and D.M. Prazeres, *Plasmid purification by hydrophobic interaction chromatography using sodium citrate in the mobile phase*. Separation and purification technology, 2009. 65(1): p. 95-104.
19. Wilson, M.J., et al., *Removal of tightly bound endotoxin from biological products*. Journal of biotechnology, 2001. 88(1): p. 67-75.
20. Darkow, R., et al., *Functionalized nanoparticles for endotoxin binding in aqueous solutions*. Biomaterials, 1999. 20(14): p. 1277-1283.
21. Razdan, S., J.C. Wang, and S. Barua, *PolyBall: A new adsorbent for the efficient removal of endotoxin from biopharmaceuticals*. Sci Rep, 2019. 9(1): p. 8867.
22. Vagenende, V., et al., *Allantoin as a solid phase adsorbent for removing endotoxins*. Journal of Chromatography A, 2013. 1310: p. 15-20.
23. Lambadi, P.R., et al., *Facile biofunctionalization of silver nanoparticles for enhanced antibacterial properties, endotoxin removal, and biofilm control*. International journal of nanomedicine, 2015. 10: p. 2155.
24. Prasad, P., et al., *Regenerative core-shell nanoparticles for simultaneous removal and detection of endotoxins*. Langmuir, 2018. 34(25): p. 7396-7403.
25. Orr, V., et al., *Recent advances in bioprocessing application of membrane chromatography*. Biotechnology advances, 2013. 31(4): p. 450-465.

26. Ghosh, R., *Protein separation using membrane chromatography: opportunities and challenges*. Journal of Chromatography A, 2002. 952(1-2): p. 13-27.
27. Hirayama, C. and M. Sakata, *Chromatographic removal of endotoxin from protein solutions by polymer particles*. Journal of Chromatography B, 2002. 781(1-2): p. 419-432.
28. Rao, J.P. and K.E. Geckeler, *Polymer nanoparticles: preparation techniques and size-control parameters*. Progress in polymer science, 2011. 36(7): p. 887-913.
29. Mendoza-Muñoz, N., S. Alcalá-Alcalá, and D. Quintanar-Guerrero, *Preparation of Polymer Nanoparticles by the Emulsification-Solvent Evaporation Method: From Vanderhoff's Pioneer Approach to Recent Adaptations*, in *Polymer Nanoparticles for Nanomedicines*. 2016, Springer. p. 87-121.
30. Badri, W., et al., *Effect of process and formulation parameters on polycaprolactone nanoparticles prepared by solvent displacement*. Colloids and Surfaces A: Physicochemical and Engineering Aspects, 2017. 516: p. 238-244.
31. Vauthier, C. and G. Ponchel, *Polymer Nanoparticles for Nanomedicines*. 2017: Springer.
32. Donnell, M.L., et al., *Endotoxin hitchhiking on polymer nanoparticles*. Nanotechnology, 2016. 27(28): p. 285601.
33. Bilensoy, E., et al., *Intravesical cationic nanoparticles of chitosan and polycaprolactone for the delivery of Mitomycin C to bladder tumors*. International journal of pharmaceutics, 2009. 371(1-2): p. 170-176.
34. Barua, S., et al., *Parallel synthesis and screening of polymers for nonviral gene delivery*. Molecular pharmaceutics, 2008. 6(1): p. 86-97.
35. Friedman, M., *Applications of the ninhydrin reaction for analysis of amino acids, peptides, and proteins to agricultural and biomedical sciences*. Journal of agricultural and food chemistry, 2004. 52(3): p. 385-406.
36. Wood, S.J., K.A. Miller, and S.A. David, *Anti-endotoxin agents. 1. Development of a fluorescent probe displacement method optimized for the rapid identification of lipopolysaccharide-binding agents*. Combinatorial chemistry & high throughput screening, 2004. 7(3): p. 239-249.
37. Lv, C., et al., *Enhanced permeation performance of cellulose acetate ultrafiltration membrane by incorporation of Pluronic F127*. Journal of membrane science, 2007. 294(1-2): p. 68-74.

38. Guillen, G.R., et al., *Preparation and characterization of membranes formed by nonsolvent induced phase separation: a review*. Industrial & Engineering Chemistry Research, 2011. 50(7): p. 3798-3817.
39. Vos, K.D. and F. Burris Jr, *Drying cellulose acetate reverse osmosis membranes*. Industrial & Engineering Chemistry Product Research and Development, 1969. 8(1): p. 84-89.
40. Ferlita, R.R., et al., *Cryo-snap: A simple modified freeze-fracture method for SEM imaging of membrane cross-sections*. Environmental Progress, 2008. 27(2): p. 204-209.
41. Stewart J. Wood, K.A.M., and Sunil A. David, *Anti-Endotoxin Agents. 1. Development of a Fluorescent Probe displacement method optimized for high throughput identification of Lipopolysaccharide-Binding Agents*. Combinatorial Chemistry & High Throughput Screening, 2004. 7(3).
42. Jesus, S., G. Borchard, and O. Borges, *Freeze dried chitosan/poly- ϵ -caprolactone and poly- ϵ -caprolactone nanoparticles: evaluation of their potential as DNA and antigen delivery systems*. J Genet Syndr Gene Ther, 2013. 4(164): p. 2.
43. Dullah, E.C. and C.M. Ongkudon, *Current trends in endotoxin detection and analysis of endotoxin-protein interactions*. Critical reviews in biotechnology, 2017. 37(2): p. 251-261.
44. Gallo, P., D. Corradini, and M. Rovere, *Ion hydration and structural properties of water in aqueous solutions at normal and supercooled conditions: a test of the structure making and breaking concept*. Physical Chemistry Chemical Physics, 2011. 13(44): p. 19814-19822.
45. Drensko, M. and S.M. Loverde, *Molecular dynamics simulations of the interaction of phospholipid bilayers with polycaprolactone*. Molecular Simulation, 2019. 45(11): p. 859-867.
46. Corporation, P., *Ion Exchange Chromatography Selection Guide*.
47. Tsumoto, K., et al., *Effects of salts on protein-surface interactions: applications for column chromatography*. Journal of pharmaceutical sciences, 2007. 96(7): p. 1677-1690.
48. Nel, A.E., et al., *Understanding biophysicochemical interactions at the nano-bio interface*. Nature materials, 2009. 8(7): p. 543.
49. Zhang, Y. and P.S. Cremer, *Interactions between macromolecules and ions: the Hofmeister series*. Current opinion in chemical biology, 2006. 10(6): p. 658-663.

50. Tallarek, U., F.J. Vergeldt, and H.V. As, *Stagnant mobile phase mass transfer in chromatographic media: intraparticle diffusion and exchange kinetics*. The Journal of Physical Chemistry B, 1999. 103(36): p. 7654-7664.
51. Cao, X., et al., *Polymyxin B immobilized on cross-linked cellulose microspheres for endotoxin adsorption*. Carbohydrate polymers, 2016. 136: p. 12-18.

SECTION

2. CONCLUSIONS AND FUTURE WORK

2.1. CONCLUSIONS

In paper-I, we reported the synthesis of polymeric PCL NPs by employing a solvent evaporation method, followed by the performance evaluation of PCL NPs for the adsorption and removal of endotoxins. It was found that PCL NPs in powder form removed around 88% of endotoxins from the water sample. The presence of salts, by adding PBS, increased the endotoxin removal efficiency further up to 100 % while maintaining 100% protein recovery from solutions. Such high removal efficiency of endotoxin from water and PBS is attributed to strong hydrophobic and van der Waals interactions. Buffers of variable pH play a very important role in determining the endotoxin binding on PCL. Acidic (pH 2.8) and alkaline (pH 9.6) buffers give ~ 90% endotoxin removal whereas intermediate pHs from 5.8 to 8 give reasonably lower % endotoxin removal, that is, between 30 and 75%. The adsorption efficiency reached almost 100% when PCL NPs were incorporated into the CA membrane where the water flow through the porous structure was directly facilitated by gravity (not requiring any pumping devices). The biocompatible PCL NPs can be reused by desorbing majority of adsorbed endotoxin using 0.2 N NaOH solution. A preliminary cost analysis showed that the manufacturing cost of the PCL NP-embedded CA membrane is quite affordable. These findings, coupled with PCL NP's known biodegradability, support the potential of

hybrid NP-membrane system use in large-scale operations that remove endotoxins efficiently and reduce the downstream process costs in biotechnological industries.

In paper-II, the goal was to test the validity of the hypothesis that endotoxin binding on PCL NP surface was due to van der Waals and hydrophobic interaction occurring between lipid-A tail of endotoxins and hydrophobic surface of PCL. This was evaluated by taking polystyrene nanoparticles, which have similar hydrophobic nature as polycaprolactone nanoparticles used as control. Subsequently, PS NPs did not show as high endotoxin removal (31%-75 %) efficiency as PCL NPs thus suggesting that in case of PCL NPs there were attractive forces other than van der Waals and hydrophobic interaction that resulted in high endotoxin binding efficiency and need further investigation. Further, the effect of pH on protein recovery for PCL NPs were also evaluated. Six different types of proteins with molecular weights varying from 14 kDa - 341 kDa and isoelectric points (pI) from 4.5- 10.7 were selected. pH values of 2.8, isoelectric point of protein and 11.5 were selected for the experiments and it was observed that protein recovery irrespective of conditions were > 93 %, which is reasonably high. Thus suggesting that pH does not have a major effect on protein recovery when using PCL NPs. It has also been shown that PCL NPs incorporated CA biofilter are effective in removing endotoxins from various protein solutions with improved flow properties and higher throughput. The maximum endotoxin removal efficiency was ~ 99 % and a protein recovery > 92 % thus indicating that majority of endotoxin binding sites within the biofilter were being utilized for endotoxin binding and very less amount of protein was getting lost during the purification operation.

2.2. FUTURE WORK

1. Expanding the application of PCL NPs loaded cellulose acetate (CA) biofilter for removal of harmful algal toxins from lake waters. To begin with our target toxins will be cyanotoxins, eg: anatoxin and microcystin-LR which are found quite extensively in the lake water.
2. Exploring the possibility of using BODIPY dye, which is a lipid biomarker as a toxin detection kit at different toxin concentrations, operating conditions and in different solutions. BODIPY has already been shown to detect endotoxins successfully as the structure of endotoxin molecules comprises of non-polar lipid-A molecules in its tail part which is hydrophobic in nature. BODIPY, which is fluorescent dye shows this unique property of quenching in its fluorescence intensity when it comes in contact with lipid molecules. Thus, this quenching property of BODIPY on coming in contact with lipid molecules was utilized to come up with a detection kit for endotoxins. Quantification of endotoxin was done by measuring the drop in fluorescence intensity (quenching) using the optical microplate reader. Our future work will comprise of testing the minimum endotoxin detection limit of BODIPY dye and also investigate the different algal toxins which can be detected using the BODIPY dye as a biomarker.

BIBLIOGRAPHY

1. Hanke, A. T.; Ottens, M. Purifying biopharmaceuticals: knowledge-based chromatographic process development. *Trends in biotechnology* 2014, 32, 210-220.
2. Gronemeyer, P.; Ditz, R.; Strube, J. Trends in upstream and downstream process development for antibody manufacturing. *Bioengineering* 2014, 1, 188-212.
3. Jozala, A. F.; Geraldles, D. C.; Tundisi, L. L.; Feitosa, V. d. A.; Breyer, C. A.; Cardoso, S. L.; Mazzola, P. G.; Oliveira-Nascimento, L. d.; Rangel-Yagui, C. d. O.; Magalhães, P. d. O.; Oliveira, M. A. d.; Pessoa, A. Biopharmaceuticals from microorganisms: from production to purification. *Brazilian Journal of Microbiology* 2016, 47, 51-63.
4. Miyagi, T.; Hori, O.; Koshida, K.; Egawa, M.; Kato, H.; Kitagawa, Y.; Ozawa, K.; Ogawa, S.; Namiki, M. Antitumor effect of reduction of 150-kDa oxygen-regulated protein expression on human prostate cancer cells. *International journal of urology* 2002, 9, 577-585.
5. McKay, R.; Hauk, P.; Wu, H. C.; Pottash, A. E.; Shang, W.; Terrell, J.; Payne, G. F.; Bentley, W. E. Controlling localization of Escherichia coli populations using a two-part synthetic motility circuit: An accelerator and brake. *Biotechnology and bioengineering* 2017, 114, 2883-2895.
6. Mack, L.; Brill, B.; Delis, N.; Groner, B. Endotoxin depletion of recombinant protein preparations through their preferential binding to histidine tags. *Anal Biochem* 2014, 466, 83-88.
7. Chen, W.; Qin, Z. Development of a gene cloning system in a fast-growing and moderately thermophilic Streptomyces species and heterologous expression of Streptomyces antibiotic biosynthetic gene clusters. *BMC microbiology* 2011, 11, 243.
8. Baeshen, M.; Al-Hejin, A.; S Bora, R.; Ahmed, M.; Ramadan, H.; Saini, K.; Baeshen, N.; Redwan, E.: *Production of Biopharmaceuticals in E. coli: Current Scenario and Future Perspectives*, 2015; Vol. 25.
9. Gonçalves, G. A. L.; Bower, D. M.; Prazeres, D. M. F.; Monteiro, G. A.; Prather, K. L. J. Rational engineering of Escherichia coli strains for plasmid biopharmaceutical manufacturing. *Biotechnology Journal* 2012, 7, 251-261.

10. Wilding, K. M.; Hunt, J. P.; Wilkerson, J. W.; Funk, P. J.; Swensen, R. L.; Carver, W. C.; Christian, M. L.; Bundy, B. C. Endotoxin-Free E. coli-Based Cell-Free Protein Synthesis: Pre-Expression Endotoxin Removal Approaches for on-Demand Cancer Therapeutic Production. *Biotechnology Journal* 2019, *14*, 1800271.
11. Berlec, A.; Štrukelj, B. Current state and recent advances in biopharmaceutical production in Escherichia coli, yeasts and mammalian cells. *Journal of Industrial Microbiology & Biotechnology* 2013, *40*, 257-274.
12. Liu, X.; Ding, W.; Jiang, H. Engineering microbial cell factories for the production of plant natural products: from design principles to industrial-scale production. *Microbial cell factories* 2017, *16*, 125.
13. Rosenfeld, L. Insulin: discovery and controversy. *Clinical chemistry* 2002, *48*, 2270-2288.
14. Hu, Y.; Huang, S.-J.; Chu, K.; Wu, T.; Wang, Z.-Z.; Yang, C.-L.; Cai, J.-P.; Jiang, H.-M.; Wang, Y.-J.; Guo, M. Safety of an Escherichia coli-expressed bivalent human papillomavirus (types 16 and 18) L1 virus-like particle vaccine: an open-label phase I clinical trial. *Human vaccines & immunotherapeutics* 2014, *10*, 469-475.
15. Schwechheimer, C.; Kuehn, M. J. Outer-membrane vesicles from Gram-negative bacteria: biogenesis and functions. *Nature Reviews Microbiology* 2015, *13*, 605.
16. Petsch, D.; Anspach, F. B. Endotoxin removal from protein solutions. *Journal of biotechnology* 2000, *76*, 97-119.
17. Ongkudon, C. M.; Chew, J. H.; Liu, B.; Danquah, M. K. Chromatographic removal of endotoxins: a bioprocess engineer's perspective. *ISRN Chromatography* 2012, *2012*.
18. Aida, Y.; Pabst, M. J. Removal of endotoxin from protein solutions by phase separation using Triton X-114. *Journal of immunological methods* 1990, *132*, 191-195.
19. Magalhães, P. O.; Lopes, A. M.; Mazzola, P. G.; Rangel-Yagui, C.; Penna, T.; Pessoa Jr, A. Methods of endotoxin removal from biological preparations: a review. *J Pharm Pharm Sci* 2007, *10*, 388-404.
20. Anspach, F. B. Endotoxin removal by affinity sorbents. *Journal of biochemical and biophysical methods* 2001, *49*, 665-681.

21. Gorbet, M. B.; Sefton, M. V. Endotoxin: the uninvited guest. *Biomaterials* 2005, 26, 6811-6817.
22. Jang, H.; Kim, H.-S.; Moon, S.-C.; Lee, Y.-R.; Yu, K.-Y.; Lee, B.-K.; Kim, J.-S. Effects of protein concentration and detergent on endotoxin reduction by ultrafiltration. *BMB Reports* 2009, 42, 462-466.
23. Dullah, E. C.; Ongkudon, C. M. Current trends in endotoxin detection and analysis of endotoxin–protein interactions. *Critical Reviews in Biotechnology* 2017, 37, 251-261.
24. Amini Tapouk, F.; Nabizadeh, R.; Nasserli, S.; Mesdaghinia, A.; Khorsandi, H.; Mahvi, A. H.; Gholibegloo, E.; Alimohammadi, M.; Khoobi, M. Endotoxin removal from aqueous solutions with dimethylamine-functionalized graphene oxide: Modeling study and optimization of adsorption parameters. *Journal of Hazardous Materials* 2019, 368, 163-177.
25. Almeida, K. M. d.; Almeida, M. M.; Fingola, F. F.; Ferraz, H. C. Membrane adsorber for endotoxin removal. *Brazilian Journal of Pharmaceutical Sciences* 2016, 52, 171-178.
26. Raetz, C. R. H.; Whitefield, C. Lipopolysaccharide Endotoxins. *Annual review of biochemistry* 2001, 71, 635-700.
27. Daneshian, M.; Guenther, A.; Wendel, A.; Hartung, T.; von Aulock, S. In vitro pyrogen test for toxic or immunomodulatory drugs. *Journal of Immunological Methods* 2006, 313, 169-175.
28. Brent, A. J. Sepsis. *Medicine* 2017, 45, 649-653.
29. Abbass, A.-N.: *Factors affecting endotoxin removal from aqueous solutions by ultrafiltration process*, 2011; Vol. 70.
30. Ramachandran, G. Gram-positive and gram-negative bacterial toxins in sepsis A brief review. *Virulence* 2014, 5, 196-218.
31. BILLIAU, A.; VANDEKERCKHOVE, F. Cytokines and their interactions with other inflammatory mediators in the pathogenesis of sepsis and septic shock. *European Journal of Clinical Investigation* 1991, 21, 559-573.
32. Angus, D. C.; van der Poll, T. Severe Sepsis and Septic Shock. *New England Journal of Medicine* 2013, 369, 840-851.

33. Johnston, M. C.; Knight, J. E.: *Septic Shock : Symptoms, Management and Risk Factors*; Nova Science Publishers, Incorporated: New York, UNITED STATES, 2012.
34. Das, A. P.; Kumar, P. S.; Swain, S. Recent advances in biosensor based endotoxin detection. *Biosensors and Bioelectronics* 2014, *51*, 62-75.
35. Anspach, F. B.; Petsch, D. Membrane adsorbers for selective endotoxin removal from protein solutions. *Process Biochemistry* 2000, *35*, 1005-1012.
36. Szermer-Olearnik, B.; Boratyński, J. Removal of endotoxins from bacteriophage preparations by extraction with organic solvents. *PLoS One* 2015, *10*.
37. Schaumberger, S.; Ladinig, A.; Reisinger, N.; Ritzmann, M.; Schatzmayr, G. Evaluation of the endotoxin binding efficiency of clay minerals using the Limulus Amebocyte lysate test: an in vitro study. *AMB Express* 2014, *4*, 1.
38. de Vries, I.; Schreiber, S.; Boßmann, D.; Hellmann, Z.; Kopatz, J.; Neumann, H.; Beutel, S. Single-use membrane adsorbers for endotoxin removal and purification of endogenous polysialic acid from Escherichia coli K1. *Biotechnology Reports* 2018, *17*, 110-116.
39. Hirayama, C.; Sakata, M. Chromatographic removal of endotoxin from protein solutions by polymer particles. *Journal of Chromatography B* 2002, *781*, 419-432.
40. Liu, S.; Tobias, R.; McClure, S.; Styba, G.; Shi, Q.; Jackowski, G. Removal of endotoxin from recombinant protein preparations. *Clinical biochemistry* 1997, *30*, 455-463.
41. Rosano, G. L.; Ceccarelli, E. A. Recombinant protein expression in Escherichia coli: advances and challenges. *Frontiers in microbiology* 2014, *5*, 172.
42. Miyamoto, T.; Okano, S.; Kasai, N. Inactivation of Escherichia coli Endotoxin by Soft Hydrothermal Processing. *Applied and Environmental Microbiology* 2009, *75*, 5058-5063.
43. Kang, Y.; Luo, R. G. Effects of ionic strength and pH on endotoxin removal efficiency and protein recovery in an affinity chromatography. *Process Biochemistry* 2000, *36*, 85-92.
44. Branston, S. D.; Wright, J.; Keshavarz-Moore, E. A non-chromatographic method for the removal of endotoxins from bacteriophages. *Biotechnology and Bioengineering* 2015, *112*, 1714-1719.

45. Saraswat, M.; Musante, L.; Ravidà, A.; Shortt, B.; Byrne, B.; Holthofer, H.: *Preparative Purification of Recombinant Proteins: Current Status and Future Trends*, 2013; Vol. 2013.
46. Straathof, A.: The Proportion of Downstream Costs in Fermentative Production Processes. 2011; Vol. 2; pp 811-814.
47. Maloney, T.; Phelan, R.; Simmons, N. Saving the horseshoe crab: A synthetic alternative to horseshoe crab blood for endotoxin detection. *PLoS biology* 2018, *16*, e2006607.
48. Gimenes, I.; Caldeira, C.; Presgrave, O. A. F.; de Moura, W. C.; Boas, M. H. S. V. Assessment of pyrogenic response of lipoteichoic acid by the monocyte activation test and the rabbit pyrogen test. *Regulatory Toxicology and Pharmacology* 2015, *73*, 356-360.
49. Hoffmann, S.; Peterbauer, A.; Schindler, S.; Fennrich, S.; Poole, S.; Mistry, Y.; Montag-Lessing, T.; Spreitzer, I.; Löschner, B.; Van Aalderen, M. International validation of novel pyrogen tests based on human monocytoïd cells. *Journal of immunological methods* 2005, *298*, 161-173.
50. Studholme, L.; Sutherland, J.; Desai, T.; Hockley, J.; Care, R.; Nordgren, I. K.; Vipond, C.; Group, C. S. Evaluation of the monocyte activation test for the safety testing of meningococcal B vaccine Bexsero: A collaborative study. *Vaccine* 2019, *37*, 3761-3769.
51. Vipond, C.; Findlay, L.; Feavers, I.; Care, R. Limitations of the rabbit pyrogen test for assessing meningococcal OMV based vaccines. *ALTEX-Alternatives to animal experimentation* 2016, *33*, 47-53.
52. Jin, Y.; Jia, J.; Li, C.; Xue, J.; Sun, J.; Wang, K.; Gan, Y.; Xu, J.; Shi, Y.; Liang, X. LAL test and RPT for endotoxin detection of CPT-11/DSPE-mPEG2000 nanoformulation: What if traditional methods are not applicable? *asian journal of pharmaceutical sciences* 2018, *13*, 289-296.
53. Ong, K. G.; Leland, J. M.; Zeng, K.; Barrett, G.; Zourob, M.; Grimes, C. A. A rapid highly-sensitive endotoxin detection system. *Biosensors and Bioelectronics* 2006, *21*, 2270-2274.
54. Sakai, H.; Hisamoto, S.; Fukutomi, I.; Sou, K.; Takeoka, S.; Tsuchida, E. Detection of lipopolysaccharide in hemoglobin-vesicles by *Limulus* amebocyte lysate test with kinetic-turbidimetric gel clotting analysis and pretreatment of surfactant. *Journal of pharmaceutical sciences* 2004, *93*, 310-321.

55. Dolejš, P.; Vaňousová, K. A collection of horseshoe crabs (Chelicerata: Xiphosura) in the National Museum, Prague (Czech Republic) and a review of their immunological importance. *Arachnologische Mitteilungen* 2015, 49, 1-9.
56. Joiner, T. J.; Kraus, P. F.; Kupiec, T. C. Comparison of endotoxin testing methods for pharmaceutical products. *International journal of pharmaceutical compounding* 2002, 6, 408-409.
57. Iwanaga, S. Biochemical principle of Limulus test for detecting bacterial endotoxins. *Proc Jpn Acad Ser B Phys Biol Sci* 2007, 83, 110-119.
58. Muta, T.; Miyata, T.; Misumi, Y.; Tokunaga, F.; Nakamura, T.; Toh, Y.; Ikehara, Y.; Iwanaga, S. Limulus factor C. An endotoxin-sensitive serine protease zymogen with a mosaic structure of complement-like, epidermal growth factor-like, and lectin-like domains. *Journal of Biological Chemistry* 1991, 266, 6554-6561.
59. Chen, L.; Mozier, N. Comparison of Limulus amebocyte lysate test methods for endotoxin measurement in protein solutions. *Journal of pharmaceutical and biomedical analysis* 2013, 80, 180-185.
60. Mohanan, P.; Banerjee, S.; Geetha, C. Detection of pyrogenicity on medical grade polymer materials using rabbit pyrogen, LAL and ELISA method. *Journal of pharmaceutical and biomedical analysis* 2011, 55, 1170-1174.
61. Hurley, J. C. Endotoxemia: methods of detection and clinical correlates. *Clinical microbiology reviews* 1995, 8, 268-292.
62. Nakamura, T.; Tokunaga, F.; Morita, T.; Iwanaga, S. Interaction between Lipopolysaccharide and Intracellular Serine Protease Zymogen, Factor C, from Horseshoe Crab (*Tachypleus tridentatus*) Hemocytes1. *The Journal of Biochemistry* 1988, 103, 370-374.
63. Schneider, C. Overcoming Low Endotoxin Recovery. *Pharmaceutical Technology Europe* 2016, 28, 40.
64. Schwarz, H.; Gornicec, J.; Neuper, T.; Parigiani, M. A.; Wallner, M.; Duschl, A.; Horejs-Hoeck, J. Biological activity of masked endotoxin. *Scientific Reports* 2017, 7, 44750.
65. Guidance for Industry Pyrogen and Endotoxins Testing: Questions and Answers. <https://www.fda.gov/regulatory-information/search-fda-guidance-documents/pyrogen-and-endotoxins-testing-questions-and-answers> (accessed December 22, 2019).

66. Elin, R. J.; Wolff, S. M. Nonspecificity of the Limulus Amebocyte Lysate Test: Positive Reactions with Polynucleotides and Proteins. *The Journal of Infectious Diseases* 1973, *128*, 349-352.
67. Morita, T.; Tanaka, S.; Nakamura, T.; Iwanaga, S. A new (1 → 3)-β-D-glucan-mediated coagulation pathway found in limulus amebocytes. *FEBS Letters* 1981, *129*, 318-321.
68. OHNO, N.; MORRISON, D. C. Lipopolysaccharide interactions with lysozyme differentially affect lipopolysaccharide immunostimulatory activity. *European Journal of Biochemistry* 1989, *186*, 629-636.
69. Mares, J.; Kumaran, S.; Gobbo, M.; Zerbe, O. Interactions of lipopolysaccharide and polymyxin studied by NMR spectroscopy. *J Biol Chem* 2009, *284*, 11498-11506.
70. Bhunia, A.; Ramamoorthy, A.; Bhattacharjya, S. Helical Hairpin Structure of a Potent Antimicrobial Peptide MSI-594 in Lipopolysaccharide Micelles by NMR Spectroscopy. *Chemistry – A European Journal* 2009, *15*, 2036-2040.
71. Kushibiki, T.; Kamiya, M.; Aizawa, T.; Kumaki, Y.; Kikukawa, T.; Mizuguchi, M.; Demura, M.; Kawabata, S.-i.; Kawano, K. Interaction between tachyplesin I, an antimicrobial peptide derived from horseshoe crab, and lipopolysaccharide. *Biochimica et Biophysica Acta (BBA) - Proteins and Proteomics* 2014, *1844*, 527-534.
72. *Guidelines for using the Test for Bacterial Endotoxins*, 2014.
73. Ding, J.; Navas, T.; Ho, B. Molecular cloning and sequence analysis of Factor C cDNA from the Singapore horseshoe crab, *Carcinoscorpius rotundicauda*. *Molecular marine biology and biotechnology* 1995, *4*, 90-103.
74. Levin, J.; Bang, F. Clottable Protein in Limulus: Its Localization and Kinetics of Its Coagulation by Endotoxin. *Thrombosis et diathesis haemorrhagica* 1968, *19*, 186-197.
75. Iwanaga, S. The limulus clotting reaction. *Current Opinion in Immunology* 1993, *5*, 74-82.
76. NAKAMURA, T.; MORITA, T.; IWANAGA, S. Lipopolysaccharide-sensitive serine-protease zymogen (factor C) found in Limulus hemocytes. *European Journal of Biochemistry* 1986, *154*, 511-521.

77. Tokunaga, F.; Nakajima, H.; Iwanaga, S. Further Studies on Lipopolysaccharide-Sensitive Serine Protease Zymogen (Factor C): Its Isolation from *Limulus polyphemus* Hemocytes and Identification as an Intracellular Zymogen Activated by α -Chymotrypsin, Not by Trypsin1. *The Journal of Biochemistry* 1991, *109*, 150-157.
78. Ding, J. L.; Ho, B. A new era in pyrogen testing. *Trends in Biotechnology* 2001, *19*, 277-281.
79. Barnett, M. J.; Wadham, J. L.; Jackson, M.; Cullen, D. C. In-Field Implementation of a Recombinant Factor C Assay for the Detection of Lipopolysaccharide as a Biomarker of Extant Life within Glacial Environments. *Biosensors (Basel)* 2012, *2*, 83-100.
80. Gall, D.; Nielsen, K.; Yu, W.; Smith, P. Rapid, field-adapted indirect enzyme-linked immunosorbent assay for detection of antibodies in bovine whole blood and serum to *Brucella abortus*. *Clin. Vaccine Immunol.* 2006, *13*, 501-506.
81. Wunderlich, C.; Schumacher, S.; Kietzmann, M. Prostaglandin E2 as a read out for endotoxin detection in a bovine whole blood assay. *Journal of veterinary pharmacology and therapeutics* 2015, *38*, 196-198.
82. Schindler, S.; Spreitzer, I.; Löschner, B.; Hoffmann, S.; Hennes, K.; Halder, M.; Brügger, P.; Frey, E.; Hartung, T.; Montag, T. International validation of pyrogen tests based on cryopreserved human primary blood cells. *Journal of Immunological Methods* 2006, *316*, 42-51.
83. (ISIA), I. S. I. A. *Frequently Asked Questions - Bovine Serum* Retrieved April 1, 2019.
84. Vipond, C.; Sutherland, J.; Nordgren, K.; Kemp, G.; Heath, A.; Care, R.; Studholme, L. Development and validation of a monocyte activation test for the control/safety testing of an OMV-based meningococcal B vaccine. *Vaccine* 2019, *37*, 3747-3753.
85. Liebers, V.; Stubel, H.; Düser, M.; Brüning, T.; Raulf-Heimsoth, M. Standardization of whole blood assay for determination of pyrogenic activity in organic dust samples. *International journal of hygiene and environmental health* 2009, *212*, 547-556.
86. Nik Mansor, N.; Leong, T.; Safitri, E.; Futra, D.; Ahmad, N.; Nasuruddin, D.; Itnin, A.; Zaini, I.; Arifin, K.; Heng, L. An amperometric biosensor for the determination of bacterial sepsis biomarker, secretory phospholipase group 2-IIA using a tri-enzyme system. *Sensors* 2018, *18*, 686.

87. Lequin, R. M. Enzyme immunoassay (EIA)/enzyme-linked immunosorbent assay (ELISA). *Clinical chemistry* 2005, 51, 2415-2418.
88. Hasiwa, N.; Daneshian, M.; Bruegger, P.; Fennrich, S.; Hochadel, A.; Hoffmann, S.; Rivera-Mariani, F. E.; Rockel, C.; Schindler, S.; Spreitzer, I. Evidence for the detection of non-endotoxin pyrogens by the whole blood monocyte activation test. *Alternatives to animal experimentation: ALTEX* 2013, 30, 169-208.
89. Stang, K.; Fennrich, S.; Krajewski, S.; Stoppelkamp, S.; Burgener, I. A.; Wendel, H.-P.; Post, M. Highly sensitive pyrogen detection on medical devices by the monocyte activation test. *Journal of Materials Science: Materials in Medicine* 2014, 25, 1065-1075.
90. Koryakina, A.; Frey, E.; Bruegger, P. Cryopreservation of human monocytes for pharmacopeial monocyte activation test. *Journal of immunological methods* 2014, 405, 181-191.
91. Spreitzer, I.; Löschner, B.; Schneider, C. K.; Hanschmann, K.-M.; Montag, T. 10 years of experience with alternative pyrogen tests (monocyte activation tests). *Jpn. Soc. Altern. Anim. Exp.* 2008, 14, 587-589.
92. Utescher, C. L. d. A.; Buosi, K. L.; Botosso, V. F.; Quintilio, W. Monocyte Activation Test (MAT) as a possibility of replacement for the rabbit pyrogen test in hyperimmune sera. *Brazilian Journal of Pharmaceutical Sciences* 2018, 54.
93. Kohl, T. O.; Ascoli, C. A. Direct Competitive Enzyme-Linked Immunosorbent Assay (ELISA). *Cold Spring Harbor Protocols* 2017, 2017, pdb.prot093740.
94. Honeychurch, K.: Printed thick-film biosensors. In *Printed Films*; Elsevier, 2012; pp 366-409.
95. Priano, G.; Pallarola, D.; Battaglini, F. Endotoxin detection in a competitive electrochemical assay: synthesis of a suitable endotoxin conjugate. *Analytical biochemistry* 2007, 362, 108-116.
96. Syaifudin, A. R. M.; Mukhopadhyay, S. C.; Yu, P.; Haji-Sheikh, M. J.; Chuang, C.; Vanderford, J. D.; Huang, Y. Measurements and Performance Evaluation of Novel Interdigital Sensors for Different Chemicals Related to Food Poisoning. *IEEE Sensors Journal* 2011, 11, 2957-2965.
97. Yeo, T. Y.; Choi, J. S.; Lee, B. K.; Kim, B. S.; Yoon, H. I.; Lee, H. Y.; Cho, Y. W. Electrochemical endotoxin sensors based on TLR4/MD-2 complexes immobilized on gold electrodes. *Biosensors and Bioelectronics* 2011, 28, 139-145.

98. Cho, M.; Chun, L.; Lin, M.; Choe, W.; Nam, J.; Lee, Y. Sensitive electrochemical sensor for detection of lipopolysaccharide on metal complex immobilized gold electrode. *Sensors and Actuators B: Chemical* 2012, *174*, 490-494.
99. Reta, N.; Michelmore, A.; Saint, C. P.; Prieto-Simon, B.; Voelcker, N. H. Label-free bacterial toxins detection in water supplies using porous silicon nanochannel sensors. *ACS sensors* 2019.
100. Liu, T.; Meng, F.; Cheng, W.; Sun, H.; Luo, Y.; Tang, Y.; Miao, P. Preparation of a peptide-modified electrode for capture and voltammetric determination of endotoxin. *ACS omega* 2017, *2*, 2469-2473.
101. Heras, J. Y.; Pallarola, D.; Battaglini, F. Electronic tongue for simultaneous detection of endotoxins and other contaminants of microbiological origin. *Biosensors and Bioelectronics* 2010, *25*, 2470-2476.
102. Richter, M. M. Electrochemiluminescence (ecl). *Chemical Reviews* 2004, *104*, 3003-3036.
103. Alahi, M.; Mukhopadhyay, S. Detection methodologies for pathogen and toxins: a review. *Sensors* 2017, *17*, 1885.
104. Inoue, K. Y.; Ino, K.; Shiku, H.; Matsue, T. Electrochemical detection of endotoxin using recombinant factor C zymogen. *Electrochemistry Communications* 2010, *12*, 1066-1069.
105. Yamamoto, A.; Ochiai, M.; Fujiwara, H.; Asakawa, S.; Ichinohe, K.; Kataoka, M.; Toyozumi, H.; Horiuchi, Y. Evaluation of the applicability of the bacterial endotoxin test to antibiotic products. *Biologicals* 2000, *28*, 155-167.
106. Shen, W.-J.; Zhuo, Y.; Chai, Y.-Q.; Yuan, R. Cu-based metal-organic frameworks as a catalyst to construct a ratiometric electrochemical aptasensor for sensitive lipopolysaccharide detection. *Analytical chemistry* 2015, *87*, 11345-11352.
107. An, Z.; Jang, C. H. Simple and Label-Free Liquid Crystal-based Optical Sensor for Highly Sensitive and Selective Endotoxin Detection by Aptamer Binding and Separation. *ChemistrySelect* 2019, *4*, 1416-1422.
108. Paul, I. E.; Raichur, A. M.; Chandrasekaran, N.; Mukherjee, A. Fluorometric sensing of endotoxin based on aggregation of CTAB capped gold nanospheres. *Journal of Luminescence* 2016, *178*, 106-114.

109. Noda, K.; Goto, H.; Murakami, Y.; Ahmed, A. B. F.; Kuroda, A. Endotoxin assay by bioluminescence using mutant firefly luciferase. *Analytical biochemistry* 2010, *397*, 152-155.
110. Fujii, H.; Noda, K.; Asami, Y.; Kuroda, A.; Sakata, M.; Tokida, A. Increase in bioluminescence intensity of firefly luciferase using genetic modification. *Analytical biochemistry* 2007, *366*, 131-136.
111. Ostronoff, C. S.; Lourenço, F. R. Measurement Uncertainty of Chromogenic LAL Assays: Reaction Time and Proportion of Endotoxin and LAL Reagent Affect Release of p-Nitroaniline. *Journal of AOAC International* 2015, *98*, 51-55.
112. Razdan, S.; Wang, J.-C.; Barua, S. PolyBall: A new adsorbent for the efficient removal of endotoxin from biopharmaceuticals. *Scientific Reports* 2019, *9*, 8867.
113. Donnell, M. L.; Lyon, A. J.; Mormile, M. R.; Barua, S. Endotoxin hitchhiking on polymer nanoparticles. *Nanotechnology* 2016, *27*, 285601.
114. Bromberg, L.; Chang, E. P.; Alvarez-Lorenzo, C.; Magarinos, B.; Concheiro, A.; Hatton, T. A. Binding of functionalized paramagnetic nanoparticles to bacterial lipopolysaccharides and DNA. *Langmuir* 2010, *26*, 8829-8835.
115. Barua, S. US Patent Number 9,918,943 entitled "Systems and Methods for Endotoxin Removal From Fluids". United States Patent.
116. Wood, S. J.; Miller, K. A.; David, S. A. Anti-endotoxin agents. 1. Development of a fluorescent probe displacement method optimized for the rapid identification of lipopolysaccharide-binding agents. *Combinatorial chemistry & high throughput screening* 2004, *7*, 239-249.
117. Prasad, P.; Sachan, S.; Suman, S.; Swayambhu, G.; Gupta, S. Regenerative core-shell nanoparticles for simultaneous removal and detection of endotoxins. *Langmuir* 2018, *34*, 7396-7403.
118. Zhang, J.; Khan, I.; Zhang, Q.; Liu, X.; Dostalek, J.; Liedberg, B.; Wang, Y. Lipopolysaccharides detection on a grating-coupled surface plasmon resonance smartphone biosensor. *Biosensors and Bioelectronics* 2018, *99*, 312-317.
119. Manoharan, H.; Kalita, P.; Gupta, S.; Sai, V. Plasmonic biosensors for bacterial endotoxin detection on biomimetic C-18 supported fiber optic probes. *Biosensors and Bioelectronics* 2019, *129*, 79-86.
120. Sheikh, S.; Blaszykowski, C.; Romaschin, A.; Thompson, M. Endotoxin detection in full blood plasma in a theranostic approach to combat sepsis. *RSC Advances* 2016, *6*, 38037-38041.

121. Li, S.; Li, Y.; Chen, H.; Horikawa, S.; Shen, W.; Simonian, A.; Chin, B. A. Direct detection of *Salmonella typhimurium* on fresh produce using phage-based magnetoelastic biosensors. *Biosensors and Bioelectronics* 2010, *26*, 1313-1319.
122. El-Moghazy, A.-N. A. Factors affecting endotoxin removal from aqueous solutions by ultrafiltration process. 2011, *70 (1)*.
123. de Mas, N.; Kientzler, D. C.; Kleindienst, D. Endotoxin Removal from a Small-Molecule Aqueous Drug Substance Using Ultrafiltration: A Case Study. *Organic Process Research & Development* 2015, *19*, 1293-1298.
124. Szymczyk, K.; Taraba, A. Properties of aqueous solutions of nonionic surfactants, Triton X-114 and Tween 80, at temperatures from 293 to 318K: Spectroscopic and ultrasonic studies. *Chemical Physics* 2017, *483-484*, 96-102.
125. Lopes, A. M.; Magalhães, P. O.; Mazzola, P. G.; Rangel-Yagui, C. O.; de Carvalho, J. C. M.; Penna, T. C. V.; Pessoa Jr, A. LPS removal from an *E. coli* fermentation broth using aqueous two-phase micellar system. *Biotechnology Progress* 2010, *26*, 1644-1653.
126. Ma, R.; Zhao, J.; Du, H.-C.; Tian, S.; Li, L.-W. Removing endotoxin from plasmid samples by Triton X-114 isothermal extraction. *Analytical biochemistry* 2012, *424*, 124-126.
127. Cunha, T.; Aires-Barros, R. Large-scale extraction of proteins. *Molecular Biotechnology* 2002, *20*, 29-40.
128. Pihlasalo, S.; Auranen, L.; Hänninen, P.; Härmä, H. Method for Estimation of Protein Isoelectric Point. *Analytical Chemistry* 2012, *84*, 8253-8258.
129. Chen, R. H.; Huang, C., Jr.; Newton, B. S.; Ritter, G.; Old, L. J.; Batt, C. A. Factors affecting endotoxin removal from recombinant therapeutic proteins by anion exchange chromatography. *Protein Expression and Purification* 2009, *64*, 76-81.
130. Janson, J.-C.; Janson, J.-C.: *Protein Purification : Principles, High Resolution Methods, and Applications*; John Wiley & Sons, Incorporated: Hoboken, UNITED STATES, 2011.
131. Fekete, S.; Beck, A.; Veuthey, J.-L.; Guillarme, D. Ion-exchange chromatography for the characterization of biopharmaceuticals. *Journal of Pharmaceutical and Biomedical Analysis* 2015, *113*, 43-55.
132. Diogo, M. M.; Queiroz, J. A.; Prazeres, D. M. F. Chromatography of plasmid DNA. *Journal of Chromatography A* 2005, *1069*, 3-22.

133. Černigoj, U.; Vidic, U.; Barut, M.; Podgornik, A.; Peterka, M.; Štrancar, A. A multimodal histamine ligand for chromatographic purification of plasmid DNA. *Journal of Chromatography A* 2013, *1281*, 87-93.
134. Ritzén, U.; Rotticci-Mulder, J.; Strömberg, P.; Schmidt, S. R. Endotoxin reduction in monoclonal antibody preparations using arginine. *Journal of Chromatography B* 2007, *856*, 343-347.
135. Hage, D. S. Affinity Chromatography: A Review of Clinical Applications. *Clinical Chemistry* 1999, *45*, 593-615.
136. Guo, W.; Shang, Z.; Yu, Y.; Zhou, L. Removal of endotoxin from aqueous solutions by affinity membrane. *Biomedical Chromatography* 1997, *11*, 164-166.
137. Stadler, J.; Lemmens, R.; Nyhammar, T. Plasmid DNA purification. *The Journal of Gene Medicine* 2004, *6*, S54-S66.
138. Wei, Z.; Huang, W.; Li, J.; Hou, G.; Fang, J.; Yuan, Z. Studies on endotoxin removal mechanism of adsorbents with amino acid ligands. *Journal of Chromatography B* 2007, *852*, 288-292.
139. Serdakowski London, A.; Kerins, B.; Tschantz, W. R.; Mackay, K. Endotoxin removal and prevention for pre-clinical biologics production. *Biotechnology Journal* 2012, *7*, 1509-1516.
140. Ryder, M. P.; Wu, X.; McKelvey, G. R.; McGuire, J.; Schilke, K. F. Binding interactions of bacterial lipopolysaccharide and the cationic amphiphilic peptides polymyxin B and WLBU2. *Colloids and Surfaces B: Biointerfaces* 2014, *120*, 81-87.
141. Issekutz, A. C. Removal of gram-negative endotoxin from solutions by affinity chromatography. *Journal of Immunological Methods* 1983, *61*, 275-281.
142. Srimal, S.; Surolia, N.; Balasubramanian, S.; Surolia, A. Titration calorimetric studies to elucidate the specificity of the interactions of polymyxin B with lipopolysaccharides and lipid A. *The Biochemical journal* 1996, *315 (Pt 2)*, 679-686.
143. McAllister, L. A.; Hixon, M. S.; Schwartz, R.; Kubitz, D. S.; Janda, K. D. Synthesis and Application of a Novel Ligand for Affinity Chromatography Based Removal of Endotoxin from Antibodies. *Bioconjugate Chemistry* 2007, *18*, 559-566.

144. Rustici, A.; Velucchi, M.; Faggioni, R.; Sironi, M.; Ghezzi, P.; Quataert, S.; Green, B.; Porro, M. Molecular Mapping and Detoxification of the Lipid A Binding Site by Synthetic Peptides. *Science* 1993, 259, 361-365.
145. Figueiredo, D. B.; Carvalho, E.; Santos, M. P.; Kraschowitz, S.; Zanardo, R. T.; Campani, G.; Silva, G. G.; Sargo, C. R.; Horta, A. C. L.; de C. Giordano, R.; Miyaji, E. N.; Zangirolami, T. C.; Cabrera-Crespo, J.; Gonçalves, V. M. Production and purification of an untagged recombinant pneumococcal surface protein A (PspA4Pro) with high-purity and low endotoxin content. *Applied Microbiology and Biotechnology* 2017, 101, 2305-2317.
146. <https://www.biovision.com/toxouttm-high-capacity-endotoxin-removal-agarose.html> (accessed January 18 2020).
147. <https://www.thermofisher.com/order/catalog/product/88270#/88270> (accessed January 18 2020).
148. https://www.genscript.com/kit/L00402-ToxinEraser_sup_TM_sup_Endotoxin_Removal_Resin.html?src=jee4FnhQu5sdR (accessed January 18 2020).
149. <https://www.abbkine.com/product/purkine-endotoxin-removal-resin-bmr21400/> (accessed January 18 2020).
150. <https://www.bio-rad-antibodies.com/proteus-endotoxin-removal-kits.html> (accessed January 18 2020).
151. <https://lionex.de/product/endotoxin-removal-resin/> (accessed January 18 2020).
152. Kaca, W.; Roth, R. I.; Levin, J. Hemoglobin, a newly recognized lipopolysaccharide (LPS)-binding protein that enhances LPS biological activity. *Journal of Biological Chemistry* 1994, 269, 25078-25084.
153. Zhang, K.; Dai, L.; Chetwyn, N. P. Simultaneous determination of positive and negative pharmaceutical counterions using mixed-mode chromatography coupled with charged aerosol detector. *Journal of Chromatography A* 2010, 1217, 5776-5784.
154. Zhang, K.; Liu, X. Mixed-mode chromatography in pharmaceutical and biopharmaceutical applications. *Journal of Pharmaceutical and Biomedical Analysis* 2016, 128, 73-88.
155. Gao, D.; Wang, L.-L.; Lin, D.-Q.; Yao, S.-J. Evaluating antibody monomer separation from associated aggregates using mixed-mode chromatography. *Journal of Chromatography A* 2013, 1294, 70-75.

156. Matos, T.; Queiroz, J. A.; Bülow, L. Plasmid DNA purification using a multimodal chromatography resin. *Journal of Molecular Recognition* 2014, 27, 184-189.
157. Zhao, G.; Dong, X.-Y.; Sun, Y. Ligands for mixed-mode protein chromatography: Principles, characteristics and design. *Journal of Biotechnology* 2009, 144, 3-11.
158. McLaughlin, L. W. Mixed-mode chromatography of nucleic acids. *Chemical Reviews* 1989, 89, 309-319.
159. Silva-Santos, A. R.; Alves, C. P. A.; Monteiro, G.; Azevedo, A. M.; Prazeres, D. M. F. Multimodal chromatography of supercoiled minicircles: A closer look into DNA-ligand interactions. *Separation and Purification Technology* 2019, 212, 161-170.
160. Wu, Q.; Xu, Y.; Yang, K.; Cui, H.; Chen, Y.; Wang, M.; Zhu, Q.; Kang, W.; Gao, C. Fabrication of membrane absorbers based on amphiphilic carbonaceous derivatives for selective endotoxin clearance. *Journal of Materials Chemistry B* 2017, 5, 8219-8227.
161. Petsch, D.; Beeskow, T. C.; Anspach, F. B.; Deckwer, W. D. Membrane adsorbers for selective removal of bacterial endotoxin. *Journal of Chromatography B: Biomedical Sciences and Applications* 1997, 693, 79-91.
162. Langer, E.; Rader, R. A.: *Top trends in biopharmaceutical manufacturing, 2017*, 2017; Vol. 30.
163. Abdullah, M. A.; Rahmah, A. U.; Sinskey, A. J.; Rha, C. K. Cell engineering and molecular pharming for biopharmaceuticals. *The open medicinal chemistry journal* 2008, 2, 49-61.
164. Waegeman, H.; Soetaert, W. Increasing recombinant protein production in *Escherichia coli* through metabolic and genetic engineering. *Journal of Industrial Microbiology & Biotechnology* 2011, 38, 1891-1910.
165. Goodman, M. Sales of biologics to show robust growth through to 2013. *Nature Reviews Drug Discovery* 2009, 8, 837.
166. Sanchez-Garcia, L.; Martín, L.; Mangues, R.; Ferrer-Miralles, N.; Vázquez, E.; Villaverde, A. Recombinant pharmaceuticals from microbial cells: a 2015 update. *Microbial cell factories* 2016, 15, 33-33.

167. Mamat, U.; Wilke, K.; Bramhill, D.; Schromm, A. B.; Lindner, B.; Kohl, T. A.; Corchero, J. L.; Villaverde, A.; Schaffer, L.; Head, S. R.; Souvignier, C.; Meredith, T. C.; Woodard, R. W. Detoxifying *Escherichia coli* for endotoxin-free production of recombinant proteins. *Microbial cell factories* 2015, *14*, 57-57.
168. Gerngross, T. U. Advances in the production of human therapeutic proteins in yeasts and filamentous fungi. *Nature Biotechnology* 2004, *22*, 1409-1414.
169. Akyar, I.: Latest Research into Quality Control. InTech, 2012.
170. Franco, E.; Garcia-Recio, V.; Jiménez, P.; Garrosa, M.; Girbés, T.; Cordoba-Diaz, M.; Cordoba-Diaz, D. Endotoxins from a pharmacopoeial point of view. *Toxins* 2018, *10*, 331.
171. Silveira, R. L.; Andrade, S. S.; Schmidt, C. A.; Casali, R. G.; Dalmora, S. L. Comparative evaluation of pyrogens tests in pharmaceutical products. *Brazilian Journal of Microbiology* 2004, *35*, 48-53.
172. Di Paolo, A.; Forti, K.; Anzalone, L.; Corneli, S.; Pellegrini, M.; Severi, G.; Cagiola, M. First evaluation of endotoxins in veterinary autogenous vaccines produced in Italy by LAL assay. *Biologicals* 2018, *55*, 71-73.
173. Magalhaes, P. O.; Lopes, A. M.; Mazzola, P. G.; Rangel-Yagui, C.; Penna, T. C.; Pessoa, A., Jr. Methods of endotoxin removal from biological preparations: a review. *J Pharm Pharm Sci* 2007, *10*, 388-404.
174. Bicho, D.; Santos, B. F.; Caramelo-Nunes, C.; Sousa, A.; Sousa, F.; Queiroz, J. A.; Tomaz, C. T. Application of ethylenediamine monolith to purify a hemagglutinin influenza deoxyribonucleic acid-based vaccine. *Separation and Purification Technology* 2015, *154*, 320-327.
175. Franco-Medrano, D. I.; Guerrero-Germán, P.; Montesinos-Cisneros, R. M.; Ortega-López, J.; Tejeda-Mansir, A. Plasmid pVAX1-NH36 purification by membrane and bead perfusion chromatography. *Bioprocess and Biosystems Engineering* 2017, *40*, 463-471.

VITA

Sidharth Razdan was born and raised in Delhi, India. Before he joined the Engineering Graduate Program in Missouri University of Science and Technology at Rolla, Missouri in 2014, he earned his Bachelor's degree in Chemical Engineering from India. He pursued his Master's Degree in Chemical Engineering from 2014 to 2016 and worked towards his PhD program in 2017 under the guidance of Dr. Sutapa Barua. His main research was focused on endotoxin removal from therapeutic solutions and water using polymeric nanoparticles and membrane adsorbers. For his research, he received the prestigious AIChE Separations Division Graduate Student Research Award (Bioseparations) in 2018. He published several papers of which one was under his principal authorship and remaining under co-authorship. In May 2020, he completed his PhD in Chemical Engineering from Missouri University of Science and Technology, Rolla, Missouri, USA.